Role of some Morin-nanoconjugates in ameliorating inflammatory diseases

Thesis submitted for degree of Doctor of Philosophy (Science)

Submitted By

SANCHAITA MONDAL

Index No. 41/20/Chem./27

Department of Chemistry

Jadavpur University

2022

To be submitted as per this format

CERTIFICATE FROM THE SUPERVISOR(S)

This is to certify that the thesis entitled **"Role of some Morin-nanoconjugates in ameliorating inflammatory disease"** Submitted by **Smt. Sanchaita Mondal** who got his / her name registered on **14/09/2020** for the award of Ph. D. (Science) Degree of Jadavpur University, is absolutely based upon his own work under the supervision of **Dr. Pradip Kumar Mahapatra** and that neither this thesis nor any part of it has been submitted for either any degree / diploma or any other academic award anywhere before.

Pradip K. Mahapatra 28.12.2022

(Signature of the Supervisor(s) date with official seal)

Dr. Pradip Kr. Mahapatra
Associate Professor
Department of Chemistry
Jadavpur University
Kolkata-700 032

Dedicated to …

Maa, Baba, Boro Masi & My Husband for their unconditional love, support and sacrifice for my higher studies and generous presence in my life…

Acknowledgements:

First and foremost I wish to express my sincere gratitude to my supervisor **Dr. Pradip Kumar Mahapatra**, Associate Professor, Department of Chemistry, Jadavpur University who supported and guided me to do my thesis works. I thank him wholeheartedly.

I would love to express my deepest gratitude to **Dr. (Mrs.) Krishna Das Saha**, Cancer Biology and Inflammatory Disorder Division, CSIR-Indian Institute of Chemical Biology. Her excellent guidance, friendly atmosphere for open and free scientific discussions, philosophical suggestions steered me throughout my Ph.D journey.

I would also like to mention the special support I got from **Dr. Chittaranjan Sinha**, Professor, Department of Chemistry, Jadavpur University. He always helped me open handedly whenever I need. His constant support and guidance make my journey easier to achieve my goal.

I would like thank the H.O.D of Chemistry department**,** Jadavpur University, **Dr. Swapan Kumar Bhattacharya** and Director of CSIR-IICB, **Dr. Arun Bandopadhyay** for providing me the permission and infrastructure to meet my research objectives.

I sincerely acknowledge the help and support that I got from several faculties of CSIR-IICB like **Dr. Krishnananda Chattopadhyay, Dr. Sanjay Dutta, Dr. Arindam Talukdar, Dr. Biswadip Banerjee, Dr. P. Jaishankar, Dr. R. Natarajan, Dr. Nakul C Maiti, Dr. Nahid Ali and Dr. Partha Chakrabarti**.

I would like to thank my labmates Sujata Das, Krishnendu Manna, Niladri Mukherjee, Snehasis Mishra, Saswati Banerjee, Tanushree Das, Saheli Roy, Sayoni Nag, Moumita Saha for and Sanjib Das for their support, all innovative discussions and fun moments we shared.

I would like to thank all the operators of instrument section of CSIR-IICB, for helping me in performing my experiments.

I would also like to specially mention the name of **Dr. Mijanur Rahaman**, Assistant Professor, Department of Chemistry, Calcutta University, for his valuable guidance which driven me in the right direction of my research work.

Most importantly, I would like to express my love and respect for my parents **Anil Kumar Mandal and Suniti Mondal** and my elder sister **Anindita Mondal**. Without their benevolent support I would have been never come this far. My parents helped me to experience the true essence of life. I learned the "never give up" attitude from them. Their constant love, support and prayer give me the strength to bounce back against all odds. Here I also like to acknowledge my Boro Masi for her unconditional love, guidance, encouragement, tremendous support and sacrifice. Her fighting spirits encourage me a lot to stay strong against all difficulties and adverse situations.

I would like to thank my husband **Kamalendu Das** for his constant love, support and encouragement. He always stands by me during my bad days and supported and motivated me endlessly whenever I need his help. I am thankful to him for being always there by my side.

Last but not the least; I would like to express my deepest love and gratitude to The Almighty for constantly blessing me.

Sanchaita Mondal

Department of Chemistry

Jadavpur University

Contents

List of abbreviations:

As: Arsenic

AFM: Atomic force microscopy

FTIR: Fourier transform infrared spectroscopy

AST: Aspartate Transaminase

ALT: Alanine Transaminase

ALP: Alkaline phosphatase

ARE: Antioxidant Response Element

Bcl-2: B-cell lymphoma 2

BAX: BCL2-associated X protein

BAD: The Bcl-2-associated death promoter protein

CS: Chitosan

CD: β-Cyclodextrin

COX-2: Cyclooxygenase-2

DLS: Dynamic Light Scattering

ELISA: Enzyme-Linked Immunosorbent Assay

GST: Glutathione-S-transferase

GPx: Glutathione peroxidise

GSH: Reduced glutathione

H_2O_2: Hydrogen Peroxide

$HO^{\cdot}$: Hydroxy radical

HO-1: Heme oxygenase 1

Akt: Protein kinase B (PKB) known as AKT

IL: Interleukin

IL-1: Interleukin-1

IL-6: Interleukin-6

Keap1: kelch-like ECH-associated protein-1

MOR: Morin

NO: Nitrogen Oxygenase

Nrf2: Nuclear factor erythroid 2 (NF-E2)-related factor 2

NAC: N-Acetylcysteine

NQO1: NAD(P)H Quinone Dehydrogenase 1

NOX1: NADPH Oxidase 1

NF-kB: Nuclear factor-kappa B

iNOS: Inducible nitric oxide synthase

O_2^-: Super Oxide anion

PARP: Poly (ADP-ribose) polymerase

PI: Propidium Iodide

PBS: Phosphate Buffered Saline

p53 : Tumor protein p53

PI3K: Phosphoinositide 3-kinase

PTEN: Phosphatase and tensin homolog

SOD: Superoxide dismutase

STPP: Sodium tripolyphosphate

ROS: Reactive Oxygen species

TEM: Transmission Electron Microscope

TNF-α: Tumor necrosis factor-α

TGF-β: Transforming growth factor-β

Vit.E : Vitamin E

UC: Ulcerative Colitis

Abstract:

Nanotechnology flourishes in the medicinal field for the treatment of chronic human diseases due to their several advantages. Recently, nanomedicine is applied in different ways such as chemotherapeutic agents, biological agents, immunotherapeutic agents etc. in the treatment of various diseases. Nanoparticles remain in the blood circulation for prolonged time. So high dose of drug is not required which reduces the adverse side effects of the drug. Nanoparticles can easily penetrate through cell membrane and reach to its preferred location which increases it's the efficiency.

Nanoparticles exhibit unique structural, chemical, mechanical, magnetic, electrical, and biological properties. In recent time, nanoparticles are used as carrier by encapsulating or attaching the drug molecules. By doing some surface modification the drugs can also be delivered to target tissues more accurately in a controlled way. Nowadays, nanoparticles are widely used in medical biology and disease prevention and remediation because of all these interesting features.

The combinatorial delivery of nano-encapsulated bioactive natural compounds along with the synthetic drugs or other natural components owes to have growing interest in recent times. Nano-carriers can enhance the half-life of drug, increase permeability and retention. So, this method of delivery of natural bioactive compounds is very impactful for the treatment of various inflammatory diseases. Currently, natural components have been thoroughly examined in curing diseases because of their characteristic features. In comparison to conventional drugs, polymer based nanoparticles encapsulated with bioactive natural components are more beneficial due to their stability, biocompatibility andbiodegradability.

Natural compounds are widely available in plants, vegetables and fruits. Its medicinal importance has been extensively studied and established. Alkaloids, flavonoids, polyphenols, tannins, terpenes, saponins are the major bioactive molecules among others. Morin, a widely available natural flavonoids which are considered to have biological activities like anticancer, antioxidant, anti-inflammatory, anti-diabetic, anti-arthitis properties. But, the low absorption, low permeability, poor solubility reduces its bioavailability and efficacy. Also due to its high systemic clearance Morin require repeated applications and/or high doses. This further lessens its therapeutic use. Formulations of various biocompatible and biodegradable biopolymers based

nanoparticles encapsulated with Morin are able to solve the above mentioned limitations, maximize their delivery efficiency and increase the desirable benefits.

In the thesis work, we formulated the different polymeric nanocomposite of morin to address those limitation , enhance the therapeutic efficacy and evaluating its protective effect on inflammatory diseases. Therapeutic efficacy of the nanoparticles is high because of unique featureslike the high surface area to volume ratio, and controllable biologic properties like enhanced solubility, improve pharmacokinetic profile and targeted delivery.

Introduction:

Natural polyphenols are commonlyavailable in food and medicinal plants [1]. The plant polyphenols are used to prevent and treat many diseases, from ancient time of human civilization. According to WHO, about 75% of people of earth currently use herbs and other folk medicine to treat different kind of malaise [2]. Plants are the most valuable sources of bioactive compounds which are also known as a natural antioxidant especially polyphenols and carotenoids, considered to have protective effect in a on health and on wide range of diseases, including allergies, cardiovascular disease, neurodegenerative, diabetes and some paticular form of cancer, hepatic injury and inflammation [3]. The biological activity of natural antioxidants can be explained by their reactive oxygen species (ROS) scavenging ability which counteracts oxidative stress [4].

Therefore, the prominence of nutraceuticals like flavoniods, polyphenols, flavonols, carotenes, and saponins in the wellness of human health has grown up not only for their anti-inflammatory, anti-diabetic, anti-arthitis, anti-cancer activity but also their non-poisonous, easy availability, and lessercomplexity than synthetic medicines [5].

The over-use of synthetic medicines is directly correlated with several side effects and drug resistance development in the human body [6]. But the natural source of drugs has more diverse structure and originality relative to synthetic materials [2]. Natural bioactive compounds are good fit to combine with proteins, and other bio-molecules. The structure of those bioactive compounds is more complex than the synthetic one. This complexity favors more binding selectivity towards the targets.

Morin

Morin hydrate (3, 5, 7, 2′, 4′ -pentahydroxyflavone) abundantly present in fruits, stem, and leaves of Moraceae family is a C15 flavonoid structure isolated as a yellow pigment from various plants. [7]

Sources of Morin

Morin is obtainedfrom various fruits and vegetables like*Prunus dulcis* (almond), *Psidium guajava* (guava), guava leaves (*Psidium guajava L.*), *Morus alba L*. (white mulberry), old fustic (*Chlorophora tinctoria*), mill (*Prunus dulcis*), osage orange (*Maclura pomifera*), *Acridocarpus*

orientalis, *Chlorophora tinctoria* (figs), *Castanea sativa* (sweet chestnut), *Artocarpus heterophyllus* (jack fruit), *Allium cepa* (onion), *Malus pumila* (apple skin) and in multiple beverages like tea, red wine, seaweeds, coffee and cereal grains [7,8,9]. Furthermore, it considered one such component of several conventionalfolk medicines.

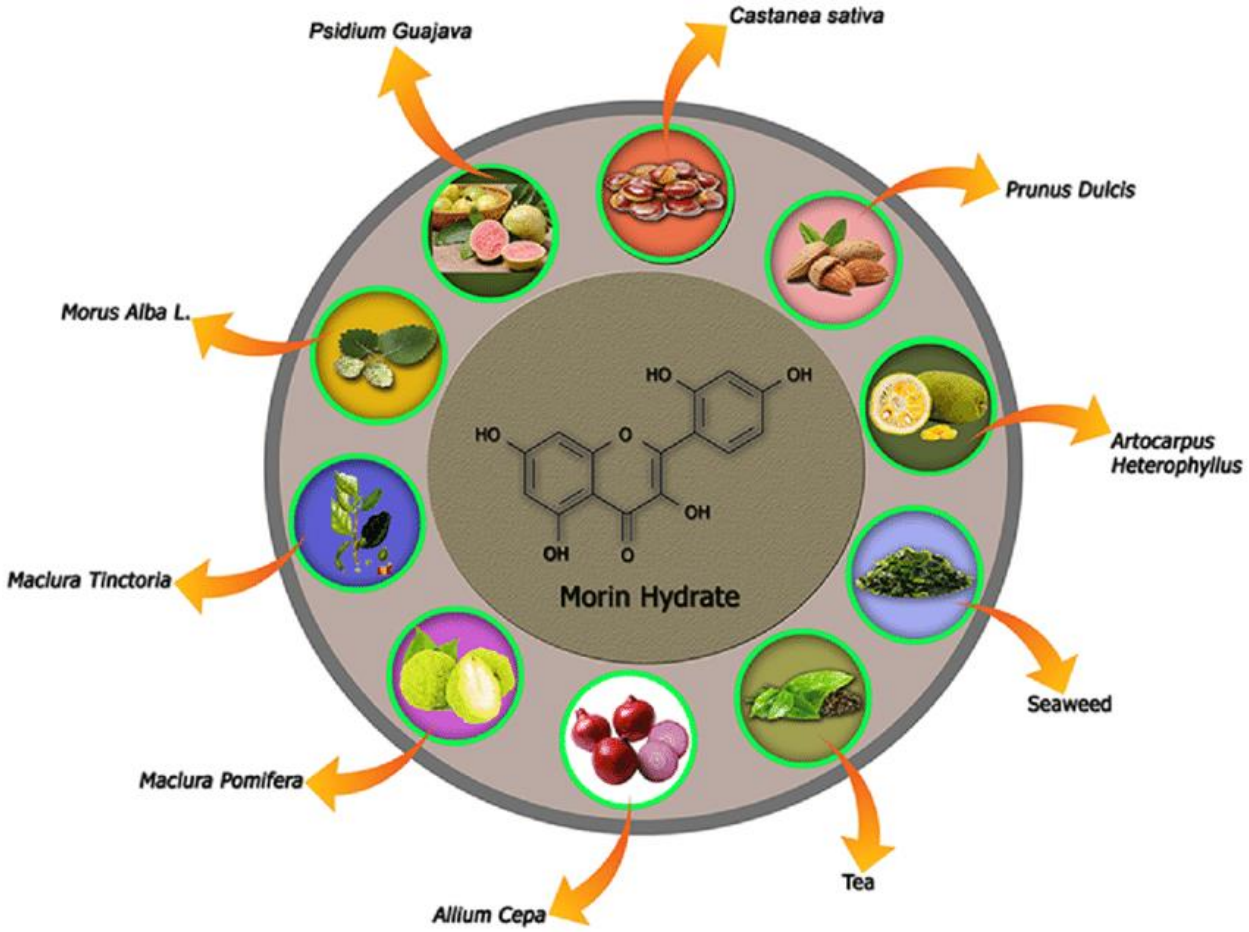

***Schematic diagram represents diverse natural sources of morin hydrate**

Chemistry of morin

Morinis a 7-hydroxy flavonol which defined by three hydroxy substituents at 2′, 4′ , and 5positions and contain a flavone (2-phenyl-1-benzopyran-4-one) backbone. This is an isomer of quercetin; but both quercetin and morin could be diversifieddepending on their B-ring's hydroxylation pattern, it is "ortho" for quercetin and "meta" for morin [8, 10]. Morin has a flexible conformation like other traditional flavonoids. Such chemical nature is found due to the electronic and intermolecular environment. Furthermore, morin has the competitive binding

affinity to transthyretin [11]. There are evidences that morin can bind with the thyroxin in more than one orientation, which shows the thyromimetic property of morin. Also, morin has the insulin mimetic properties because of its unique structural configuration.

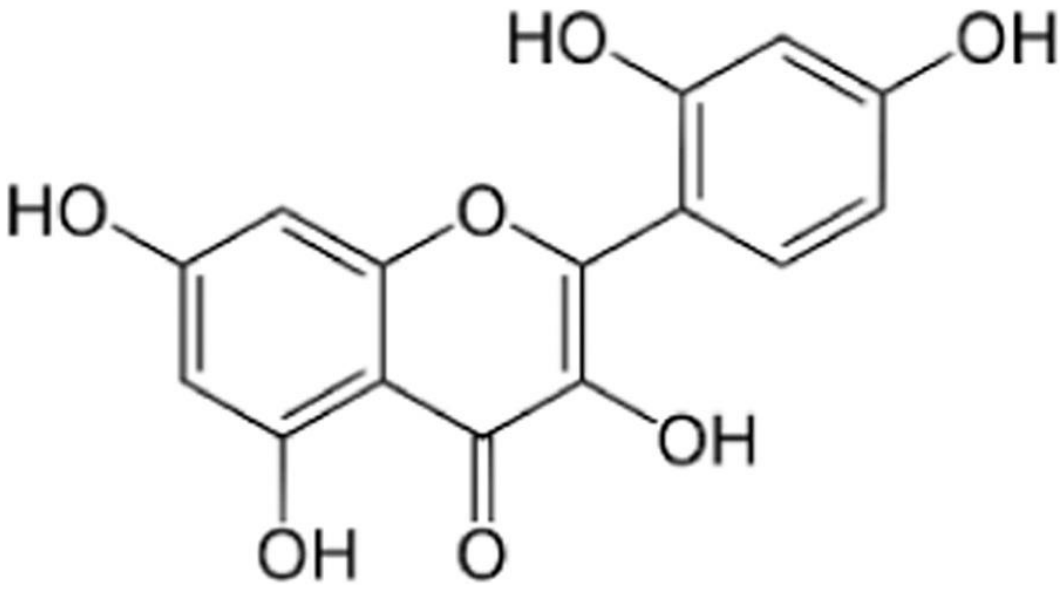

***Chemical structure of morin hydrate**

Biological activity of Morin

Like other flavonoids morin also has a broad spectrum of pharmacological properties, including anti-inflammatory [12, 13] antioxidant [14–16], anticancer [17–19], lung injury [20, 21], liver injury [22], neuro-inflammatory disorders [23, 24], nephrotoxicity [25], diabetes [26], gastritis [27], mastitis [21], and myocardial infarction [28] due to low toxicity. But the main drawbacks of morin are the bitter taste, poor water solubility, bio inavailability, susceptible to chemical degradation, instability to changing physiological environments in the gastrointestinal (GI) tract (pH, enzymes) for therapeutic application.

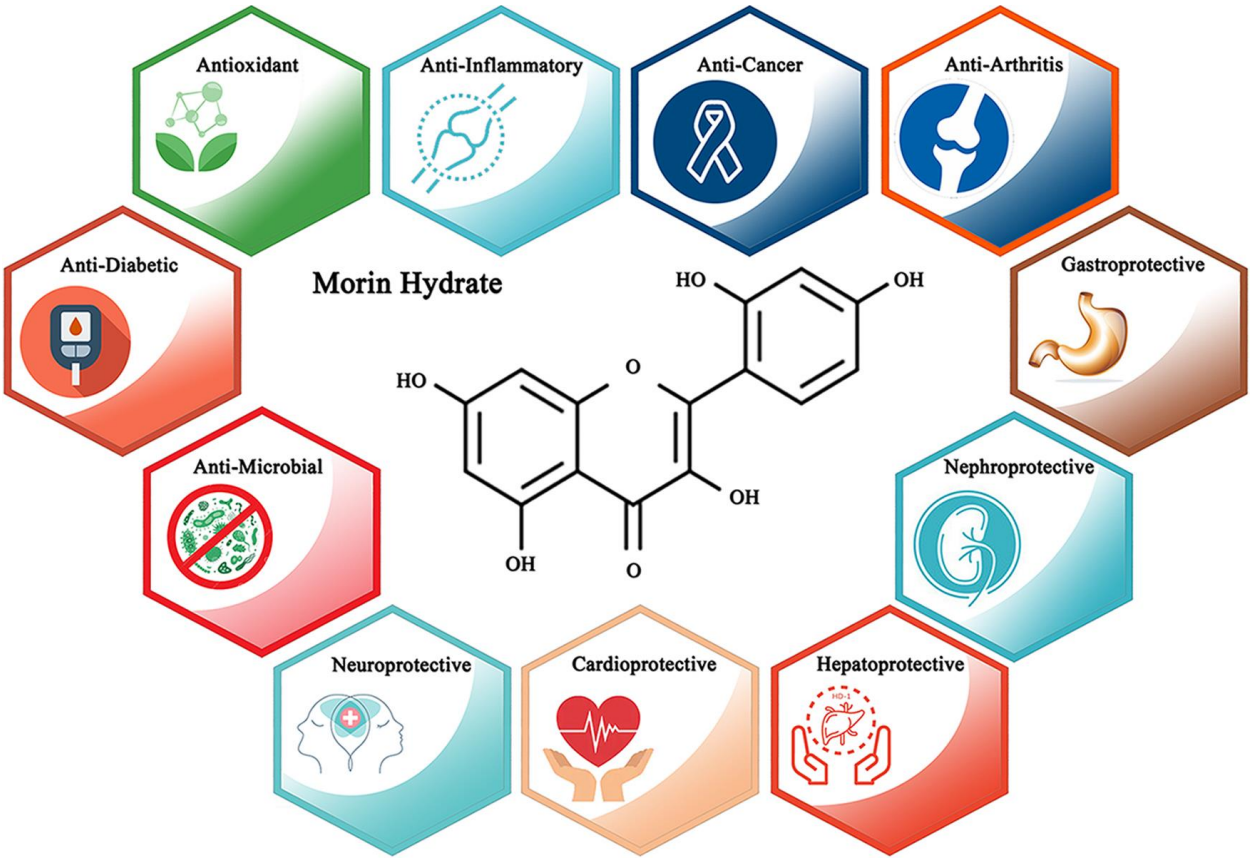

***Schematic diagram represents pharmacological potential of morin hydrate**

Nanotechnology

Nanotechnology is a process in which distinct feature of materials is utilized at nanoscale level [29].The implementation of nanotechnology in medicine and healthcare is called as nanomedicine.Nanomedicine offers a miraculous path to improve the way of disease treatment [30]. Among these, nanoparticles are widely used in the past few years in various medical applications, including drug and gene delivery, imaging, vaccine formulations, and biodetection [31]. The use of those nanomaterials could be revolutionized in order to improve the therapeutic effects and to overcome the other clinical challenges.

Nanoparticles & its advantages

Nanoparticles are actually a well-defined polymeric matrix in which active molecules can easilydissipated [32]. Nanoparticles provide the suitable cage for a drug or bioactive molecule to entrap within itwithout any chemical changes. As nanoparticles are smaller than micron and sub-

cellular in size, they have multipurposeuses for selected, site-specific delivery [33]. So by counting all those positive sites of nanotechnology it can be stated that it has a noteworthy prospect in the medication and multiplicated values in the wide range of disease pathology such as cancer, diabetes, cardiovascular disease etc.

Bioavailability is defined as the percentage of the active moiety (drug, phytochemicals or metabolites) reaching in the systemic circulation in unaltered form [34].
In pharmacology bioavailability falls in the subcategory of absorption. So bioavailability is affected by factors like hydrophobicity, low chemical stability, insufficient gastric residence time that influences absorption. The proper formulation of a nanoparticle has a significant impact on bioavailability to improve the therapeutic potential.

Chitosan

Chitosan is a natural polymerobtained by deacetylation of chitin using sodium hydroxide [35].Chitosan is stable at neutral pH and solubilizes in acidic environments. So in acidic medium it can transport the drug to the preferred locations. Chitosan nanoparticles are small in size, have better stability, low toxicity, cost-effective, easy to prepare and fabricate the outer surface and versatile means of administration [36].Chitosan alsoshows comparatively prolonged blood circulation time and moderate absorption by the reticulo-endothelial system (RES) [37]. Because of its innate physicochemical and biological features, it can be used as a promising drug and gene delivery.

Vitamin E

The chemical name of Vitamin E is alpha-tocopherol. It is a naturally obtained fat soluble vitaminand an antioxidant. It is available in many foods like vegetable oils, cereals, meat, poultry, eggs, and fruits [38].Vitamin E plays a crucial role for the appropriate functioning of living-organism.Reports have suggested that vitamin E can act as a scavenger for ROS by detoxifying their reactivity in several tissues [39]. Some previous reports have shown that chemicals and drugs mediated oxidative stress is suppressed or ameliorated by vitamin E as it acting like a ROS scavenger in the liver [40].

β-cyclodexrtrin

Cyclodextrins (CDs) are naturally obtained non-toxic cyclic oligosaccharideswith six, seven, or eight glucose units linked by α-1, 4 glucoside bonds, named, α-, β- and γ-CD, respectively [41]. They have received considerable attention owing to their low biotoxicity, high biocompatibility and unique structural features to effectively entrap and release of the drug molecules in a controlled way based on different stimuli [42].

All CDs have cone-like structure which offersa hydrophilic outer-surface and a comparatively hydrophobic inner-face. So it can form inclusion complexes with a wide range of hydrophobic guest molecules *via* the host-guest interactions andimprovethe solubility [43], stability, permeability, efficacy, biosafety and bioavailability of drugs [44].
All of this uniqueness of CDs makes themextraordinary from other materials, proposing a shining future for their biological implementations.

GNP

Metal Nanoparticles (NPs) hasgained increasing attentionbecause of their universal medical, consumer, industrial, and military applications [45].GNPs have been extensivelyexamined in several biomedical applications, such as bioimaging, single molecule tracking, biosensing, drug deliveryand as contrast-enhancing agents in X-ray and computed tomography (CT) applications [46].Gold Nanoparticles (GNPs) is extremely promising metal nanoparticles in biological applications due to their biocompatibility, inert reactivity, good photostability, facile synthesis, non-cytotoxicity and solubility, easy outer sphereremodeling with peptides, DNA and antibodies [47-48] and distinct physicochemical characteristicse.g.greater absorbance and light scattering [49]. Production of gold nanoparticles by biological method (“green synthesis”) is eco-friendly and minimizes the amount of harmful chemical and toxic byproducts [50]. Reports have shown that gold nanoparticles (GNPs) were much effective and less toxic than standard gold(I) drugs when it was administered orally, subcutaneously, or intra-articularly [51]. Based on these qualities, GNPs have widely applied forremedial treatment [52] cell labeling [53] targeted drug delivery [54] medical imaging [55] cancer therapy [55-58] and inflammatory diseases [59-60].

Inflammation

Inflammation performs amain role in the healing process [61]. Inflammation is classified as two: acute and chronic. The inflammation occurs due to sudden body damage, such as cutting your finger is called acute inflammation [62].When there is a continuous inflammation occur for a elongated times, and the immune system constantlyextruding white blood cells and chemical messengers that particular timeof the process, is known as chronic inflammation [63].Chronic inflammation can damage normal cells, tissues and organs which are linked to the development of several diseases [64]. Inflammation mediated tissue injury is observed in many organs including liver, kidney, intestinal tract, brain, lung, heart and reproductive system which sometime becomes life threatening [61]. Standard treatment schedule for these inflammatory diseases has more maleficent intricacy than the disease itself [65]. Therefore, there is a burning need of improvement of the healing compounds through application of nanotechnology. As curing agents of natural sources are safer, less hazards and cost-effective, aim of this study is to prepareand deliver the nanoparticles of morin in inflammation and organ damage.

Oxidative stress and antioxidants:

Oxidative stress arises because of the disparity between the generation of ROSand the antioxidant factors [66].Oxidative stress and inflammation are interrelated pathophysiological processes [67] and they are accompanied with several chronic diseases e.g. liver and lung diseases, diabetes, hypertension and cardiovascular diseases, and neurodegenerative diseases [68]. Inflammatory cells produceseveral reactive species from affected site which lead to excessive oxidative stress [69]. Because the enhanced level of ROS which exceeds the cellular counteracting antioxidant capacity, damages biological molecules such as lipid, proteins, DNA etc. ROS are also producedin the time of enzymatic reactions. ROS comprise several radicalslikesuperoxide, hydroxyl radicals, lipid hydroperoxides, and singlet oxygen ($^1O_2$), hydrogen peroxide, hypochlorous acid, chloramines and ozone [70]. Lipid peroxidationcan take place due to the over production of hydroxyl radical, thus damage the cell membranes and lipoproteins [71]. Alcohol, chemicals, drugs various heavy metals like arsenic, cadmium, environmental stresses give rise excessive ROS production which accelerate oxidative damage followed by cell death [72].ROS generation occur through the activation of redox signaling,

which is againstimulated by NADPH oxidase, and various growth factors and cytokines [73]. ROS is the main signaling molecules that play a crucial role in the development of inflammatory disorders. An increasing ROS generation by polymorphonuclear neutrophils (PMNs) at inflammation site instigates endothelial dysfunction and tissue injury. Oxidative stress performs a vital role in several pathological conditions, such as hypertension, pulmonary hypertension, diabetes, and chronic kidney disease, in target organs including the heart, liver, pancreas, kidney, and lung [74].

Antioxidants are compounds or chemicals that decrease or prevent the effects of free radicals by inhibiting their formation or by interrupting their propagation by several pathways [75]. Antioxidants can decrease oxidative stress induced by chemicals, metals, environmental factors by a direct scavenging of ROS that is they donate an electron to free radicals. Antioxidants may reduce the cellular ROS level either by constraining the activities free radical generating enzymes e.g. NAD(P)H oxidase and xanthine oxidase or by increasing the activities and expressions of antioxidant enzymes e.g. SOD, catalase, GSH [76]. So, antioxidants protective activity against reactive oxygen species and other free radicals and can act as a safeguard fortissues. Therefore, they prevent undesirable inflammatory responses, which may play a role in heart disease, cancer and other diseases.

The natural antioxidants obtain from plants and herbs are mostly polyphenols (phenolic acids, flavonoids, anthocyanins, lignans and stilbenes), carotenoids (xanthophylls and carotenes), vitamins etc [77]. Traditionally, the natural plant antioxidants are used to treat different diseases. Several reports suggest that the medicinal effects of natural antioxidants correlatedwith their interactions with specific proteins in the cell and activating or deactivating the signaling cascades [78], their rectification of the expression and activity of vital proteins.

Supplementation ofantioxidants including Vitamin E, Vitamin C, and various natural polyphenols can alleviate oxidative stress. Biological systems have redox balance properties to prevent damage of enzymatic and non-enzymatic natures which favor ROS inactivation. Nrf2 is known as the “key regulator” of the antioxidant response [79, 80]. Under physiological condition, Nrf2 stays inactivate and bounded with Keap1 in the cytoplasm. Under oxidative stress,Nrf2 become separated form Keap1 and got activated [81, 82]. The activated Nrf2 become translocated from cytoplasm to nucleus where it combine with the antioxidant response element

(ARE), stimulatesdifferent anti-oxidant enzymes and non-enzymatic factors. So, activation of Nrf2 signalling pathway improves the internal antioxidants defense system and amplifying the expression of antioxidants and detoxifying enzymes. The antioxidant enzymes e.g. CAT, SOD, GSH, GR and GPx, GST, NQO1, HO-1, NOX1 and the anti-oxidant factors Coenzyme Q10, GSH and ROS binding proteins like thioredoxin (Trx) become elevated [83-85]. They give electrons to free radicals without turning into electron-scavenging substances themselves.

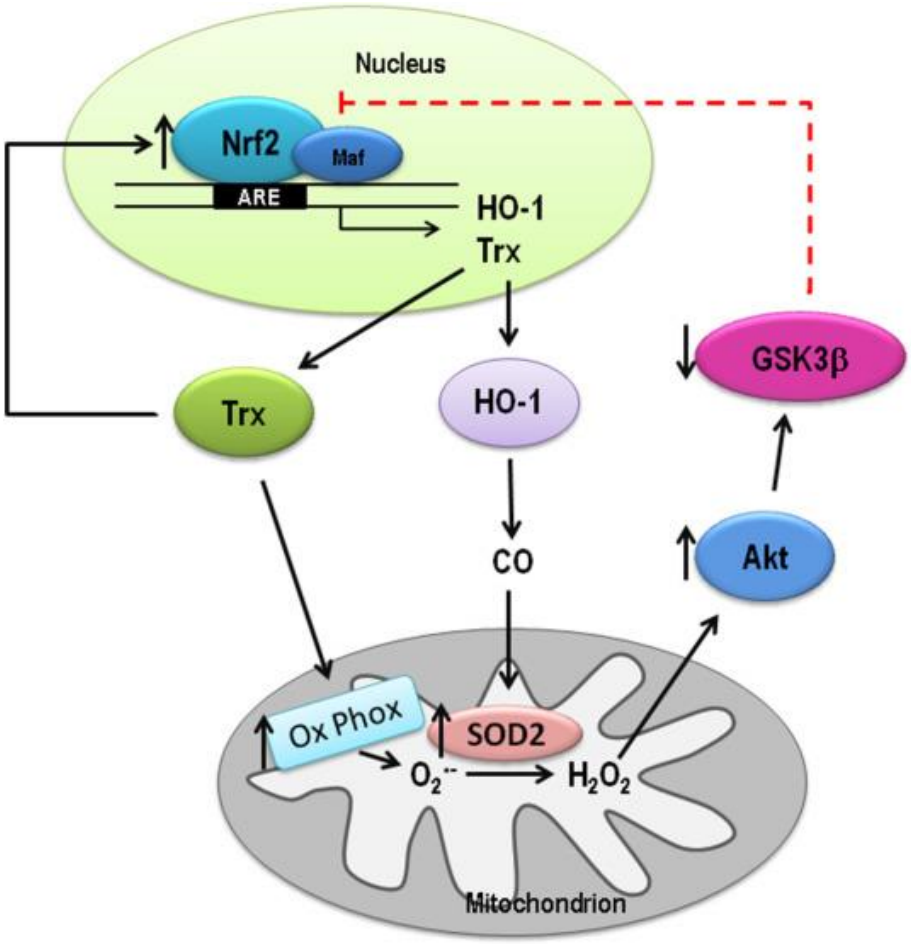

***Schematic diagram of Nrf2-keap1 signaling pathway**

Apoptosis:

Cell death can occur by necrosis or apoptosis or both. Apoptosis is characterized as an active, programmed cell death in multicellular organisms. Necrosis is described as passive, accidental cell death with uncontrolled inflammatory responses [86]. Apoptosis is also prompted by some

external and internal stimuli like ultraviolet radiation, oxidative stress and genotoxic chemicals in the body. Apoptosis may occur via two well-defined pathways - extrinsic and intrinsic [88].

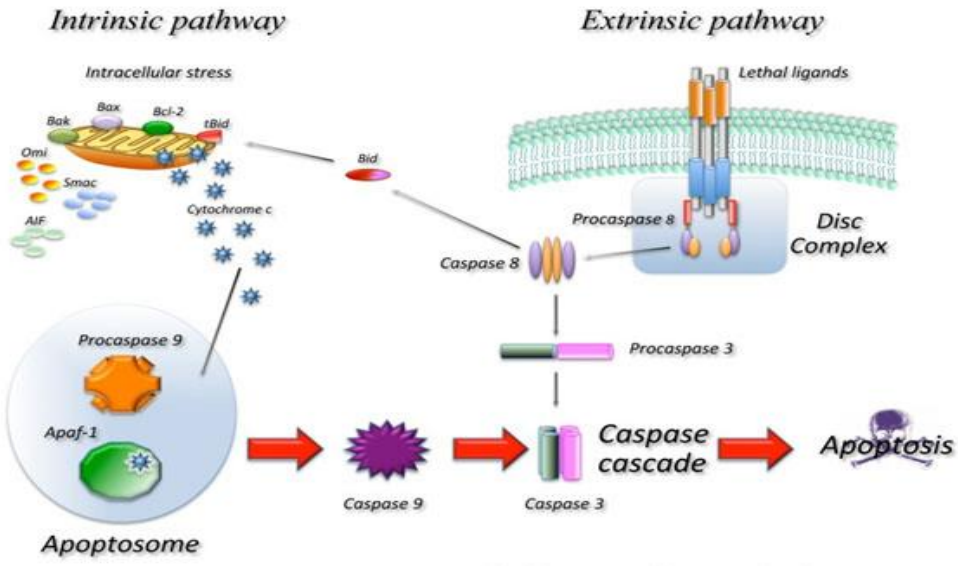

***Schematic diagram of apoptotic pathway**

During apoptosis,several morphological, cellular, nuclear modifications such as cell shrinkage, cell rounding, nuclear condensation and fragmentation, protein cleavage, DNA breakdown are observed [88]. Caspases (cysteine proteases) normally exists as inactive proenzyme forms in various cells and activated by intrinsic or extrinsic death factors. Once activated through its cleavage, it can activate other procaspases through proteolytic cleavage [89]. In the proteolytic cascade, one caspase can activate other caspases, stimulates the apoptotic signaling pathway resulting cell death. Caspases are classified as initiators (caspase-2,-8,-9,-10), and effectors or executioners (caspase-3,-6,-7) and inflammatory caspases (caspase-1,-4,-5). Executer caspase, caspase-3 is activated by initiator caspases (caspase-8, -9 or -10) [89]. Apoptosis is primarilydriven by cell survival and the proliferative signal transduction pathway. The bcl-2 proteins family (bcl-2 and bcl-XL) is anti-apoptotic, whereas Bad, Bax or Bid are pro-apoptotic [90]. Cell growth and survival depends on the level of pro- and anti-apoptotic proteins [91]. Enhanced level of pro-apoptotic proteins increase the cell apoptosis, and for anti-apoptotic proteins the thing is altered. Apoptosis may occur by intrinsic pathway (named as the mitochondrial pathway) or by the extrinsic pathway or both. The intrinsic pathway is activated through binding of BAX to mitochondria when membrane pore size increases and Cytochrome C

is released from mitochondria to cytosol [92]. Cytochrome c along with ATP and Apaf-1 promotes the cleavage and activation of Caspase-9 (initiator caspase) [93]. Caspase-3 then initiates activation of caspase-3 (executioner caspase). Caspase-3 in its activated form activates the specific cleavage of many significant cellular proteins and finally leading to the apoptotic cell death [94].

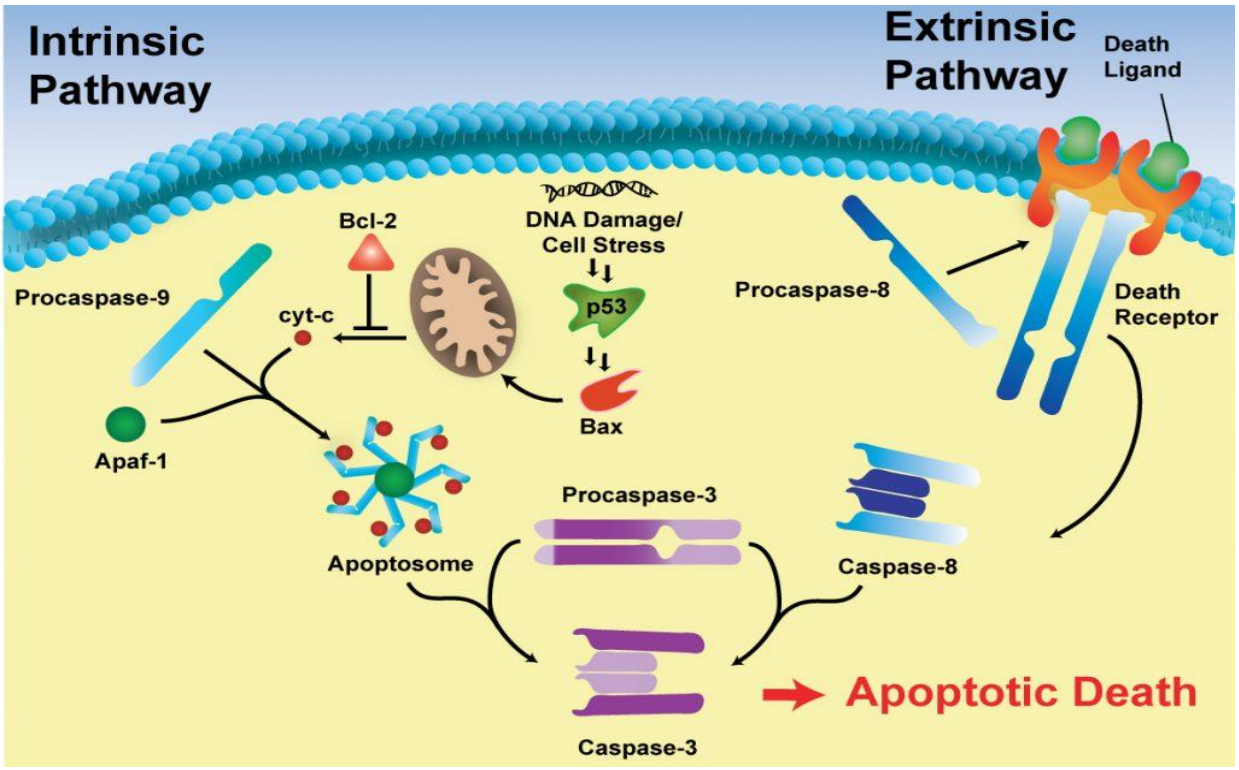

***Schematic Diagram of casepase-3/9 pathway of apoptosis**

AKT is a cell survival factor of the body [95]. The PI3K/AKT pathway is the main signal transduction pathway that arbitrates cell growth and inhibits apoptosis [96]. Activation of PI3K/AKT cascade is a the innate properties of cell survival. This PI3K/AKT signaling is suppressed by the tumor suppressor gene PTEN-10. AKT could also activate NF-kB via regulating IkB kinase (IKK), resulting transcription of pro-survival factors.AKT phosphorylate the anti-apoptotic protein, Bcl-2 [97]. Tumor suppressor protein p53 is another central regulator of signalling cascades regulating cell growth and apoptosis [98]. P53 promotes cell death [99]. Hepatic injury is also regulated by p53 [100].

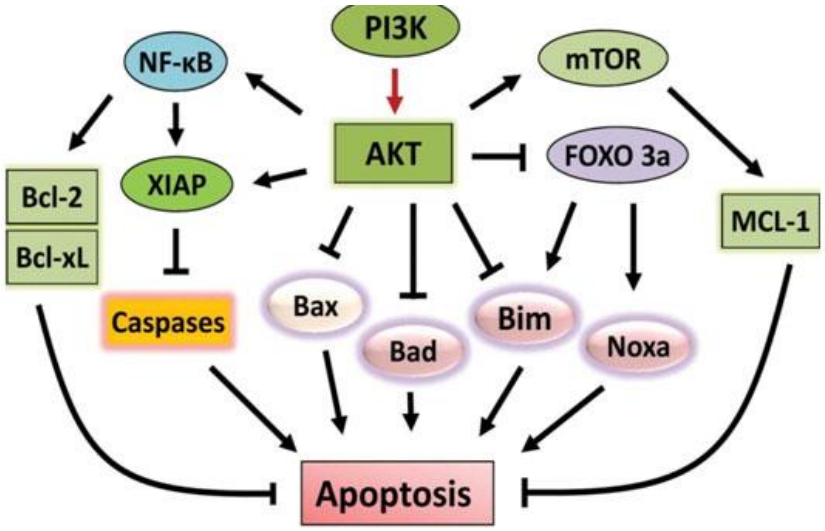

PI3K/AKT pathway of apoptosis

Liver injury

Liver is aprime organ of human body. It plays a significant role in metabolism and detoxification of compounds [101]. So, toxicological problems associated with several diseases also affect the liver tissues. Basically, hepatic cells are damaged by hepatoxins by triggering oxidative stress [102]. Arsenic a metalloid and environmental contaminated are related with human health problems in several areas [103]. Arsenic contamination majorly occurs through ground water and prolonged inflammation through chronic arsenic exposure induction via drinking water leads to liver toxicity [104]. During arsenic exposure, there is enhanced oxidative stress which lowers antioxidant systems like SOD, catalase, GSH, GST, GPx, GR and NQO1, HO-1, Nrf2 [105]. Whereas NOXs is increased as prime origin of reactive oxygen species (ROS). Generation of proinflammatory gene, NF-kBand its translocation to the nucleus is initiated by ROS. Nuclear NF-kB enhances the production of TNF-α, IL-1β, IL-6, NO, iNOS, activation of COX-2 [105]. In particular, chornic inflammation is considered to be the hallmark of liver damage.

Liver injury primarily developes from hepatic apoptosis [106]. The regulation of apoptosis and its regulatory factors can provide the necessary tools to combat liver diseases. The level of pro-apoptotic and apoptosis inducing factors like caspase-3, caspase-9, Bax, p53, PTEN are elevated and that of anti-apoptotic factors such as Bcl-2, AKT, PI3K are suppressed during chronic exposure to arsenic [107].

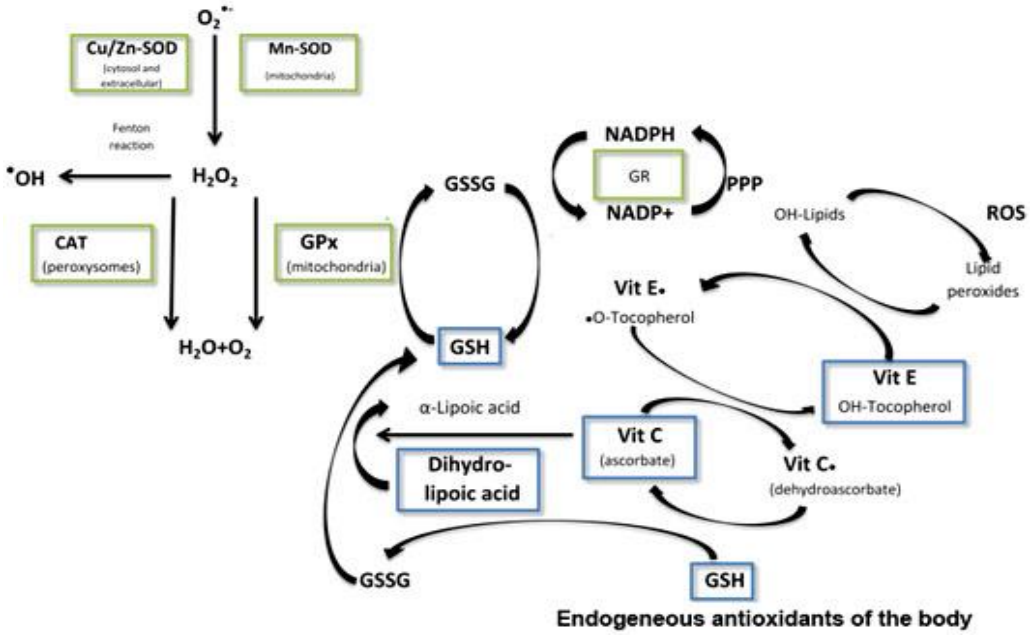

Ulcerative colitis

Ulcerative colitis (UC) is an inflammatory bowel disease (IBD) which occurs due to inflammation and ulcers in the digestive tract [108]. Most of the patients suffer with acute abdominal pain, fecal blood, weight loss, and diarrhea. This type of inflammatory irregularities of the gastrointestinal tract is very frequent and it consider as a chronic disorder [109]. There are an increasing number of reports of these inflammatory diseases globally and presently no such effective treatment is available.UC is characterized by pathological mucosal damage, immune dysregulation and ulceration [110]. Remarkably, it leads to imbalanced and enhanced inflammatory cells, over-production of cytokine and aberrant apoptosis of intestinal epithelial cells (IECs) [111]. Inflammatory cytokines likeTNF-α, IL-1β and IL-6 have been contributed in the virulent of UC [111]. And the enhanced level of inflammatory cytokines was linked with the infiltration of leukocytes, neutrophils and macrophages in the progression of UC [112]. Inflammation and apoptosis are interlinked with each other [113]. Several evidences focused the significant roles in the development of IECs apoptosis in the colonic tissue injury and the abnormality of immunology in UC [114]. Hence, UC was developed through inflammation and IECs apoptosis. So, the constrained of inflammation and apoptosis are the primary targets to heal UC.

Objectives:

Liver damage and ulcerative colitis are being a rising health problem with no cure. These diseases are associated with oxidative stress, inflammation and apoptosis. Natural compounds specially polyphenols have strong anti-oxidant, anti-inflammatory and anti-apoptotic properties. This study aims to prepare various nanoocomposites of morin, and examine the potency in liver damage and ulcerative colitis model. Following studies have been performed.

(1) Morin encapsulated Chitosan Nanoparticles (MCNPs) was prepared, characterized and its hepatoprotective effect was evaluatedinmurine model of arsenic induced liver damage.

(2) Morin, Vitamin E and β-cyclodextrin inclusion complex loaded chitosan nanoparticles (M-Vit.E-CS-CD NPs) was prepared, characterized and its hepatoprotective role was assessed in murine model of arsenic induced liver damage.

(3) Morin reduced gold nanoparticles ameliorates dextran sulfate sodium-induced Ulcerative Colitis via down-regulation of TLR4/NF-κB and NLRP3-inflammasome pathways and modulation of redox balance.

Research plan For Morin encapsulated Chitosan Nanoparticles (MCNPs):

i. Preparation of Morin encapsulated Chitosan Nanoparticles (MCNPs)

ii. Characterization of these above mention nanoparticles using FT-IR, UV-VIS, DLS, TEM, AFM.

iii. Determination of Drug loading capacity and encapsulation efficacy of nanoparticles.

iv. Invitro drug release at pH 6.8 and 7.4

Invivo Study:

v. Liver injury disease model development in mice via arsenic contaminated drinking water.

vi. Selection of nontoxic dose of MCNPs

vii. Treatment of the experimental group of mice by the prepared NPs with different dosages in every alternate day along with arsenic via drinking water upto 30 days.

viii. Examine the effect of MCNPs on liver function markers, blood parameters, anti-oxidant and anti-inflammatory factors.

ix. Liver tissue histology study by H&E staining.

x. Western blot analysis of anti-oxidant, anti-inflammatory and anti-apoptotic proteins expression.

xi. Organ distribution study by HPLC.

Research plan For Morin, Vitamin E and β-cyclodextrin inclusion complex loaded chitosan nanoparticles (M-Vit.E-CS-CD NPs):

i. Preparation and characterization of Morin, Vitamin E and β-cyclodextrin inclusion complex loaded chitosan nanoparticles (M-Vit.E-CS-CD NPs)

ii. Characterization of M-Vit.E-CS-CD NPs using FT-IR, UV-VIS, DLS,TEM, AFM, TGA, DSC, XRD, 1HNMR.

iii. Determination of Drug loading capacity and encapsulation efficacy of nanoparticles.

iv. Invitro drug release at pH 6.8 and 7.4

Invivo Study:

v. Liver injury disease model development in mice via arsenic contaminated drinking water.

vi. Selection of nontoxic dose of M-Vit.E-CS-CD NPs

vii. Treatment of the experimental group of mice by the prepared NPs with different dosages in every alternate day along with arsenic via drinking water upto 30 days.

viii. Examine the effect of M-Vit.E-CS-CD NPs on liver function markers, blood parameters, anti-oxidant and anti-inflammatory factors.

ix. Liver tissue histology study by H&E staining.

x. Western blot analysis of anti-oxidant, anti-inflammatory and anti-apoptotic proteins expression.

xi. Organ distribution study by HPLC.

Research plan ForMorin reduced Gold Nanoparticles (MGNPs):

i. Preparation of Morin reduced gold nanoparticles (MGNPs).

ii. Characterization of MGNPs using FT-IR, UV-VIS, DLS, TEM, AFM.

Invivo Study:

iii. Ulcerative colitis disease model development in mice via DSS-induced drinking water.

iv. Selection of nontoxic dose of MGNPs

v. Treatment of the experimental group of mice by the prepared NPs with different dosages in every alternate day along with arsenic via drinking water upto 15 days.

vi. Examine the effect of MGNPs on disease activity index (DAI), liver& kidney function markers, blood parameters, anti-oxidant and anti-inflammatory factors.

vii. Liver, kidney and colon tissue histology study by H&E staining.

viii. Western blot analysis and immunohistochemistry (IHC) of anti-oxidant, anti-inflammatory and anti-apoptotic proteins expression.

ix. Organ distribution study by HPLC.

Chapter I

Preparation and Characterization of Morin encapsulated Chitosan Nanoparticles (MCNPs) and evaluation of its hepatoprotective effect on arsenic induced murine model

Introduction:

Arsenic, a natural metalloid which is carcinogenic and genotoxic in nature, affect the living organism worldwide [115]. Utilization of arsenic derivatives as herbicides, rodenticides, insecticides, food preservatives and fossil fuel markedly polluted the drinking water. Previous report showed that arsenic induced toxicity is associated with liver dysfunction, renal failure, dermatitis, cardiovascular diseases, peripheral neuropathy, diabetes mellitus and varieties of cancers [116]. Due to environmental arsenic pollution liver disease is in the major risk in the whole world. The liver is the main target organ for the metabolism of arsenicals [115]. In humans liver is the main site for the methylation of inorganic arsenic which is the major metabolic pathway. Arsenite salt may exert its toxicity through reactions with thiols in cells and generation of reactive oxygen species (ROS) during their metabolism in cells [117].

Arsenic exposure elevated the serum level of liver function markers such as alanine amino transferase (ALT), asparatate amino transferase (AST) and alkaline phosphatase (ALP) [118].

It is established that the arsenic intoxication promotes Reactive Oxygen Species (ROS) generation, along with quick reduction of antioxidant enzymes such as superoxide dismutase (SOD) and catalase [116]. Nrf2, which act as a key redox regulator, remains attached with the kelch-like ECH-associated protein-1 (Keap1) in the cytoplasm, and is inactive at this bound state. Under oxidative stress condition Nrf2 is dissociated form Keap1 and are thus activated [119]. The activated Nrf2 being translocatedto the nucleus where it interacts with the antioxidant response element (ARE) and promotes the expression of different anti-oxidant enzymes such as Catalase (CAT), superoxide dismutase (SOD), glutathione (GSH), GSH peroxidase (GPx), glutathione-S-transferase (GST), heme oxygenase-1 (HO-1), NADPH quinone oxidoreductase 1(NQO1), etc.. Antioxidant enzyme and non-enzymatic anti-oxidant factors are affected in arsenic induced liver injury [118].

Arsenic induced liver injury is an outcome of inflammatory response with the generation of the inflammatory mediators like the cytokines TNF-α, IL-1β and IL-6, NO, COX-2 etc. Nuclear transcription factor-kB (NF-kB) remains inactive through attachment with its inhibitor called IkB in the cytosol. Dissociation of NF-kB from IkB leads to its activation following its translocation to the nucleus and where it regulates the transcription of pro-inflammatory genes. Transforminggrowth factor-β plays a key role in progression of liver diseases including liver toxicity. NLRP3 inflammasome activation occurs in severe liver injury with increased expression of casepase-1, IL-1β etc.

Oxidative stress mediated DNA damage and hepatocyte apoptosis is the focal point in arsenic induced hepatic injury (Nithyananthan et al. 2020).Therefore, the prevention of hepatocytes apoptosis is one of the pointers to examine the effectiveness of liver protective drugs (Kim et al., 2004; Ozaki, 2019).

Several research studies report the protective efficacy of plant polyphenols on hepatic injury against arsenic induced toxicity[120].Morin hydrate (MH; 2′,3,4′,5,7-pentahydroxyflavone), a yellowish pigment and a potent flavonoid present in various edible fruits and vegetables, belonging to Moraceae family, is used as a herbal medicine. Morin has a hepatoprotective activity [121].Anti-oxidant and anti-inflammatory properties of Morin mainly attributed to the protective efficacy and also the distinct structural feature of morin assists to interact with nucleic acids, enzymes and proteins [121].

But morin shows low water solubility in their free form, a high rate of metabolism and rapid elimination from the human body like other flavonoids [122]. Moreover, it undergoes degradation in water or oxidation, with a consequent loss in activity. All these factors contribute to a lack in long-term stability and to a poor vascular and oral bioavailability that drastically reduce the effectiveness of the compound which depends on preserving the stability, bioactivity and bioavailability. Therefore, the advancement of new ideas to conquer the drawbacks associated with MOR can provide a relatively cost effective and indigenous therapeutic lead in the treatment of liver ailments.

Chitosan, a natural polysaccharide derivative of chitin, is a poly-cationic linear polymer which has high potential to encapsulate natural ingredients. Chitosan is biocompatible, non-toxic and biodegradable, and has good bio-adhesive properties, making it capable of *in vivo* use through oral, intraperitoneal or intravenous administrations. Additionally, chitosan nanoparticles (CNPs)

can be easily prepared based on ionic gelation between positively charged chitosan polymer tripolyphosphate (TPP) anions. Therefore, CNPs have high capacity for delivering naturally available hydrophobic compounds like Morin.

Currently, polymeric nanoparticles have been widely used as a promissing drug delivery system. The remarkable advantage of polymeric nanoparticles is that they can be easily synthesized with different chemical methods. The topological and morphological control of nanoparticles is vitalfor specific applications in emerging areas of nanotechnology.The high surface area and internal void space present in the nanoparticles can make it an ideal medium as a drug delivery vehicle [123]. Specifically, the structures of polymeric nanoparticles are very attractive because of the unique topology that offers low density, high surface area, high pore volume, narrow pore size distribution, its non-toxic nature and biocompatibility. Consequently, nanotechnology can play a pivotal role in the development of nanomaterials that can be used for the therapeutic application of various inflammatory diseases [124].

So, in this study, we have synthesized and characterized morin encapsulated chitosan nanoparticles (MCNPs) and evaluated its hepatoprotective role, potential to ameliorate oxidative stress, inhibit apoptosis and inflammation.

Materials and Methods:

Chemicals

Morin Hydrate (purity ≥ 99.0%), Chitosan (low MW, extrapure), dichloromethane (DCM) and poly-(vinyl alcohol) (PVA), were purchased from Sisco Research Laboratories (Gurugram, India), Erlotinib hydrochloride (purity ≥98.0%) and all primary and secondary antibodies Sodium TPP were purchased from Sigma (USA) were purchased from Sigma-Aldrich, MO, USA. Assays kits for the detection of serum ALT, AST, AP, SOD, catalase, GPx, HDL, LDL, triglyceride (TG), total cholesterol (TC) were bought from ARKRAY Healthcare Pvt. Ltd (Surat, India). IL-1β, IL-6, TGF-β and TNF-α were measured by ELISA kits from R&D system (MN, USA). All other chemicals were available commercially and of a high degree of purity.

Preparation and Characterization of MCNPs:

Morin encapsulated chitosan nanoparticles (MCNPs) were synthesized by using the ionic gelation method [125]. Briefly, a desired amount of chitosan dissolved in acetic acid (1%) was mixed with a certain amount of Morin hydrate solution which was dissolved in slightly alkaline double distilled water under magnetic stirring (1000 rpm) at room temperature. After 5 min of

stirring, TPP solution was added dropwise to the mixture to form nanoparticles. To get the highest encapsulation efficacy 3:5:5 ratio of chitosan, Morin and TPP were used respectively for the preparation of nanoparticles in according to Bardania et al. The prepared nanoparticlessolution was centrifuged at 10000 rpm for 10 min. To determine the amount of morin encapsulated into the nanoparticles the UV-VIS spectra of the supernatant was recorded.The CNPs packed with morin have been examined for characterization in terms of Fourier transform IR, size distribution, morphological characteristics, zeta-potential, shape, the efficacy of drug encapsulation, percentage of drug loading and release of *in vitro* product.

Encapsulation efficiency & drug loading:

NPs (5 mg) were soaked in 5 ml of phosphate buffer for 30 min. The solution was centrifuged at 4000 rpmat 4˚C for 40 min, and the unconjugated drug was removed by washingthe precipitate twice with fresh solvent. Using a UV spectrophotometer (JASCO V-730, Spectrophotometer, Tokyo, Japan) at λ_{max} values of 270 and 395 nm, the clear supernatant solution was analyzed for unencapsulated morin. Morin standard curves were obtained by plotting the concentration against the absorbances from 10 to 50 mg/ml.

By using the following formula the percentages of drug loading and entrapment efficiency were evaluated:

Encapsulation efficiency (%) = (The total amount of drug released from the lyophilized MCNPs/Amount of drug initially taken to synthesize the MCNPs*)* × 100.

Drug loading (%) = (Amount of drug found in the lyophilized MCNPs/Amount of lyophilized MCNPs) × 100.

Particle size & zeta potential measurement:

To measure particle size analysis, distribution and zeta potential a Zetasizer 3000 HSA (Malvern Instruments, Malvern, UK) was used. For the DLS measurements, NPs were diluted with double distilled water, and 500 µl was loaded into the cuvette and transferred to zeta sizer cells for zeta potential measurement.

Fourier transform infrared spectroscopy:

FT-IR was recorded to identify the various functional group present in Morin, Chitosan and MCNPs. Morin, Chitosan and synthesized NPs which was centrifuged and lyophilized eariler; and the powdered of all three were analysed in the IR spectrum to interprete the presence of

different functional groups using the Perkin Elmer FT-IR spectrometer (MA, USA), in the absorbance mode.

Atomic force microscopy (AFM):

5 μL of the samples (1 mM) were deposited onto a freshly cleaved muscovite Ruby mica sheet (ASTM V1 Grade Ruby Mica from MICAFAB, Chennai) for 5–10 minutes, and then the sample was dried by using a vacuum dryer. AAC mode AFM was performed using a Pico plus 5500 AFM (Agilent Technologies USA) with a piezo scanner with a maximum range of 9 μm. Micro-fabricated silicon cantilevers of 225 μm in length with a nominal spring force constant of 21–98 N m^{-1} from Nano sensors were used. Cantilever oscillation frequency was tuned into resonance frequency. The cantilever resonance frequency was 150–300 kHz. The images (256 by 256 pixels) were captured with a scan size between 0.5 and 5 μm at a scan rate of 0.5 lines per s. The images were processed by flatten using Pico view1.4 version software (Agilent Technologies, USA). Image analysis was done through Pico Image Advanced version software (Agilent Technologies, USA).

Transmission electron microscopy (TEM):

A freshly prepared solution of the MCNPs in double distilled water was placed on a TEM grid (300-mesh carbon-coated Cu grid). The samples were allowed to dry in air at room temperature for a few hours before the measurements were recorded.

In vitro drug release studies:

MCNPs was solubilized in phosphate-buffered saline (PBS) medium (1M, NaCl = 8 gm, KCl = 0.2 gm, Na_2HPO_4 = 1.44 gm, KH_2PO_4 = 0.24 gm were dissolved in double distilled water and pH was adjusted to 7.4). To study the in vitro release kinetics MCNPs (10 mg) was filled in the dialysis bag of cut off size 5 kDa, put in a 200 ml of PBS of pH 7.4 and stirred at 1 g for 4 days. After a certaintime, interval 2 ml of the buffer solution was removed and replaced with fresh buffer. Using a UV-visible spectrophotometer (JASCO V-730 spectrophotometer, Tokyo, Japan) at 270 and 395 nm, respectively, the release of drugs has been tested. The experiments were repeated thrice, and the average values were evaluated.

Animals:

Male BALB/c mice of 6-8 weeks weighing 20-22gms were procured from animal house division of our Institute (CSIR- Indian Institute of Chemical Biology, Kolkata) and fed with standard

chow diets and drinking water. The animals were kept at 22−24 °C temperature, 50−60% humidity, and subject to light and dark cycles of 12:12 h. By following theinstitutional guidelines of the CSIR-Indian Institute of Chemical Biology Animal Ethics Committee the experiments were carried out. The institutional Animal Ethics Committee(s) approved the experiments.

Dose selection of MOR and MCNP:

After acculturation for 7 days, each group of mice were treated with 0mg, 100mg, 200mg, and 400 mg/kg body weight of MOR or 75mg, 150mg, 300 mg/kg body weight of MCNPs on every alternate day upto 30 days by oral gavage. AST and ALT were measured at different time intervals. Doses of MOR or MCNPs those did not affect the level of AST or ALT were chosen for further study.

Survival Study:

Different doses of arsenic were given to the mice for 30days along with the treatment without or with different doses of MOR or MCNP. Number of mice survived on day 30 was monitored and % survival of mice was calculated.

Experimental design:

The experimental plan of this study was as follows: Group I: Mice were exposed to arsenic (40mg/L) only via drinking water for 30 days. Arsenic exposed mice were given orally 0mg, 50mg, 100mg, and 200 mg/kg body weight of MOR (Group II-V) and 25, 50, 100 mg/kg body weight of MCNPs (Group VI-VIII). Both MOR and MCNPs were given on every alternate day by suspending in 0.1% Tween 80 in PBS starting from day 2 to 28 days of arsenic exposure. Blood was drawn by tail vein puncture at different time points from each group of mice, for serum analysis. The mice were sacrificed after 30days and the livers sections were collected for histology, Immunohistochemistry and Western blot analysis. For biochemical testing, one part of liver was stored at -80◦C freezer, and the other part was cut and placed in a bottle containing 10% neutral-buffered saline for performing histopathological analysis the next day.

Measurement of serum ALT, AST, HDL, LDL, TG, TC, LDL, HDL, uric acid, creatinine, and MDA

Blood samples were obtained by tail-vein puncture and kept at 4˚C undisturbed o/n. Samples were centrifuged the next day(1100×*g*, 10 min, 4˚C) to obtain the serum from the experimental groups. Serum AST, ALT, ALP, HDL, LDL, TG, TC, SOD, GPx and catalase activities were calculated according to the instruction brochure provided with the commercial assay kits.

Assessment of arsenic deposition in organs:

A simple spectrophotometric method has been followed for the determination of arsenic in various organ of the murine samples. The method is based on the reaction of arsenic(III) with potassium iodate in acid medium to liberate iodine. This liberated iodine bleaches the red color of Rhodamine B. A calibration curve was prepared by adding 2 ml of potassium iodate and 1 ml of HCl to an aliquot of a working standard solution containing 1.0–10.0 μg of arsenic in a 25 ml calibrated flask and the mixture was shaken gently. This was followed by addition of 2 ml of 0.05% Rhodamine-B. The solution was kept for 15 min and made upto the mark with deionised water. The decrease in absorbance at 550 nm is directly proportional to arsenic (III) concentration and obeys Beer's law [126].Then a measured amount of liver and spleen samples were taken in a 15 ml polypropylene tube in the presence of 3 ml of nitric acid (61%). The tubes were capped properly and incubated at 80°C for 48 hrs, followed by cooling for 1 hr to room temperature. After cooling, 3 ml of hydrogen peroxide (30%) was added to each tube, followed by incubation at 80°C for 3 hrs. After suitable dilution of the digested materials with ultrapure water, levels of arsenic in the samples were determined. Sample solution (1mL) obtained after digestion of the tissue was mixed with 2 mL of KIO_3 and 1 mL of HCl. And the mixture was shaking gently followed by addition of 0.1% Rhodamine-B. The solution was kept for 15 min. The absorbance was measured at 550 nm.

Determination of ROS:

Liver samples (200 mg each) were homogenized (1:10 w/v) in Tris-HCl buffer (40 mM, pH = 7.4, 0◦C). One hundred mililiter of tissue homogenate was mixed with 1 ml of Tris-HCl buffer and 5 μl of 2, 7-dichlorofluorescein diacetate solution (10 mM). The mixture was incubated for

half an hour at 37˚C. Finally, the sample fluorescence intensity was measured using a spectrofluorometer at 480 and 525 nm wavelengths of excitation and emission.

Estimation of Lipid Peroxidation Levels in the Liver

The level of lipid peroxidation in liver tissues was measured as the amount of thiobarbituric acid reactive substances (TBARS) [127].Thiobarbituric acid reactswith MDA (malondialdehyde), a major lipid oxidation product to form a red product (TBARS) that can be detected colorimetrically at 532nm or fluorometrically at Ex/Em 532/553 nm. Briefly, supernatants of tissue lysate were mixed with equal volume of TCA-BHT (BHT = butylated hydroxytoluene) in order to discard proteins. BHT stops further sample peroxidation during experimental process. After centrifugation (1000 g, 10 min, 4°C), 200 ml of the resulting supernatant was mixed with 40 ml of HCl (0.6 M) and 160 ml of thiobarbituric acid (TBA) 20% dissolved in Tris. The mixture was heated at 80°C for 10 min, and after cooling at room temperature, the absorbance was read at 530 nm and TBARS values were calculated and expressed in nmol/mg protein.

Estimation of SOD, GSH, catalase:

Blood samples were obtained by tail-vein puncture and kept at 4˚C undisturbed o/n. Samples were centrifuged the next day(1109×*g*, 10 min, 4˚C) to obtain the serum from the experimental groups. Serum, SOD, GSH and catalase activities were calculated according to the instruction brochure provided with the commercial assay kits.

Histological evaluation:

The fixed liver tissues in 10% neutral buffered formalin (NBF) were embedded in paraffin, thinly sectioned, de-paraffinated and rehydrated using the standard histology procedure. Various pathological changes were assessed by using hematoxylin and eosin stains.

Assessment of serum cytokines:

Blood samples were isolated at different time points as mentioned above, and the serum levels of TNF-α, IL-1β, TGF-β and IL-6 were determined using the commercially available ELISA kit according to the manufacturer's instruction and guidelines (R&D Systems, MN, USA).

Tissue Distribution Study:

All mice were fasted overnight and were fed only water before the experiments. Standard stock solutions of MOR and MCNPs (1 mg/mL) were prepared by dissolving the specific amounts of the drug in ethanol. After oral administration of MCNPs mice were sacrificed at 2, 6, 12, 24, 48, and 72 h. Various tissues (liver, lung, kidney, spleen) were collected and washed with 0.9% NaCl to remove the extra blood and contents. After blotting them with filter paper, 1 mg equivalent from the tissues was weighed and homogenized in 1mL of 0.9% NaCl. Then, 100 μL of it was used as the tissue sample. Blood samples were drawn from the tail vein and coagulated for half an hour in an MCT tube. The blood samples were centrifuged at 2000 rpm for 10 min (4 °C), and serum was obtained from the supernatant. Then, 100 μL of the serum was used as the sample. Tissues were stored at −80 °C for further use [128].

Western blot analysis:

Dissected tissues frozen in liquid nitrogen were disrupted using homogenizer and RIPA lysis buffer and then centrifuged. Protein concentrations in the supernatant of tissue lysate were assessed using the Bradford method [129]. SDS-PAGE was carried out on an acrylamide gel to separate the proteins, which were then transferred to a polyvinylidene difluoride membrane. The membrane is blocked with 10% skimmed milk or 5% BSA and incubated overnight with primary antibody of different proteins and β-actin (1:1,000; Santa Cruz, CA, USA), and next day after washing the membrane 3 times with wash buffer, was incubated with the alkaline phosphatase conjugated secondary antibody for 2 h. At last, protein expressions were detected using NBT/BCIP solution.

Immunohistochemical analysis:

Paraffin-embedded blocks of liver tissues were cut into thin sections and mounted onto slides. Xylene was used to deparaffinize liver sections, and various concentrations of alcohol were used to rehydrate the tissues. Antigen retrieval step was performed using sodium citrate buffer (10 mM sodium citrate, 0.05 percent between 20, pH = 6.0) for 20 min in a water bath at 100◦C. A 5%solution of BSA was used for blocking in Tris-buffered saline (TBS, 20mM Tris–HCl, pH 7.4 containing 150 mM NaCl) for 2 h. For permeabilization, the tissue sections were washed with TBST (Tris-buffered saline, 0.1% Tween 20). Finally, at a dilution of 1:500 at 4˚C overnight in a humidified chamber, the sections were incubated with the primary antibody. The tissue sections were washed with 1× TBS and incubated with 1:400 dilution of Alexa fluor 555 (red) and Alexa fluor 488 (green) conjugated secondary antibodies for 2 h at room temperature. The nucleus was

visualized by Hoechst (Invitrogen, CA, USA) stain. The images were observed using an automated laser scanning confocal microscope (Olympus FV10i, Shinjuku, Tokyo, Japan).

Statistical analysis

All data from at least three experiments with replicates were expressed as mean standard deviation (SD). Using GraphPad Prism software (CA, USA), statistical significance and differences between control and five other treatment groups were analyzed using a one-way analysis of variance.

Results:

Characterization of MCNP:

Morin encapsulated chitosan nanoparticles (MCNPs) prepared by Ionic gelation method were characterized. Figure 1A shows the UV-Vis absorbance spectra of morin and MCNPs. The DLS shows that MCNPs has a diameter of 124±1.5 nm (Figure 1B), with a polydispersity index value of 0.18, suggesting low polydispersity. MCNP's zeta potential value is -28.4±0.39 mV, which tended to stabilize NPs' suspension. Fourier Transform IR (FTIR) demonstrates the compatibility between MOR, chitosan and morin loaded chitosan nanoparticle as shown in Figure 1C. The FTIR spectra cover the region from 4000 cm^{-1} to 500 cm^{-1}. The significant peaks assigned for MOR, chitosan and MCNP confirm the presence of their different functional groups. The strong, broad peak at 3400 cm^{-1} is due to O-H (stretching), while a sharp peak at 1650 cm^{-1} corresponds to the presence of aromatic ester (C=O) and alkene (C=C) groups and an another strong, sharp peak at 1200 cm^{-1} indicates the C-OH stretching. The strong, sharp peak at 3100 cm^{-1} is due to O-H (stretching), and a sharp peak at 1647 cm^{-1} corresponds to the presence of alkene (C=C) groups, and a sharp peak observed at 1160 cm^{-1} is the indication of C-OH (stretching) in Chitosan. The MCNP shows a peak at 3100 cm^{-1}, which suggests that the O-H groups of MOR and Chitosan are conserved. Another small peak at 1645 cm^{-1} and 1120 cm^{-1} denotes the conservation of the alkene (C=C) and ester (C=O) groups and C-OH bond of MOR and Chitosan in the MCNP. Atomic force microscopy (AFM) and Transmission Electron Microscopy (TEM) reveal that the surface topology of MCNPs is spherical, and they are uniformly distributed without aggregation. The size of MCNPs ranges between 100 and 200 nm, as seen in Figure 1D& 1E.

The encapsulation efficiency of MOR is 73±2.5%. The formulation optimized for spherical shaped NPs results high drug encapsulation efficiency. The drug loading for MOR is 58±3.3% (Figure 1F). The drug release kinetics morin-loaded Chitosan NPs are shown in (Figure 1G). The nanoparticles release 53% MOR in 24 h. A constant slow release of MOR is observed for 4 days, but the maximum release is observed at 72 h which is 86.5%.

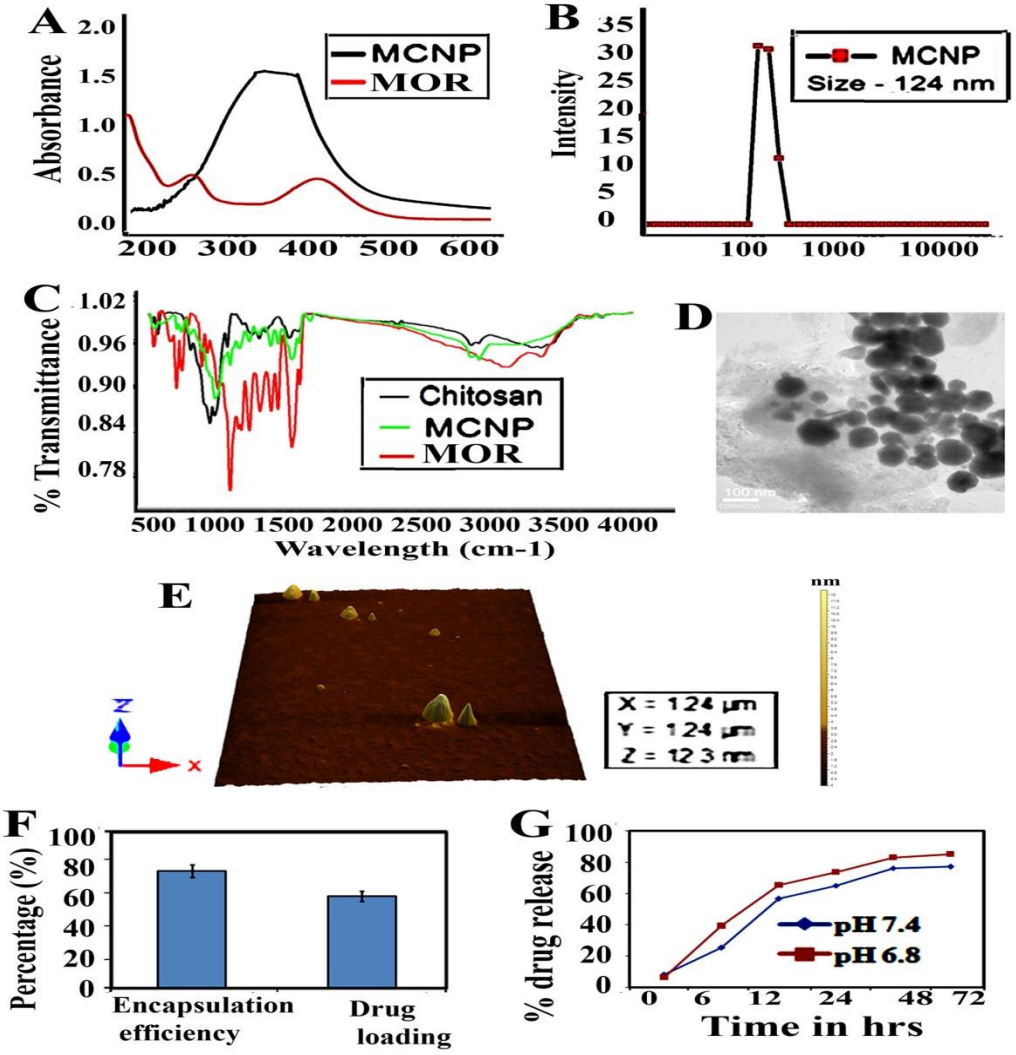

Figure 1: Characterization of Morin loaded Chitosan nanoparticles. (A) UV–Visible spectra of morin and MCNPs. The red line shows the spectra of morin, black line shows the spectra of MCNPs. (B) Particle size distribution from differential light scattering (DLS) with MCNPs. (C) Fourier transform infrared spectroscopy (FTIR) spectra of Morin, chitosan, and MCNPs. (D) TEM images of MCNPs. (E) MCNPs particle surface topology determination using atomic force microscopy (AFM). The acquired images were analyzed using scanning probe microscopy

(SPM) tools for laboratory study. (F) Encapsulation efficiency percentage and drug-loading percentage of MCNPs. (G) Percentage of release of Morin from MCNPs over a time period of 0−72 h. Result is the mean ± standard deviation (SD) from triplicate independent experiments.

Effect of MOR and MCNP on AST, ALT, body weight, hematological parameters, kidney function markers and lipid profiles

Non-toxic doses of MOR and MCNPs in mice were determined by measuring the effect of their different doses on the serum level of AST and ALT. Upto 200 mg/kg of MOR and 100mg/kg of MCNPs given orally on alternate day upto 30 days did not raise the serum level of AST and ALT (Fig. S1 and S2). However, the level of AST and ALT increased following treatment of 400 mg/kg body weight of MOR and 200 mg/kg body weight of MCNPs. So, the effect of MOR and MCNPs against arsenic induced toxicity was performed using maximum doses 200 mg/kg and100 mg/kg respectively.

S1

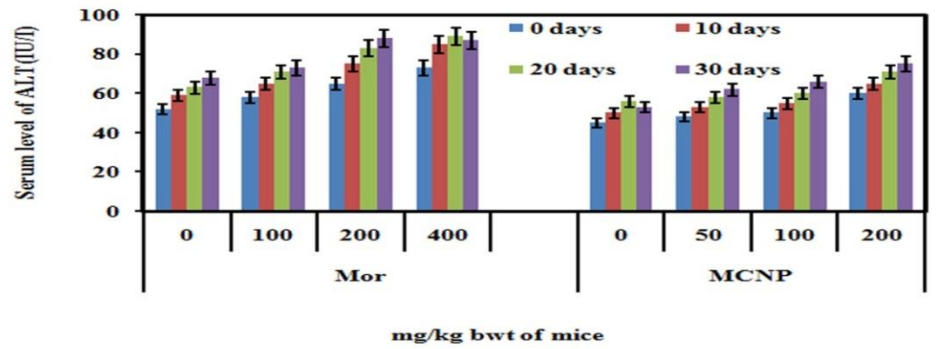

S2

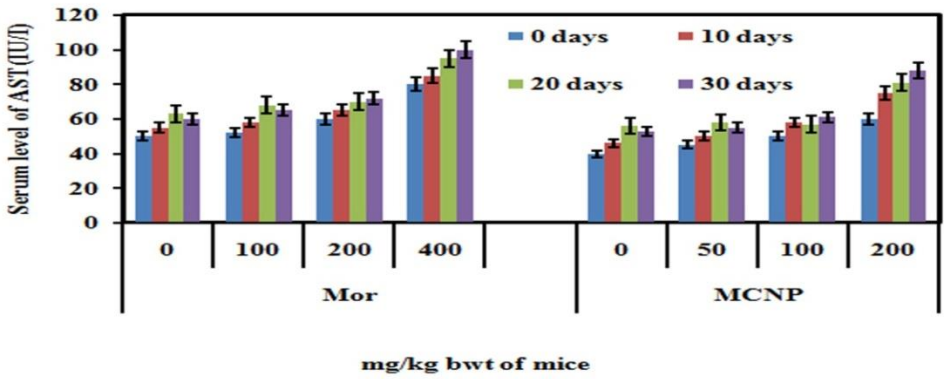

Fig S1 and S2: Effect of Morin (MOR) and MCNPs on liver function markers (ALT and AST). Different dosage of Morin (MOR) and MCNPs were orally given to the normal BALB/c mice and the serum level of ALT and AST were measured. Data is one of the three representative experiments ± SD.

Serum level of AST and ALT increased with time in arsenic exposed mice (40 mg/L). Treatment of MOR (50, 100 and 200 mg/Kg bwt) and MCNPs (25, 50, and 100 mg/Kg bwt) on alternate day during arsenic exposure dose dependently lowered the level of AST and ALT (Figure 2A and 2B). Effect of 25mg/kg and 50mg/kg MCNP was comparable with 100mg/kg and 200mg/kg bwt of MOR respectively. Thus, potency of MCNPs was nearly four times higher than MOR and optimum effect was observed with 50mg/kg MCNP and 200mg/kg bwt of MOR.

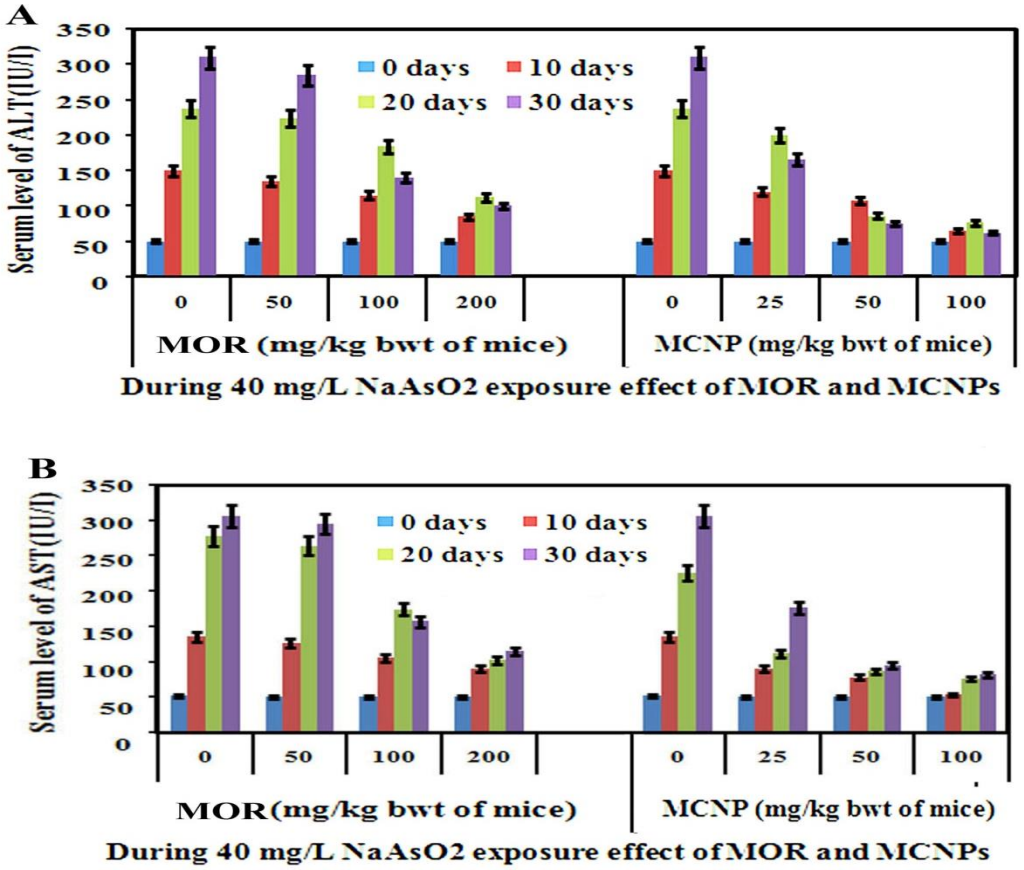

Figure 2: Effect of Morin (MOR) and MCNPs on arsenic induced elevation of ALT and AST. Morin (MOR) and MCNPs level with the duration of its exposure. Indicated doses of Morin (MOR) and MCNPs were treated during arsenic exposure. Data is one of the three representative experiments ± SD.

Arsenic exposure suppressed the increase of body weight, lowered the level of RBC, hemoglobin (Hb), platelet (PLT), HDL (good cholesterol) and increased WBC, LDH, kidney function markers such as uric acid and creatinine, lipid markers such as cholesterol, triglycerides, and LDL (bad cholesterol). High LDH level is the indication of tissue damage. Treatment of mice with 50mg/kg bwt MCNP and 200mg/kg bwt of MOR reversed the arsenic induced alteration in body weight, level of the blood parameters and kidney function markers **(Table 1).** Also, higher serum level of LDL, TG and TC, low level of HDL were significantly altered following treatment with 50mg/kg bwt MCNP and 200mg/kg bwt of MOR **(Table 1).**

Table 1: Effect of oral administration of MOR and MCNPs on haematological Parameters

Parameters	**Control Group**	**Arsenic (40 mg/L) treated mice**	**Arsenic + MOR (200 mg/kg) treated mice**	**Arsenic + MCNPs (50 mg/kg)**
Body weight gain (gm)	**0.61 ± 0.04**	**0.34 ± 0.05**	**0.46 ± 0.02**	**0.39 ± 0.04**
RBC : No. of cells (10^6/µL)	**7.5 ± 0.82**	**5.6 ± 0.54**	**6.5 ± 0.44**	**7.1 ± 0.38**
WBC : No. of cells (10^3/µL)	**12.4 ± 0.06**	**15.8 ± 0.22**	**14.1 ± 0.54**	**13.5 ± 0.42**
Hb (gm/dl)	**12.9 ± 0.42**	**10.1 ± 0.3**	**11.9 ± 0.23**	**12.5 ± 0.31**
PLT (10^3/µL)	**542 ± 34.2**	**422 ± 37.6**	**502 ± 26.7**	**526 ± 18.1**
LDH (U/L)	**391 ± 26.3**	**751 ± 41.6**	**481 ± 24.6**	**415 ± 21.8**
Uric acid (mg/dL)	**2.79 ± 0.62**	**4.66 ± 0.71**	**3.12 ± 0.22**	**2.88 ± 0.21**
Creatinine (mg/dL)	**0.45 ± 0.04**	**2.6 ± 0.16**	**1.1 ± 0.08**	**0.62 ± 0.08**
Cholesterol (mg/dL)	**135 ± 9.8**	**287 ± 25.2**	**159 ± 15.2**	**142 ± 8.5**
TG (mg/dL)	**82.1 ± 7.7**	**159 ± 11.8**	**91.4 ± 6.5**	**86.5 ± 5.8**
HDL (mg/dL)	**58.8 ± 3.9**	**36.6 ± 5.1**	**46.9 ± 2.7**	**53.6 ± 2.7**
LDL (mg/dL)	**74.2 ± 6.7**	**168.7 ± 11.8**	**88.1 ± 8.7**	**78.6 ± 5.5**

Phospholipid (mg/dL)	**44.5 ± 3.5**	**24.1 ± 1.3**	**35.1 ± 2.5**	**41.3 ± 2.1**

Values are expressed as mean ± SEM (n=3). P>0.05 when compared to normal group.

Effect of MOR and MCNP on survival of mice against arsenic induced mortality, arsenic deposition in different organs

Therapeutic benefit of MOR and MCNPs was assessed by measuring its survival effect on arsenic induced mortality in mice model. Following treatment of 0mg/, 25mg, 50mg and 100mg/kg of MCNPs, survival of mice were (a) 0%, 30%, 60%, and 80% respectively on day 40, (b) 20%, 45%, 70% and 90% respectively on day 30, (c) 40%, 60%, 85%, and 100% respectively on day 20, (d) 100% on day 10 against the mortality induced by 60mg/L of arsenic exposed via drinking water (Figure 3A). Similarly, percent survival resulted from treatment of 0mg/, 50mg, 100mg and 200mg/kg of MOR were (a) 0%, 0%, 15%, and 25% respectively on day 40, (b) 20%, 25%, 40% and 50% respectively on day 30, (c) 35%, 40%, 55%, and 70% respectively on day 20, (d) 100% on day 10 (Figure 3B).

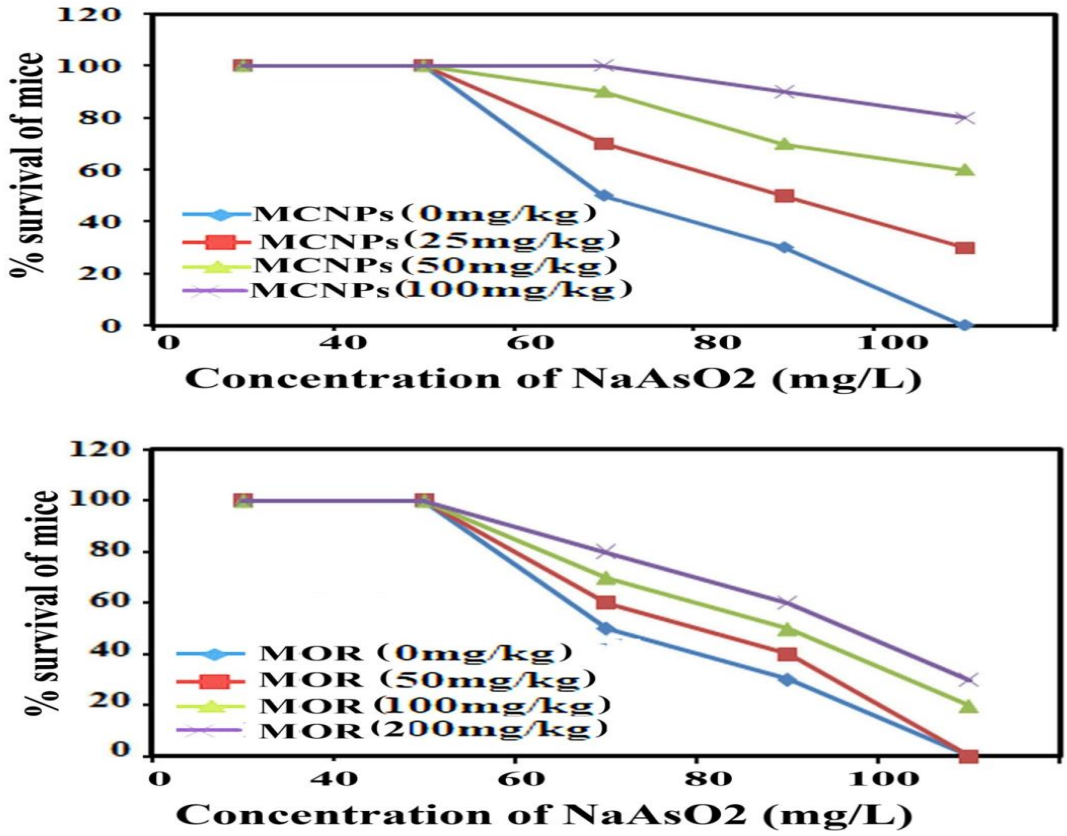

Figure 3: Effect of different concentrations of MOR and MCNPs against 60mg/L arsenic-induced mortality in mice on indicated days. Percent survival of mice following oral treatment of (A) MCNPs (0, 25, 50, 100 mg/kg bwt) and (B) MOR (0, 50, 100, 200 mg/kg bwt) in mice on every alternate day from the day 2 upto 30 days.

Table 2 shows the effect of MOR and MCNPs treatment on arsenic deposition in liver, kidney, brain, lung, heart and skin. Exposure to arsenic resulted in a significant increase in arsenic concentration in these organs. Arsenic deposition is found to be higher in liver than any other organs. Administration of MCNPs and MOR lowered the amount of arsenic deposited in these organs **(Table 2)**.

Table 2: Arsenic deposition in different organ

	Arsenic concentration in µg/g of tissue in 30 days					
	Liver	**Kidney**	**Cerebellum**	**Lung**	**Heart**	**Skin**
Arsenic, 40 mg/L	**139.3 ± 6.3**	**25.7 ± 1.7**	**11.6 ± 0.47**	**12.6 ± 0.35**	**11.4 ± 0.66**	**4.2 ± 0.26**
Arsenic + MOR (200 mg/kg)	**112.7 ± 6.5**	**17.3 ± 0.45**	**8.8 ± 0.21**	**8.9 ± 0.29**	**7.5 ± 0.41**	**1.3 ± 0.06**
Arsenic + MCNP (50 mg/kg)	**45.6 ± 2.5**	**3.6 ± 0.42**	**0.82 ± 0.06**	**1.5 ± 0.04**	**1.8 ± 0.11**	**0**

Values are expressed as mean ± SEM (n=3). P>0.05 when compared to normal group.

MCNPs suppress oxidative stress in mice liver

Treatment with MOR or MCNPs significantly prevented arsenic-induced ROS generation and increase of MDA level **(Figure 4A and 4B). Figure 4C**shows the change in ROS level as seen in confocal microscopy study using DCFDA (green) and change is same like Figure 4A.

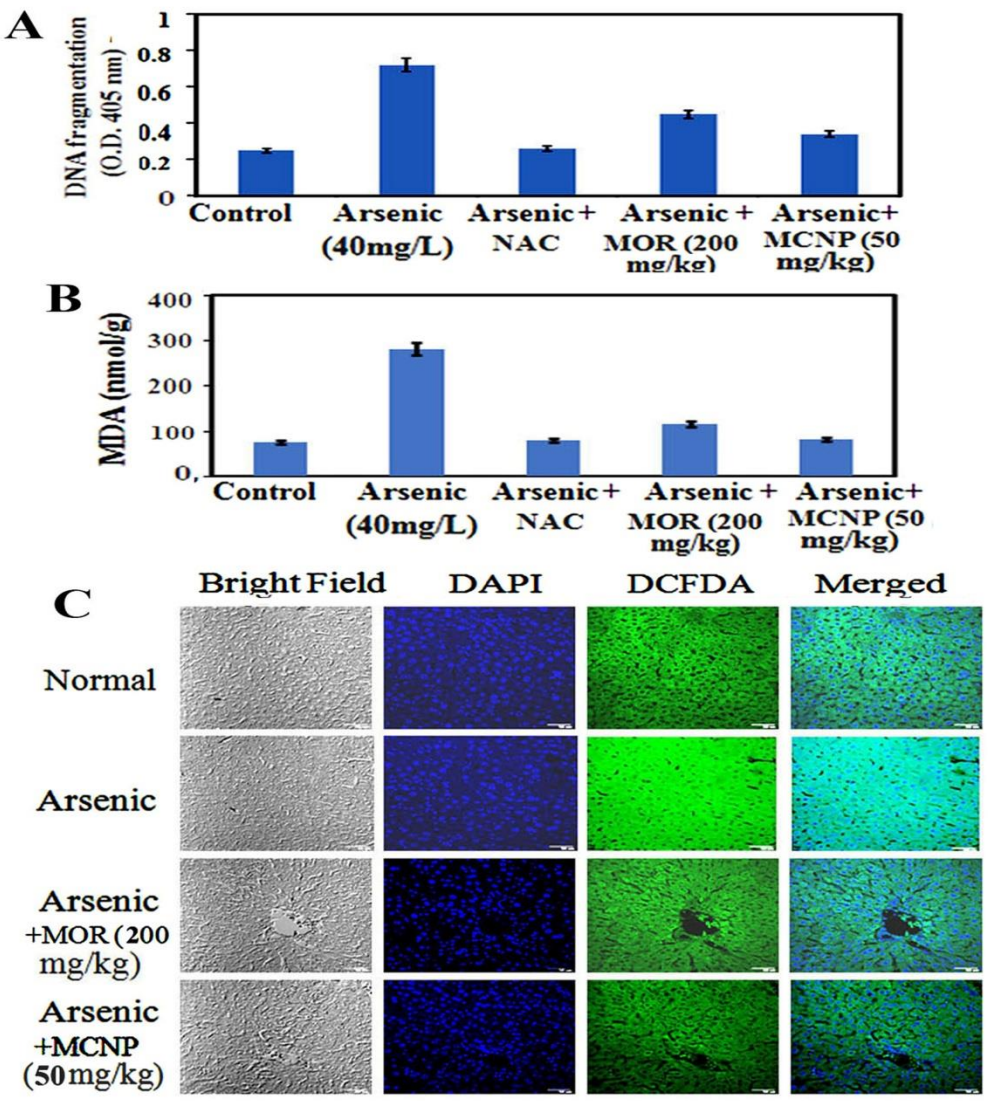

Figure 4: Effect of MOR and MCNPs on ROS generation and MDA level.

Mice exposed to arsenic via drinking water were treated with MCNPs (50 mg/kg bwt) and MOR (200 mg/kg bwt) orally on every alternate day and the level of (A) ROS, (B) MDA were determined. (C) ROS detection in liver tissues after staining with DAPI and DCFDA (green fluorescence) followed by Fluorescence imaging using confocal microscope.

MCNPs enhance the production of antioxidant factors in mice liver

Nrf2 activation induces *phase II detoxifying enzymes such as* glutathione (GSH), catalase (CAT), glutathione S-transferase (GST), hemeoxygenase-1 (HO-1) and NAD(P)H:quinone oxidoreductase 1 (*NQO1*), glutathione peroxidase (GPx), etc. against oxidative stress.SOD was up-regulated by MOR (200mg/kg) and MCNPs (50mg/kg) in arsenic exposed mice **(Figure 5A).** Catalase and

GSH level were low in arsenic group. It increased in the arsenic group receiving MCNPs **(Figure5B and 5C).** MCNPs treatment increased the level of nuclear Nrf2, GST, and GPx those were decreased due to arsenic exposure **(Figure 5D).** Also, Figure 5D shows that cytosolic Nrf2 and Keap1 markedly increased in arsenic group are lowered following MCNPs treatment. Similar findings were observed in the level of HO-1 and NQO1 **(Figure 5E).**Effect of 50mg/kg bwt MCNPs was same as that of 200mg/kg of MOR. This indicated MCNPs has a strong antioxidant capacity against arsenic-induced liver injury.

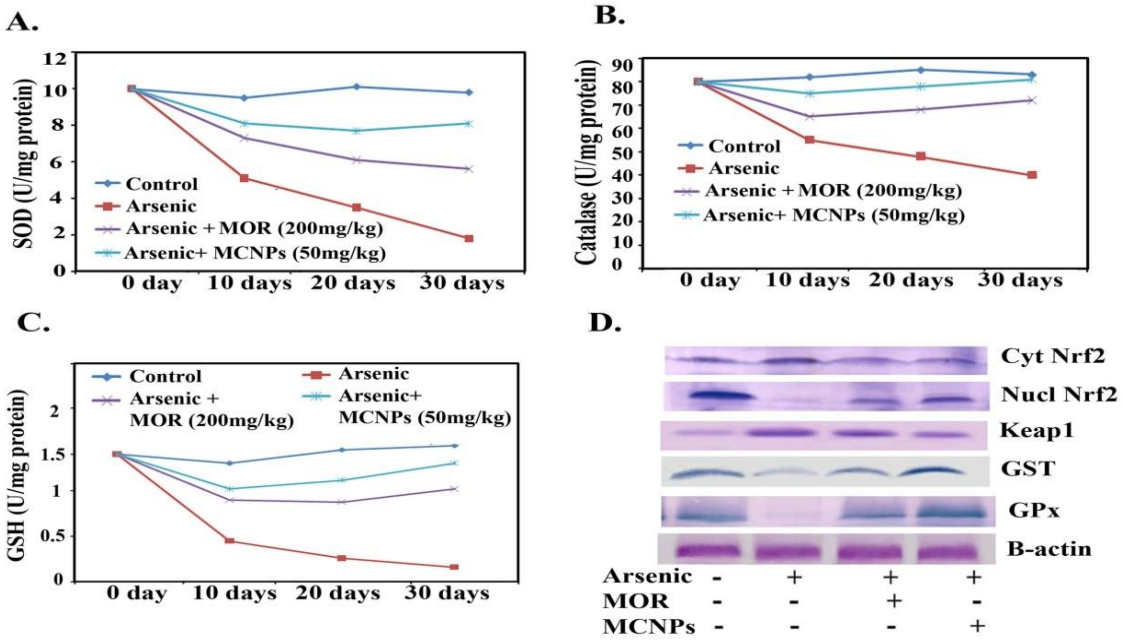

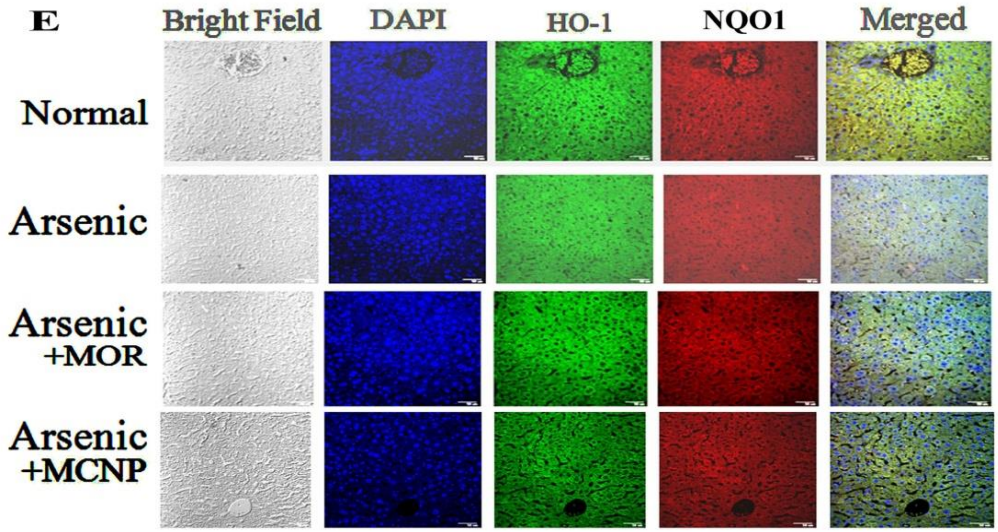

Figure 5: Effect of MCNPs and MOR on antioxidant factors. MCNPs (50mg/kg bwt) and MOR (200 mg/kg bwt) were treated orally in mice during its exposure to arsenic. The level of (A) SOD (B) catalase (C) GSH in the liver tissue lysate of arsenic was measured by using assay kits. (D) shows the effect of MCNPs and MOR on protein expression of cytosolic Nrf2, nuclear Nrf2, Keap1, GST, GPx (western blot analysis) in the liver tissue lysate. (E) Expression of HO-1 and NQO1 as seen in immunohistochemical analysis.

MCNPs inhibitapoptosis and improve histology of liver

To further investigate the role of MCNPs in As (III)–induced liver cells dysfunction, the expression of apoptosis related proteins was detected. Excessive ROS production by arsenic triggers cell death through apoptosis [130]. The apoptosis is associated with activation of pro-apoptotic Bax/Bak, Bad, release of cytosolic cytochrome C, and apoptotic protease activating factor-*1* (*Apaf-1*), stimulation of caspase-3 and caspase-9, activation of PUMA (p53 upregulated modulator of *apoptosis)* and DNA fragmentation [131].

Arsenic mediated enhancement of DNA fragmentation, active caspase-3/caspase-9, and cytosolic cytochrome C were suppressed by MCNPs in the liver tissue lysate **(Figure 6A and 6B).** Bax, Bak, Bad, Apaf-1, and PUMA were found to be suppressed in the liver tissue lysate of arsenic+MOR and arsenic+MCNP group in contrast to their higher level in arsenic group. Anti-apoptotic protein Bcl-2 suppressed by arsenic was enhanced following the treatment of MOR and MCNP **(Figure 6C).**

H&E staining of liver tissue sections was performed to evaluate the histopathological changes.

The livers of the nomal, only MOR and MCNPs treated groups showed undamaged hepatocytes in which normal looking sinusoids lined by Kupffer cells whereas exposure with arsenic showed severe injury characterized by diffused Kupffer cells, vascular changes, inflammatory cells infiltration**(Figures 6D).** Treatment of mice with MOR and MCNPs during arsenic exposureshowed minor or no hepatocellular damage, inflammatory cell infiltration, and no marked histopathological alteration were noticed. Treatment with MCNPs significantly alleviated chronic arsenic-induced deleterious effects.

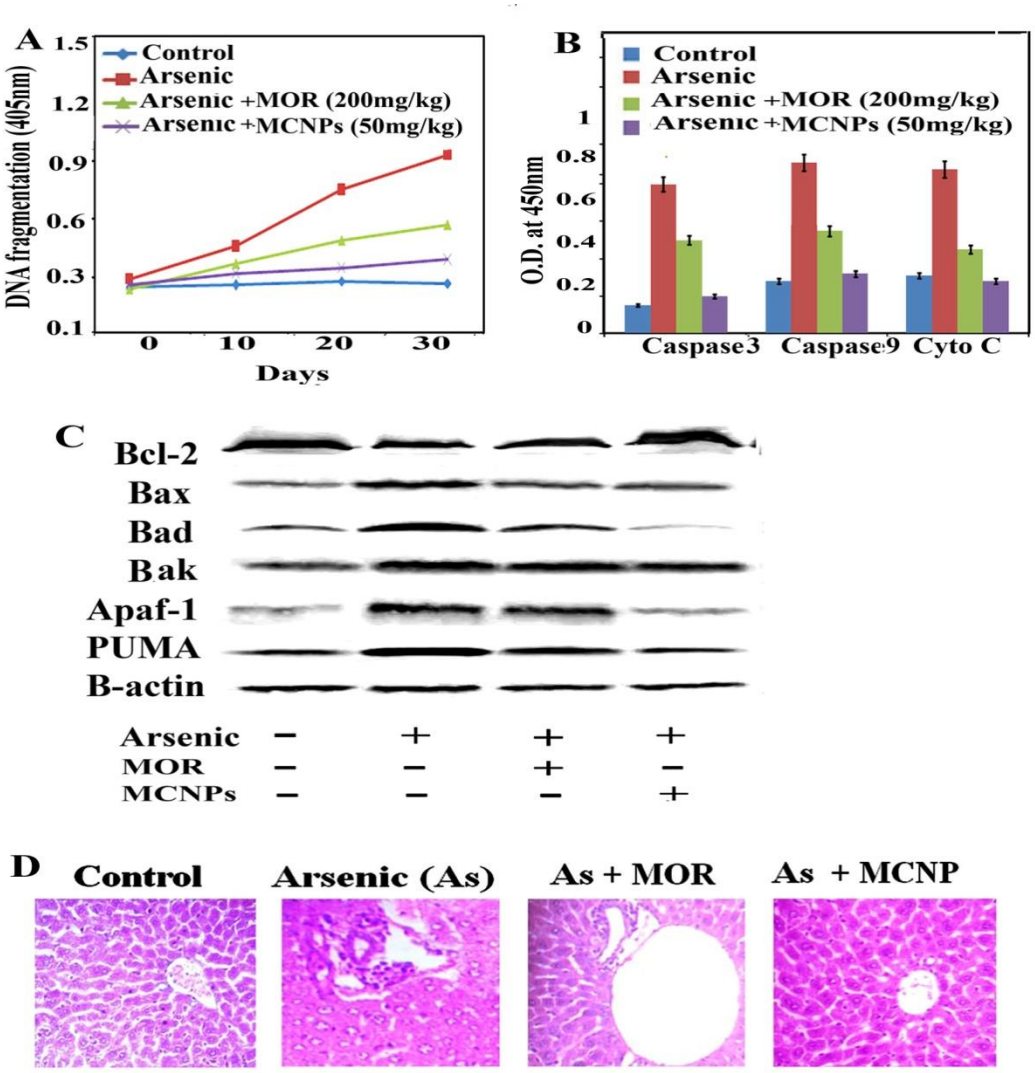

Figure 6: Effect of MCNPs and MOR on liver tissue apoptosis and histology. (A) Level of DNA fragmentation obtained using DNA fragmentation kit, (B) the level of active caspase-3, active caspase-9, and cytosolic cytochrome C obtained using respective colorimetric assay kits. (C) shows the effect of MCNPs and MOR on the protein expression (western blot analysis) of Bcl-2, Bax, Bad, Bak, Apaf-1 and PUMA in mice exposed to arsenic, (D) Architecture of liver tissue section following treatment without or with MCNPs and MOR in arsenic exposed mice.

.MCNPs suppressed arsenic induced inflammatory responses:

Dissociation of IkBα from NF-kB in cytosol leads to its translocation into (activation) nucleus resulting enhanced production of pro-inflammatory mediators [132]. During arsenic exposure, NF-kBp65 is highly activated with the release of high level of inflammatory cytokines.

Treatment of MOR and MCNPs attenuated the scale of these cytokines such as TNF-α, IL-1β and IL-6 elevated by arsenic **(Figure 7A).**NF-kBp65 and NF-kBp50, both the subunits of NF-kB activated in arsenic exposed mice are suppressed following the treatment of MCNPs or MOR (Figure 7B). Chronic arsenic exposure is also associated with the activation of NLRP3 inflammasome and the release of pro-inflammatory factors Caspase-1, IL-1b and IL-8 those cause pyroptosis. MCNPs alleviated the level of NLRP3 inflammasome that was elevated by arsenic and the level of Caspase-1, and IL-8 in liver tissue **(Figure 7B).**Downregulation of the expression of NF-kBp65 and NLRP3 by MOR and MCNPs in the liver tissue of arsenic exposed mice shown by confocal microscopy were depicted in **Figure 7C.**

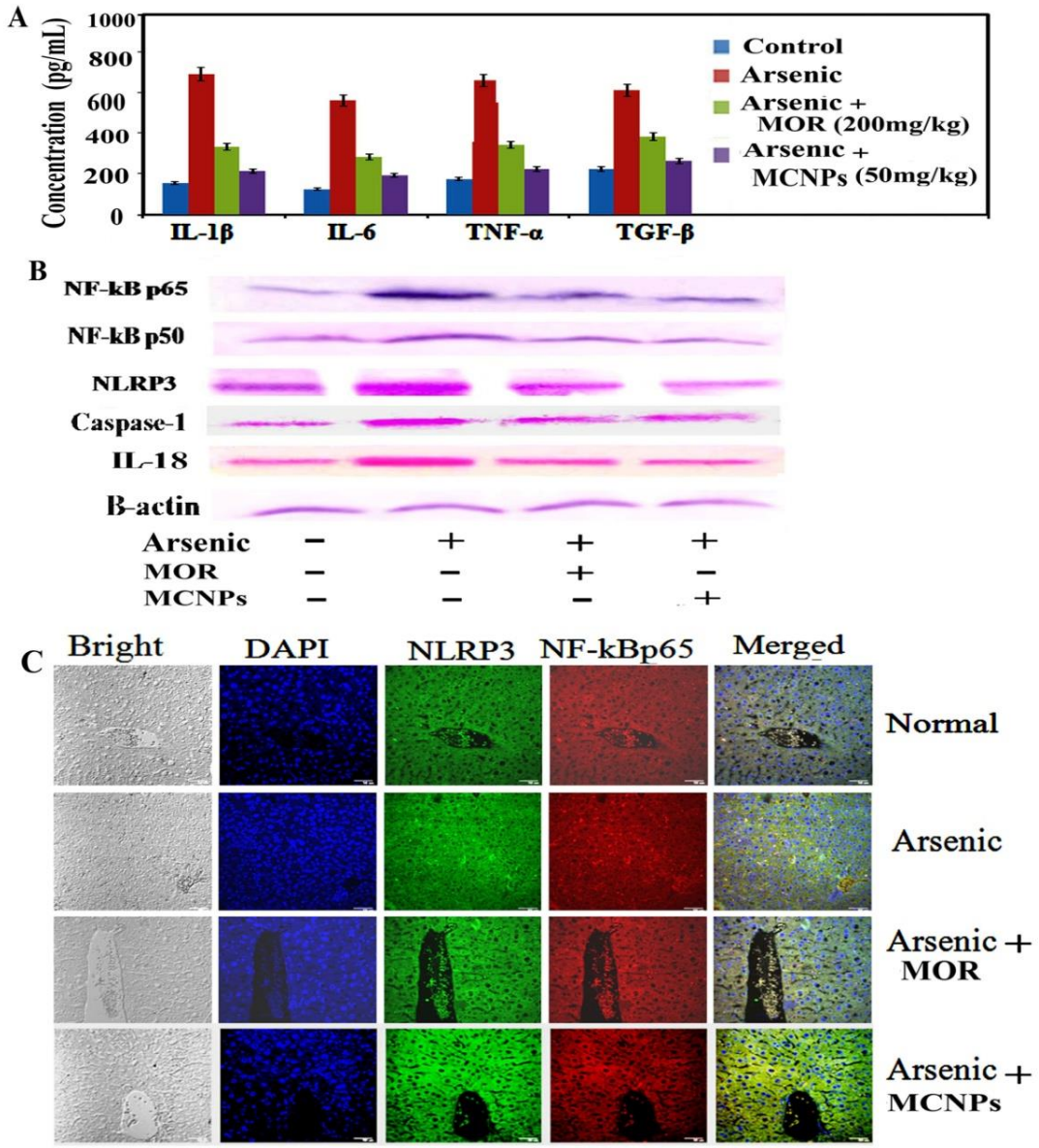

Figure 7: Effect of MCNPs and MOR on the level of (A) TNF-α, IL-β, IL-6, TGF-β in the liver tissue lysate of arsenic challenged mice as seen in ELISA analysis. Data are one of the three representative experiments ± SD. (B) shows the effect of MCNPs and MOR on protein expression of nuclear NF-kBp65 and NF-kBp50, NLRP3, Caspase-1, IL-18 (western blot analysis). (C) show the expression of NF-kBp65and NLRP3(confocal images) in arsenic exposed mice.

Tissue Distribution Study of MCNPs in Various Organs

After oral administration of single dose of MCNPs and MOR in mice for various time intervals, content of free morin in liver, spleen, lungs, kidneys, and serum were monitored by High-Performance Liquid Chromatography (HPLC). As shown in Figure 8A, morin content from MCNPs showed its different concentrations in the organs. Its highest concentration was found in the liver at 2h that gradually decreased with time and was low at 72h. Order of concentration of morin in different organs was liver> kidney≥spleen> lung>serum. Over time, the main trend of the concentration of morin in all organs was reduced slowly suggesting negligible or no accumulation in the tissues and a slow elimination of this compound. Amount of morin accumulated in the organs of free morin treated mice were about 4-5 times less compared to the MCNPs treatment. The trend of reduction of morin concentration in the organs was same as that of MCNPs (Figure 8B)

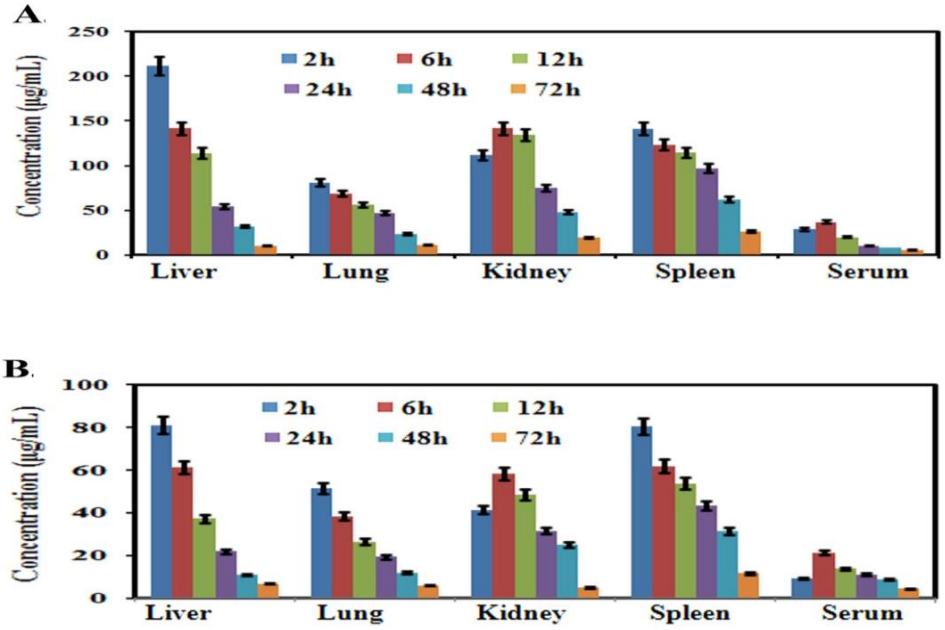

Figure 8: Tissue distribution studies of MCNPs and MOR in various organs.

Mean concentration of morin in liver, lungs, kidneys, spleen, and serum at 2, 6, 12, 24, 48, and 72 h after oral administration of single dose of (A) MCNPs and, (B) MOR (n = 3, mean ± SD) in mice.

Discussion:

The current research work shows that arsenic hazard causes hepatic injury. It increases thelevel of the liver function markers, alters the level of lipid profiles, and rises the arsenic accumulation in organs bypromoting the ROS production, inflammation and apoptosis. Supplementation of morin encapsulated chitosan (MCNPs) and morin (MOR) regularized the irregularitiescaused by arsenic. Effect of MCNPs is higher than free MOR.

Arsenic pollution has become a curse for human healthnot onlyin India but also in the globe. The major complications occur due to long term deposition of arsenic is liver damage as it increases ROS production like ethoxy, superoxide, hydroxyl, peroxyl and hydrogen peroxide radicals [132]. Many pathological events occur due to lipid peroxidation which is induced by the oxidative stress.High triglyceride (TG) level increases the risk of the diseases like Diabetes mellitus, obesity, chronic renal disease, and cardiovascular disorder. ROS attack the hepatocytes, stellate cells, Kupffer cells and their signaling mediators' interleukins, growth factorswhich ultimately acceleratehepatic fibrosis and cirrhosis [131]. The mecation expenses for liver damage are very costlyand also haveseveral side effects [132]. Therefore, there is urge in seraching alternative pathway of treatments nowadays. Polyphenols widely present in plants and food origin exhibit protective efficacy against various chronic diseases including liver disorderdue to their strong antioxidant and anti-inflammatory activity [133]. Some reports showed that the hepatoprotective activity of polyphenols like Silibinin/silymarin, quercetin, morin, genistein, Naringenin, resveratol, EGCG, curcumin, chlorogenic acid, berberine [134]. Also, some research articles established the fact that arsenic toxicity can be resolved by the potential application of polyphenols, EGCG, quercetin, lutein, grape seed extract, gallic acid, and tannic acid [134]. Several researchers reported the anti-oxidant and hepatoprotective effect of morin against hepatic damage induced by different drugs, chemicals [135, 136]. Protective efficacy of curcumin, quercetin and resveratrol NPs against liver injury are well documented [137, 138]. There are reports showed that Chitosan NPs also has protective role in the impairment of hepatic injury

caused by acetaminophen, alcohol, diethylnitrosamine (DEN), CCl4, and concanavalin A [139-142]. So all these previous study justified the hepatoprotective activity of MCNPs against arsenic induced hepatotoxicity. Improvement of normal liver architecture by MCNPs treatment in arsenic exposed mice is in harmony of the previous report [143, 144].

This study suggests that MCNPs may works as stronger antioxidant agents than free morin to ameliorate arsenic-induced hepatotoxicity caused by ROS generation. During arsenic exposure, ROS level is extremelyupliftedand the level of anti-oxidant enzymes and anti-oxidant factors are decreased. Increased level of ROS and MDA and decreased level of SOD, catalase, GSH, nuclear Nrf2, HO-1 and NQO-1 in the liver tissue lysate was reflected in the result. Several researchers have shown that arsenic induced hepatic injury results from excessive oxidative stress and DNA damage [116]. MCNPs significantly inhibit DNA damage and hepatic injury. Thus, the protective effects of MCNPs against arsenic toxicity are reflected in its ability to suppress ROS/MDA and activate Nrf2 and its downstream anti-oxidant enzymes SOD, catalase, HO-1, GPx etc. Identical effect was seen with MOR. But compare to MCNPs, MOR effect was much low. Findings of Hussein et al and Tzankova et al on hepatoprotective activity of quercetin, curcuminloaded nanoparticles through enhancement of these antioxidants support our data [143,145].Arsenic induced hepatic damage occurs through apoptosis [146].Due to arsenic exposuregroups ofpro-apoptotic proteins of Bax family, apoptosis inducer initiator protease caspase-9 and effector protease caspase-3, apoptosis triggering protein cytochrome C are activated and anti-apoptotic Bcl-2 protein is suppressed in mice [147]. Treatment of MCNPs prevented liver tissue damage by inhibiting apoptosis via alteration of the expression of above proteins regulating apoptosis.

Production of proinflammatory cytokines TNF-α, IL-1β, IL-6 via activation of NF-κB and/or inflammasome NLRP3 is the indication of inflammatory response [148]. Arsenic exposure triggered these pro-inflammatory factors which aggravate further tissue damage via its binding with the thiol groups of cellular proteins and ROS generation [132]. Elevated expression of NF-κB and its target cytokines TNF-α, IL-1β, and IL-6 in liver tissue confirms arsenic induced hepatotoxicity. MCNPs restricted the level of these inflammatory factors. Some evidences prove that morin can exert protective efficacy through inhibition of inflammation [138]. So our findings can be justified by these observations.

Some previous reports showed that liver tissue can absorb up to 250 nm of particle size, and better internalization was shown by spherical-shaped NPs [148]. MCNPs were spherical, 124.5nm in diameter, indicating the continuous release of MOR for 72h. All the important functional groups of MOR were conserved in its Chitosan-encapsulated form. MCNP showed significant inhibition (nearly 4 times higher) with respect to morin. Our data showed that effect of MOR (100 mg/kg) is analogus to MCNPs (25 mg/kg). This could be due to the increase in water solubility, bioavailability and sustained drug released from the nanocomposites.

MCNP treated mice along with arsenic showed more or less similar architecture of hepatic tissue of control. The data revealed that the hepatocytes arranged in cords radiating from the central vein. They are polygonal cells with pale vesicular nuclei and prominent nucleoli. Blood sinusoids were found as a network between the plates of hepatocytes converging towards the central vein. In contrast with the control the architect of the liver in arsenic exposed mice showed loss of cellular architecture, degeneration of hepatocytes, infiltration of inflammatory cells, dilated sinusoidal and focal necrosis (Figure 6D). Some hepatocytes showed early signs of apoptosis with fragmented nuclei, and hazy vacuolated cytoplasm. Apoptotic hepatocytes were also detected, showing nuclear and cytoplasmic condensation into deeply stained apoptotic bodies. When MCNP was administered with arsenic, liver sections appeared somewhat normal in histological architecture. Almost normal hepatocytesseparated by clear sinusoids were observed. Loss of cellular architecture, degeneration of hepatocytes, infiltration of inflammatory cells, dilated sinusoidal and focal necrosis showed the damage of liver by arsenic as compared to normal mice. Improvement of regeneration was seen by the well recovered hepatocytes separated by clear sinusoids in groups treated with MOR and MCNPs.

Recently, several nanoparticles have shown successful results to treat different kind of inflammatory diseases [149]. Polymeric nanoparticles size 50 and 200 nm gratify a faster and more oral absorption, can efficiently transport across the intestinal membrane, and mostly accumulate in the liver [150]. Small-sized nanoparticles (<5 nm) are filtered out by the kidneys.Spheres shaped nanoparticles are consumed by cells more easily than any other shaped nanoparticles and have received great attention. Natural polymers are biodegradability, biocompatibility, and economic and environmental friendliness. So it’shave more acceptances compared to the synthetic variety.

Previous report shows that oral treatment of Resveratrol, quercetin, curcumin and EGCG loaded Polymeric nanoparticles have higher water solubility, sustained release of the drug, better bioavailability and higher biodistribution efficacy compared to the pure drug [143-145]. Also, these nanoparticles can readily cross the intestinal barrier after their oral administration and therefore, it is effectively applied for oral drug delivery. Polyphenol-loaded polymeric nanoparticles can easily move through the membrane and be internalized by cells, give better absorptivity as compared to the pure drug [150]. Also, polymeric nanoparticles of polyphenols show better anti-inflammatory and antioxidant effects than free drug and strongly inhibit apoptosis, and lipid peroxidation [150]. These evidences strongly support the higher antioxidant, anti-inflammatory and anti-apoptotic effect of Chitosan encapsulated morin nanoparticles than free morin as observed in our study.

Conclusion:

Our study suggests that MCNPs showed better protective efficacy than MOR against arsenic-induced hepatotoxicity in mice. The greater hepatoprotective activity of MCNPs can be attributed by the increased solubility and bioavailability of MOR due to formulation of chitosan nanoparticle. The antioxidant, anti-inflammatory and antiapoptotic activities can be considered as key factors accountable for the hepatoprotective effect of MCNPs. The results showed that MCNPs suppressed ROS production and increased antioxidant potential. MCNPs also ameliorated inflammatory responses andapoptosis. Therefore, MCNPs may represent a potential therapeutic alternative to prevent liver tissue injury induced by arsenic exposure.

Chapter II:

Preparation and characterization of Morin, Vitamin E and β-cyclodextrin inclusion complex loaded chitosan nanoparticles (M-Vit.E-CS-CD NPs) and its hepatoprotective role on arsenic induced liver damage in murine model.

Introduction:

Cyclodextrins (CDs) are natural, cyclic oligosaccharides and non-toxic in nature, contain a hydrophilic outer surface as the hydroxyl groups are faced to the outward direction and a lipophilic central cavity due to the hydrogen and glycosidic oxygen bonds are facing inside the core. Therefore, cyclodextrin acts as a host, can form inclusion complex interacting through soft bonds with guest compound in the hydrophobic region without affecting the host framework structure [151]. Among three types of CDs, β-CD is commonly used because the size of the internal pocket of β-CD is appropriate for the guest's molecule with molecular weights 200-800 g/mol. However, β-CD is able to interact with different type of molecules in higher molecular weights by a specific moiety [152]. Several studies suggested that β-CD can enhance the drug loading efficiency of nanoparticles and decelerate the release of drugs.

Chitosan (CS), as a biocompatible and biodegradable polymer, has been heavily used in the nanoparticle formation. Chitosan has the ability of drug release in controlled and sustained way, good solubility in aqueous acidic solution [153]. Several researchers have reported the application of CS nanoparticles for the delivery of hydrophobic drugs [154, 155] along with hydrophilic protein [156, 157].

Morin hydrate (2′,3,4′,5,7-pentahydroxyflavone), a yellowish bioflavonoid, mainly obtained from fruits, stem, and leaves of Moraceae family members plant [158] prevents broad spectrum of disease pathologies including liver toxicity, diabetes, ischemia, cardiovascular anomalies, cancer, neurotoxicity and renal complications [159]. Several researches have shown that, Morin administration does not show any harmful outcome [160]. Besides, it is inexpensive and readily obtainable [161]. Morin exhibits protective effect due to its strong anti-oxidant efficacy and its distinct architecture helps to bind it with nucleic acids, enzymes and proteins [162]. Vitamin E is

a naturally available, fat-soluble antioxidant [163]. Its hepatoprotective activity results from its scavenging effect on ROS [164].

In arsenic induced liver injury serum level of asparatate amino transferase (AST), alanine amino transferase (ALT) and alkaline phosphatase (ALP) become uplifted [165]. Excess Reactive Oxygen Species (ROS) are generated due to arsenic intoxication in addition to quick attenuation of antioxidant enzymes such as catalase and superoxide dismutase (SOD) [166]. The leading ROS-affected pathways following arsenic exposure include Nrf2-antioxidant response element (ARE) signaling pathways [167]. Nrf2, a prime transcription factor in antioxidant system remains bound to kelch-like epichlorohydrin-associated protein1 (Keap1) in the cytoplasm [168]. Under oxidative stress or in response to antioxidant agents, Nrf2 is dissociated from Keap1 and translocated to the nucleus where it binds to the ARE motif and activates the production of numerous antioxidant enzymes and detoxification enzymes e.g. superoxide dismutase (SOD), Catalase (CAT), glutathione (GSH), glutathione-S-transferase (GST), GSH peroxidase (GPx), NADPH quinone oxidoreductase 1(NQO1), heme oxygenase-1 (HO-1) etc. to neutralize the ROS [169-171]. Excessive levels of ROS induce apoptotic signaling pathways. Therefore, the inhibition of apoptosis in the liver tissue is one of the indicators to explore the protective efficacy of drugs.

NF-κB is responsible for transcriptional induction of pro-inflammatory cytokines such as IL-1, IL-6, IL-12, TNF-α, chemokines and additional inflammatory mediators [172]. NF-κB also has a role in controlling the activation of NLRP3 inflammasomes. So, deregulated NF-κB activation is the sign of chronic inflammatory diseases. The elevated level of NF-κB and NLRP3 confirm the inflammatory responses in arsenic induced liver injury.

So, in the present study we have synthesized and characterized MOR-Vitamin E-β-CD inclusion complex loaded chitosan nanoparticles and evaluated its hepatoprotective role through measurement of inhibition of excessive ROS production, inflammation and apoptotic responses and improvement of anti-oxidant factors.

Materials and Methods:

Chemicals

Morin Hydrate (purity ≥ 99.0%), Chitosan (low MW, extrapure), dichloromethane (DCM), β-Cyclodextrin (β-CD), vitamin E (α-Tocopherol)and Sodium TPP were purchased from Sisco

Research Laboratories (Gurugram, India), and all primary and secondary antibodies were purchased from Sigma (USA) were purchased from Sigma-Aldrich, MO, USA. Assays kits for the detection of serum ALT, AST, AP, SOD, catalase, GPx, HDL, LDL, triglyceride (TG), total cholesterol (TC) were bought from ARKRAY Healthcare Pvt. Ltd (Surat, India). IL-1β, IL-6, TGF-β and TNF-α were measured by ELISA kits from R&D system (MN, USA). All other chemicals were available commercially and of a high degree of purity. Dulbecco's modified Eagle's medium (DMEM), Fetal Bovine Serum (FBS), penicicillin, streptomycin, neomycin (PSN) antibiotic, ethylenediaminetetraaceticacid (EDTA) and trypsin were bought from Gibco BRL (Grand Island, NY, USA). 3-(4, 5-Dimethylthiazol-2-yl)-2,5-diphenyltetrazolium bromide(45989,MTT-CAS 298-93-1-Calbiochem), DMSO were bought from Merck-Millipore. Tissue culture plastic wares were bought from Genetix Biotech Asia Pvt. Ltd. Zinc acetate was purchased from Sigma-Aldrich. HepG2 cell line was obtained from National Centre for Cell Science (NCCS), Pune.

Preparation of MOR-Vit.E-β-CD inclusion complex:

A particular amount of β-CD (15 mg/mL) was dissolved in deionized water in a glass tubecontaining a magnetic bar. To this solution, equivalent amounts of MOR and vitamin E (1:1 ratio) in 70 μL acetone were prepared and stirring for 16 h [172]. Stirring was allowed to evaporate acetone without a cap. The solution was stirred overnight until a clear solution was acquired. The solution was then centrifuged at 4000 rpm for 15 min, and a supernatant containing highly water soluble MOR-Vit.E-β-CD inclusion complexes was dried in a freeze dryer (DFU-1200, Tokyo Rikakikai Co., Ltd., Japan). The dried MOR-Vit.E-β-CD inclusion complexes were stored at 4˚C until further use.

Preparation of MOR-Vit.E-β-CD inclusion complex loadedchitosan NPs:

MOR-Vit.E-β-CD inclusion complex loaded chitosan NPs (M-Vit.E-CD-CS NPs) were synthesized by using the ionic gelation method. Briefly, a desired amount of chitosan dissolved in acetic acid (1%) was mixed with a certain amount of MOR-Vit.E-β-CD inclusion complexes solution at room temperature. After 5 min of stirring, TPP solution was added dropwise to the mixture to form nanoparticles. For the preparation of nanoparticles with highest encapsulation efficacy chitosan, MOR-Vit.E-β-CD inclusion complexes and TPP were used in 3:5:5 ratios respectively according to Bardania et al [173]. The solution of the prepared nanoparticles was

centrifuged at 10000 rpm for 10 min. To obtain the respective NP powder, M-Vit.E-CD-CS NPs pellets were lyophilized for three days and preserved at −20 °C.

Determination of MOR and Vitamin E encapsulation efficiency and drug-loading:

NPs (5 mg) were soaked in 5 ml of phosphate buffer for 30 min. The solution was centrifuged at 4000 rpmat 4˚C for 40 min, and the precipitate was washed twice with fresh solvent to remove the unconjugated drug. Using a UV spectrophotometer (JASCO V-730, Spectrophotometer, Tokyo, Japan) at λ_{max} values of 270 and 395 nm, the clear supernatant solution was analyzed for unencapsulated morin and vitamin E. Standard curves morin and vitamin E were obtained by plotting the concentration against the absorbances from 10 to 50 mg/ml.

The percentages of drug loading and entrapment efficiency were calculated by using the following formula:

Encapsulation efficiency (%) = (The total amount of drug released from the lyophilized M-Vit.E-CD-CS NPs /Amount of drug initially taken to synthesize the M-Vit.E-CD-CS NPs*)* × 100.

Drug loading (%) = (Amount of drug found in the lyophilized M-Vit.E-CD-CS NPs/Amount of lyophilized M-Vit.E-CD-CS NPs) × 100.

Particle Size Measurement:

A Zetasizer 3000 HSA (Malvern Instruments, U.K.) was used to measure particle size and distribution. Using 12 mm cells at 90 degrees and a temperature of 25 °C, differential light scattering (DLS) was used to determine the mean NP diameter. Before the tests, the NPs were diluted with double-distilled water, and 500 μL was loaded into the cuvette for DLS and polydispersity index readings.

Fourier transform infrared spectroscopy:

To identify the various functional group present in Morin, Chitosan, β-cyclodextrin, vitamin E and M-Vit.E-CD-CS NPs, FT-IR was performed. All the compound and synthesized NPs which was centrifuged and lyophilized eariler; and the powdered of all compound were analysed in the IR spectrum to interprete the presence of different functional groups using the Perkin Elmer FT-IR spectrometer (MA, USA), in the absorbance mode.

Atomic force microscopy (AFM):

5 µL of the samples (1 mM) were deposited onto a freshly cleaved muscovite Ruby mica sheet (ASTM V1 Grade Ruby Mica from MICAFAB, Chennai) for 5–10 minutes, and then the sample was dried by using a vacuum dryer. AAC mode AFM was performed using a Pico plus 5500 AFM (Agilent Technologies USA) with a piezo scanner with a maximum range of 9 µm. Micro-fabricated silicon cantilevers of 225 µm in length with a nominal spring force constant of 21–98 N m^{-1} from Nano sensors were used. Cantilever oscillation frequency was tuned into resonance frequency. The cantilever resonance frequency was 150–300 kHz. The images (256 by 256 pixels) were captured with a scan size between 0.5 and 5 µm at a scan rate of 0.5 lines per s. The images were processed by flatten using Pico view1.4 version software (Agilent Technologies, USA). Image analysis was done through Pico Image Advanced version software (Agilent Technologies, USA).

Transmission electron microscopy (TEM):

A freshly prepared solution of the M-Vit.E-CD-CS NPs in double distilled water was placed on a TEM grid (300-mesh carbon-coated Cu grid). The samples were allowed to dry in air at room temperature for a few hours before the measurements were recorded.

Differential scanning calorimetry (DSC) and X-ray powder diffraction (XRD):

The thermal and crystallographic characterization was performed by DSC and XRD respectively. Thermogravimetric analysis (TGA) was performed using a TGA Q500 system from TA Instruments Inc. under a N2 atmosphere from 0- 500 °C at a heating rate of 5 °C /min. Differential Scanning Calorimetry (DSC) was performed using a DSC Q200 RCS system from TA Instruments Inc. with refrigerated Cooling System. The sample was heated with constant ramp rate of 10 °C/min between -30 °C and 90 °C.

Nuclear magnetic resonance (NMR) spectroscopy:

2 mg of MOR, Vit.E, β-CD, chitosan was dissolved using different solvent according to their solubility. Then 1H NMR was recorded.

In vitro drug release studies:

M-Vit.E-CD-CS NPs was solubilized in phosphate-buffered saline (PBS) medium (1M, NaCl = 8 gm, KCl = 0.2 gm, Na_2HPO_4 = 1.44 gm, KH_2PO_4 = 0.24 gm were dissolved in double distilled

water and pH was adjusted to 7.4). To study the in vitro release kinetics M-Vit.E-CD-CS NPs (10 mg) was filled in the dialysis bag of cut off size 5 kDa, put in a 200 ml of PBS of pH 7.4 and stirred at 1 g for 4 days. 2 ml of the buffer solution was removed after a fixed time interval and replaced with fresh buffer. Using a UV-visible spectrophotometer (JASCO V-730 spectrophotometer, Tokyo, Japan) at 270 and 395 nm, respectively, the release of drugs has been tested. The experiments were repeated thrice, and the average values were evaluated.

Cell culture:

HepG2 (human hepatocellular carcinoma) cells were grown in DMEM with 10% fetal bovine serum and 1% pen-strep at 37˚C at 5% CO2 in a humid environment. After 60–70% confluency, cells were treated with arsenic for 24 h and cotreated without and/or with MOR, vitamin E, M-Vit.E-CD-CS NPs. Then MTT assay was done for cell survivability and ROS was measured by fluorometry assay with DCFDA. Cell imaging study was done using nuclear staining DAPI.

Animals:

Male BALB/c mice of 6-8 weeks weighing 20-22gms were procured from animal house division of our Institute (CSIR- Indian Institute of Chemical Biology, Kolkata) and fed with standard chow diets and drinking water. The animals were kept at 22−24 °C temperature, 50−60% humidity, and subject to light and dark cycles of 12:12 h. The research procedure conducted on animals was as per the recommendations of the CSIR-Indian Institute of Chemical Biology Animal Ethics Committee.

Dose selection of MOR, vitamin E and M-Vit.E-CD-CSNPs:

We have used the dose of the morin from the previous study [174]. And for the dose selection of vitamin E &M-Vit.E-CD-CS NPseach group of mice were treated with 0, 25, 50, 100 mg/kg body weight of vitamin E or 0, 10, 20, 40 mg/kg body weight of M-Vit.E-CD-CS NPs on every alternate day upto 28 days by oral gavage, after acclimatization for 7 days. AST and ALT were measured at different time intervals. Doses of vitamin E or M-Vit.E-CD-CS NPs those did not elevated the level of AST or ALT were selected for experimental study.

Experimental design:

The experimental plan of this study was as follows: Mice were exposed to arsenic (40mg/L) only via drinking water for 30 days [175]. Arsenic exposed mice were given orally 0, 50, 100, 200 mg/kg body

weight of MOR, 0, 25, 50, 100 mg/kg body weight of vitamin E and 0, 10, 20, 40 mg/kg body weight of M-Vit.E-CD-CS NPs. MOR, vitamin E and M-Vit.E-CD-CS NPs were given on every alternate day by suspending in 0.1% Tween 80 in PBS starting from day 2 to 28 days of arsenic exposure. Blood was drawn by tail vein puncture at different time points from each group of mice, for serum analysis. The mice were sacrificed after 30days and the livers sections were collected for histology and Western blot analysis. For biochemical testing, one part of liver was stored at -80◦C freezer, and the other part was cut and placed in a bottle containing 10% neutral-buffered saline for performing histopathological analysis the next day.

Measurement of serum ALT, AST, HDL, LDL, TG, TC, LDL, HDL, uric acid, creatinine, and MDA

Blood samples were obtained by tail-vein puncture and kept at 4˚C undisturbed o/n. Samples were centrifuged the next day(1100×*g*, 10 min, 4˚C) to obtain the serum from the experimental groups. Serum AST, ALT, ALP, HDL, LDL, TG, TC, SOD, GSH and catalase activities were calculated according to the instruction brochure provided with the commercial assay kits.

Assessment of arsenic deposition in organs:

Levels of arsenic in the tissue samples of As-exposed mice were measured by the method described previously [176].Briefly, liver and spleen samples were taken in a 15 ml polypropylene tube in the presence of 3 ml of nitric acid (61%). The tubes were capped properly and incubated at 80°C for 48 hrs, followed by cooling for 1 hr to room temperature. After cooling, 3 ml of hydrogen peroxide (30%) was added to each tube, followed by incubation at 80°C for 3 hrs. After suitable dilution of the digested materials with ultrapure water, levels of arsenic in the samples were determined by colorimetric method based on the reaction of As (III) with potassium iodate in acid medium to liberate iodine. This liberated iodine bleaches the orangish red color of Rhodamine B. Sample solution (1mL) obtained after digestion of the tissue was mixed with 2 mL of KIO_3 and 1 mL of HCl. And the mixture was shaking gently followed by addition of 0.1% Rhodamine-B. The solution was kept for 15 min. The absorbance was measured at 550 nm. The decrease in absorbance is directly proportional to the concentration arsenic (III).

Determination of ROS:

Liver samples (200 mg each) were homogenized (1:10 w/v) in Tris-HCl buffer (40 mM, pH = 7.4, 0◦C). One hundred mililiter of tissue homogenate was mixed with 1 ml of Tris-HCl buffer and 5 µl of 2,7-dichlorofluorescein diacetate solution (10 mM). The mixture was incubated for half an hour at 37˚C. Finally, the sample fluorescence intensity was measured using a spectrofluorometer at 480 and 525 nm wavelengths of excitation and emission.

Estimation of Lipid Peroxidation Levels in the Liver

The level of lipid peroxidation in liver tissues was measured as the amount of thiobarbituric acid reactive substances (TBARS) [177].Thiobarbituric acid reactswith MDA (malondialdehyde), a major lipid oxidation product to form a red product (TBARS) that can be detected colorimetrically at 532nm or fluorometrically at Ex/Em 532/553 nm. Briefly, supernatants of tissue lysate were mixed with equal volume of TCA-BHT (BHT = butylated hydroxytoluene) in order to discard proteins. BHT stops further sample peroxidation during experimental process. After centrifugation (1000 g, 10 min, 4°C), 200 ml of the resulting supernatant was mixed with 40 ml of HCl (0.6 M) and 160 ml of thiobarbituric acid (TBA) 20% dissolved in Tris. The mixture was heated at 80°C for 10 min, and after cooling at room temperature, the absorbance was read at 530 nm and TBARS values were calculated and expressed in nmol/mg protein.

Estimation of SOD, GSH, catalase:

Blood samples were obtained by tail-vein puncture and kept at 4˚C undisturbed o/n. Samples were centrifuged the next day(1109×*g*, 10 min, 4˚C) to obtain the serum from the experimental groups. Serum, SOD, GSH and catalase activities were calculated according to the instruction brochure provided with the commercial assay kits.

Histological evaluation:

The fixed liver tissues in 10% neutral buffered formalin (NBF) was embedded in paraffin, thinly sectioned, de-paraffinated and rehydrated using the standard histology procedure. Variouspathological changes were assessed by using hematoxylin and eosin stains. The damage scores were estimated by counting the morphological alterations in 10 randomly selected microscopic fields from six samples of each group and from at least three independent

experiments. Themorphological liver integrity was graded on a scale of 1 (excellent) to 5 (poor). Liver damage scores was adopted from the study of t'Hartet al. [178] and described as: 1. normal rectangular structure, 2. rounded hepatocytes with an increase of the sinusoidal spaces, 3. vacuolisation, 4. nuclear picnosis and 5. necrosis.

Assessment of serum cytokines:

Blood samples were isolated at different time points as mentioned above, and the serum levels of TNF-α, IL-1β, TGF-β and IL-6 were determined using the commercially available ELISA kit according to the manufacturer's instruction and guidelines (R&D Systems, MN, USA).

Tissue Distribution Study:

All mice were fasted overnight and were fed only water before the experiments. Standard stock solutions of M-Vit.E-CD-CS NPs (1 mg/mL) were prepared by dissolving the specific amounts of the drug in ethanol. After oral administration of M-Vit.E-CD-CS NPs mice were sacrificed at 2, 6, 12, 24, 48, and 72 h. Various tissues (liver, lung, kidney, spleen) were collected and washed with 0.9% NaCl to remove the extra blood and contents. After blotting them with filter paper, 1 mg equivalent from the tissues was weighed and homogenized in 1mL of 0.9% NaCl. Then, 100 µL of it was used as the tissue sample. Blood samples were drawn from the tail vein and coagulated for half an hour in an MCT tube. The blood samples were centrifuged at 2000 rpm for 10 min (4 °C), and serum was obtained from the supernatant. Then, 100 µL of the serum was used as the sample. Tissues were stored at −80 °C for further use [179].

Western blot analysis:

Dissected tissues frozen in liquid nitrogen were disrupted using homogenizer and RIPA lysis buffer and then centrifuged. Protein concentrations in the supernatant of tissue lysate were assessed using the Bradford method. 25µg of total protein from tissue homogenate was used for western blot analysis.SDS-PAGE was carried out on an acrylamide gel to separate the proteins, which were then transferred to a polyvinylidene difluoride membrane. The membrane is blocked with 10% skimmed milk or 5% BSA and incubated overnight with primary antibody of different proteins and β-actin (1:2000 dilution; Santa Cruz, CA, USA), and next day after washing the membrane 3 times with wash buffer, was incubated with the alkaline phosphatase conjugated secondary antibody (1:5000 dilution) for 2 h. At last, protein expressions were detected using NBT/BCIP solution.

Statistical analysis

All data from at least three experiments with replicates were expressed as mean standard deviation (SD). Using GraphPad Prism software (CA, USA), statistical significance and differences between control and five other treatment groups were analyzed using a one-way analysis of variance.

Results:

Characterization of M-Vit.E-CD-CS NPs:

MOR-Vit.E-β-CD inclusion complex loaded chitosan NPs (M-Vit.E-CD-CS NPs) prepared by two steps and were characterized. Fourier Transform IR (FTIR) exhibits the compatibility between MOR-Vit.E-β-CD inclusion complex encapsulated CS nanoparticle (Figure 1A). The FT-IR spectrum covers the range from 4000 cm^{-1} to 400 cm^{-1}. The notable peaks attributed for MOR, vitamin E, β-CD, chitosan, and M-Vit.E-CD-CS NPs validate the existence of their distinct functional groups. The strong peak at 3400 cm^{-1} signify O-H (stretching), and a absorption band at ~1600 cm^{-1} indicate the existence of alkene (C=C) groups, and a sharp peak observed at ~1180 cm^{-1} denoted C-OH (stretching) in MOR, vitamin E, β-CD and chitosan. The M-Vit.E-CD-CS NPs shows a band at 3400 cm^{-1}, which assigned that the hydroxyl groups of MOR, vitamin E, β-CD and CS are preserved. One more short hump at 1640 cm^{-1} and 1150 cm^{-1} implies the protection of the alkene (C=C) and ester (C=O) groups and C-OH bond of MOR, vitamin E, β-CD and chitosan in the M-Vit.E-CD-CS NPs.The DLS data shows that size of M-Vit.E-CD-CS NPs is 178±1.5 nm as shown in the Figure 1B, with the polydispersity index (PDI) value of 0.18. M-Vit.E-CD-CS NPs zeta potential value is -22.4±0.31 mV, which have a propensity to balance NPs' suspension. Atomic force microscopy (AFM) and Transmission Electron Microscopy (TEM) show that the outward topology of M-Vit.E-CD-CS NPs is spherical, and they are systematically divided without conglomeration. The size of M-Vit.E-CD-CS NPs ranges within 100-200 nm (Figure 1C& 1D).

The encapsulation efficacy of M-Vit.E-CD-CS NPs for MOR is 78±2.5% and for vitamin E 73±1.8%. Earlier report suggests that the NPs with spherical shape show high level of drug encapsulation efficacy. The drug loading efficacy of M-Vit.E-CD-CS NPs for MOR is 58±3.1% and for vitamin E 42±1.5% (Figure 1E). The in vitro drug release kinetics of M-Vit.E-CD-CS NPs (Figure 1F). 60% MOR and 52% vitamin E are released from the nanoparticles in 24 h. A

prolonged release of MOR and vitamin E were monitored upto 4 days, but the highest release is detected at 72 h which was 82.5% for MOR and 71.8% for vitamin E.

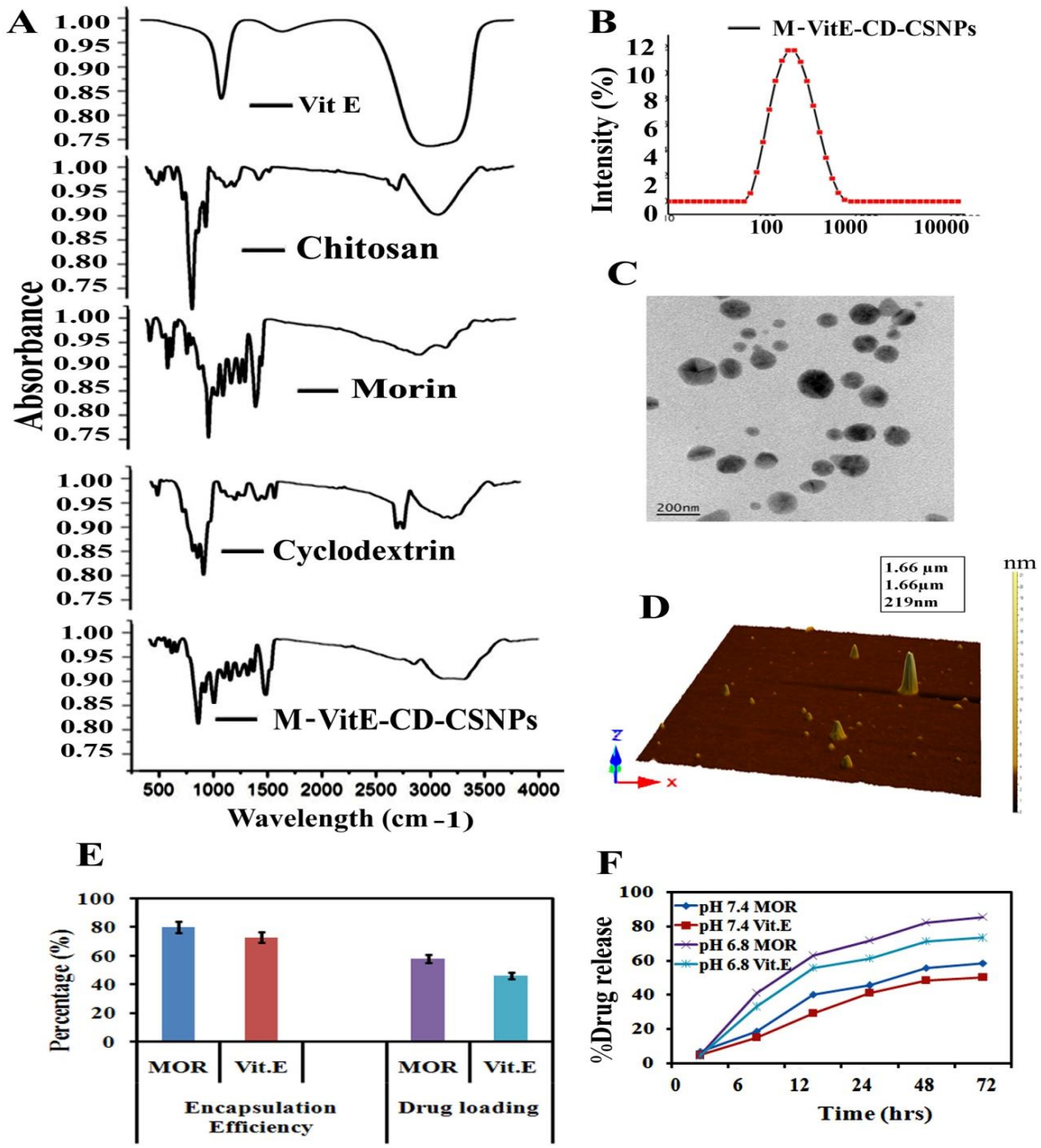

Figure 1: Characterization of Morin, vitamin E and β-CD inclusion complex loaded Chitosan nanoparticles. (A) Fourier transform infrared spectroscopy (FTIR) spectra of Morin, vitamin E, β-CD, chitosan, and M-Vit.E-CD-CS NPs (B) Particle size distribution from differential light scattering (DLS) with M-Vit.E-CD-CS NPs. (C) TEM images of M-Vit.E-CD-CS NPs. (D) M-Vit.E-CD-CS NPs particle surface topology determination using atomic force microscopy

(AFM). The acquired images were analyzed using scanning probe microscopy (SPM) tools for laboratory study. (E) Encapsulation efficiency percentage and drug-loading percentage of M-Vit.E-CD-CS NPs. (F) Percentage of release of Morin from M-Vit.E-CD-CS NPs over a time period of 0−72 h. Result is the mean ± standard deviation (SD) from triplicate independent experiments.

^{1}HNMR was recorded for MOR, Vit.E, β-CD, chitosan and M-Vit.E-CD-CS NPs (Figure 2A). And the results showed that in nanoparticles there is no significant peak of MOR and vitamin E. Only the peak of chitosan and cyclodextrin were observed. That again proved the successful encapsulation of the drug in the cycodextrin cavity.

TGA data showed that the % weight loss of NPs from 235°C (Figure 2B & C). In the case of NPs, the DSC thermogram showed an endothermic peak at 84.33°C (Figure 2D) which is quite similar with the Tg values of chitosan nanoparticles reported in the literature [180]. That indicated the incorporation of the M-Vit.E-CD inclusion complex in polymer matrix of chitosan. XRD spectra were recorded for the nanoparticles and it revealed the loss of crystalline character of the NPs as no sharp peak was observed (Figure 2E). This indicated that due to formation of the nanoparticles the crystallinity of the used compounds has been lost. And the XRD value was consistent with the results obtained from DSC studies.

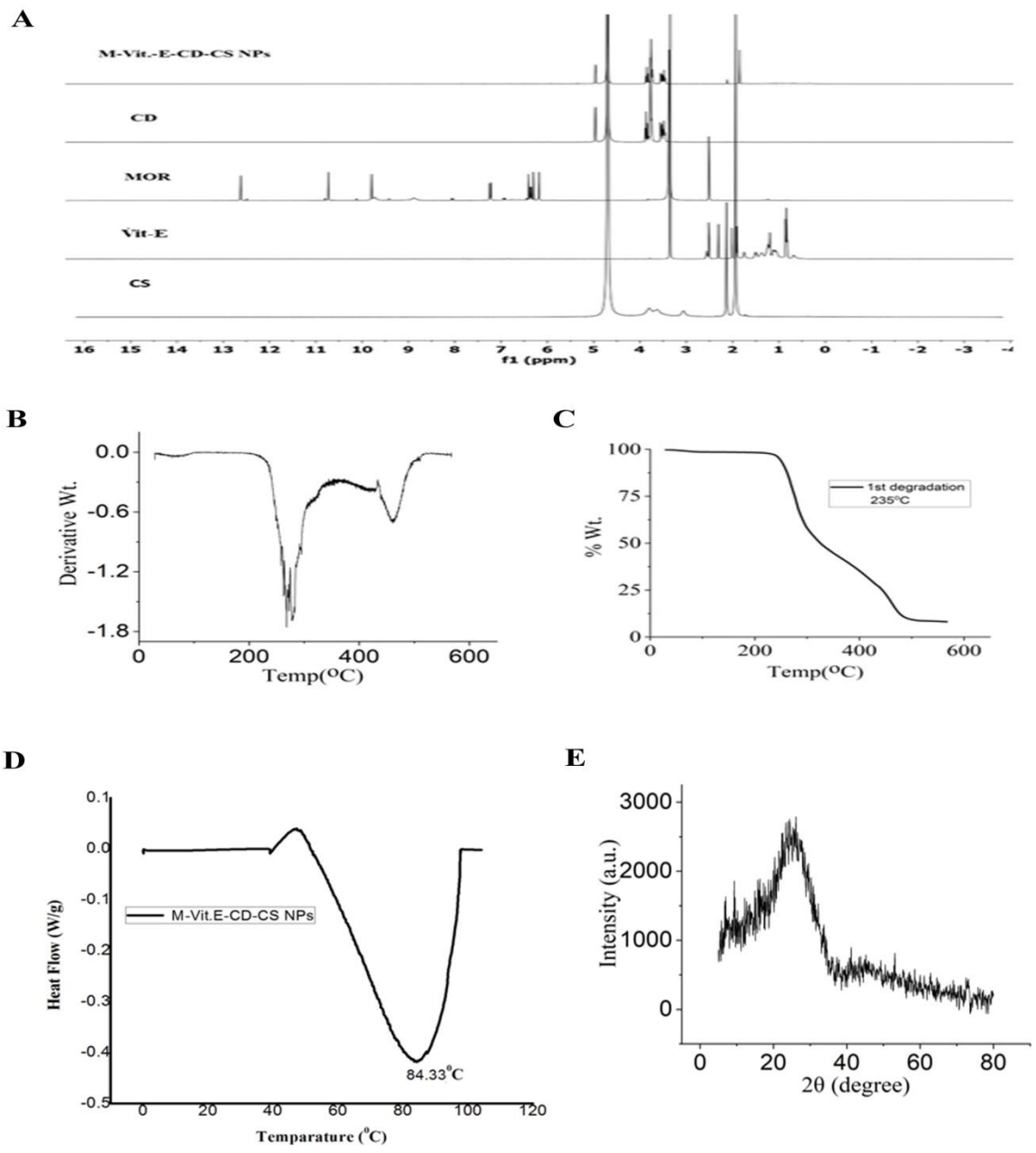

Figure 2: (A) 1HNMR spectra of MOR, Vitamin E, β-CD, Chitosan and M-Vit.E-CD-CS NPs. (B) & (C) Thermogravimetric analysis (TGA) was performed using a TGA Q500 system from TA Instruments Inc. under a N2 atmosphere from 0- 500 ℃ at a heating rate of 5 ℃ /min. (D) Differential Scanning Calorimetry (DSC) was performed using a DSC Q200 RCS system from TA Instruments Inc. with refrigerated Cooling System. The sample was heated with constant ramp rate of 10 ℃/min between -30 ℃ and 90 ℃.

Effect of MOR, Vitamin E andM-Vit.E-CD-CSNPs on arsenic treated HepG2 cells:

The mortality rate of cells due to arsenic exposure was analyzed by MTT assay. The cells were treated with different concentration of arsenic (5, 10, 20, 30, 40 µg/mL) upto 24h and then the percentage cell death was evaluated (Figure S1).

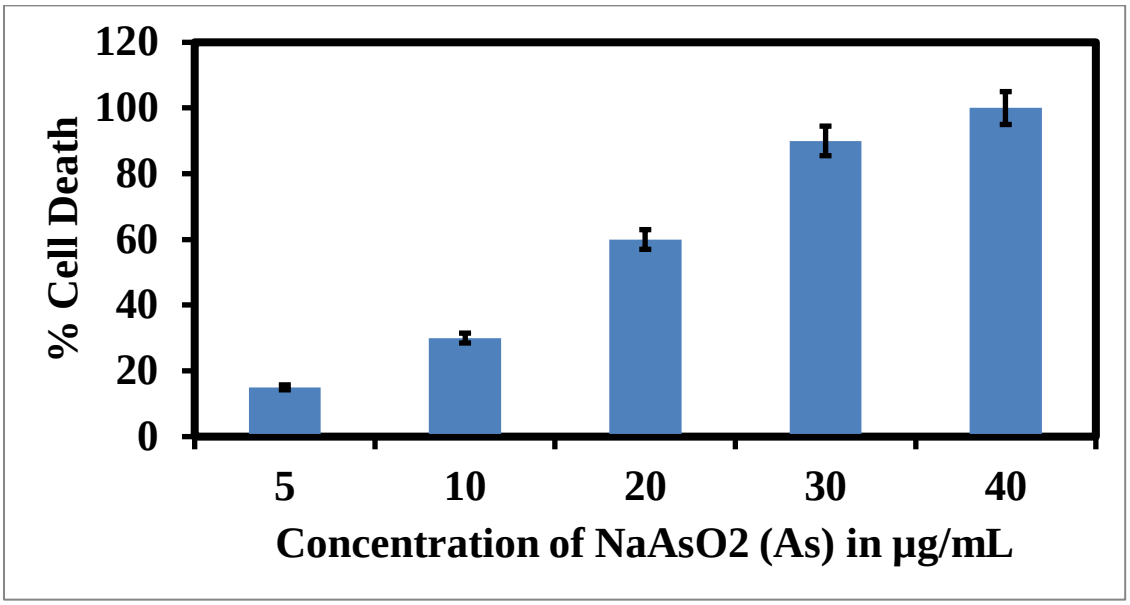

HepG2 (human hepatocellular carcinoma) cells ($1x10^6$ cells/mL) were treated with different concentrations of sodium arsenite ranging from 5 to 40µg/mL for 24 h. % cell death values were calculated from an MTT assay. Results presented here are one of the three representative experiments ±S.D.

To further investigate the role of MOR, vitamin E and M-Vit.E-CD-CS NPs in As (III)–induced liver cells dysfunction, the percentage cell survival was detected in HepG2 cell line. The result showed that there was a decrease in percentage of cell survivability with the treatment of arsenic which increased with the treatment of MOR, vitamin E and M-Vit.E-CD-CS NPs (Figure 3A).

ROS generation triggers cell death. So, ROS level was studied in arsenic cotreated with MOR, vitamin E and M-Vit.E-CD-CS NPs HepG2 cells fluorometrically. Increased ROS level was observed with treatment of arsenic which was altered following the treatment of MOR, vitamin E and M-Vit.E-CD-CS NPs (Figure 3B). This result also indicated that the effect of M-Vit.E-CD-CS NPs was higher than MOR and vitamin E.

DNA fragmentation is the indication of cell death.So, we investigated DNA fragmentation level induced by arsenic in HepG2 cells and the effect of MOR, vitamin E and M-Vit.E-CD-CS NPs on it. Level of fragmented DNA increases with arsenic treatment and decreased with the treatment of MOR, vitamin E and M-Vit.E-CD-CS NPs in HepG2 (Figure 3C). Similar rise in DNA fragmentation like ROS level was observed. And the effect of M-Vit.E-CD-CS NPs was comparable the ROS-inhibitor NAC. Also the noticeable part of this study was only M-Vit.E-CD-CS NPs on the hepG2 cell line did not affect the survivability of the HepG2 cell line.

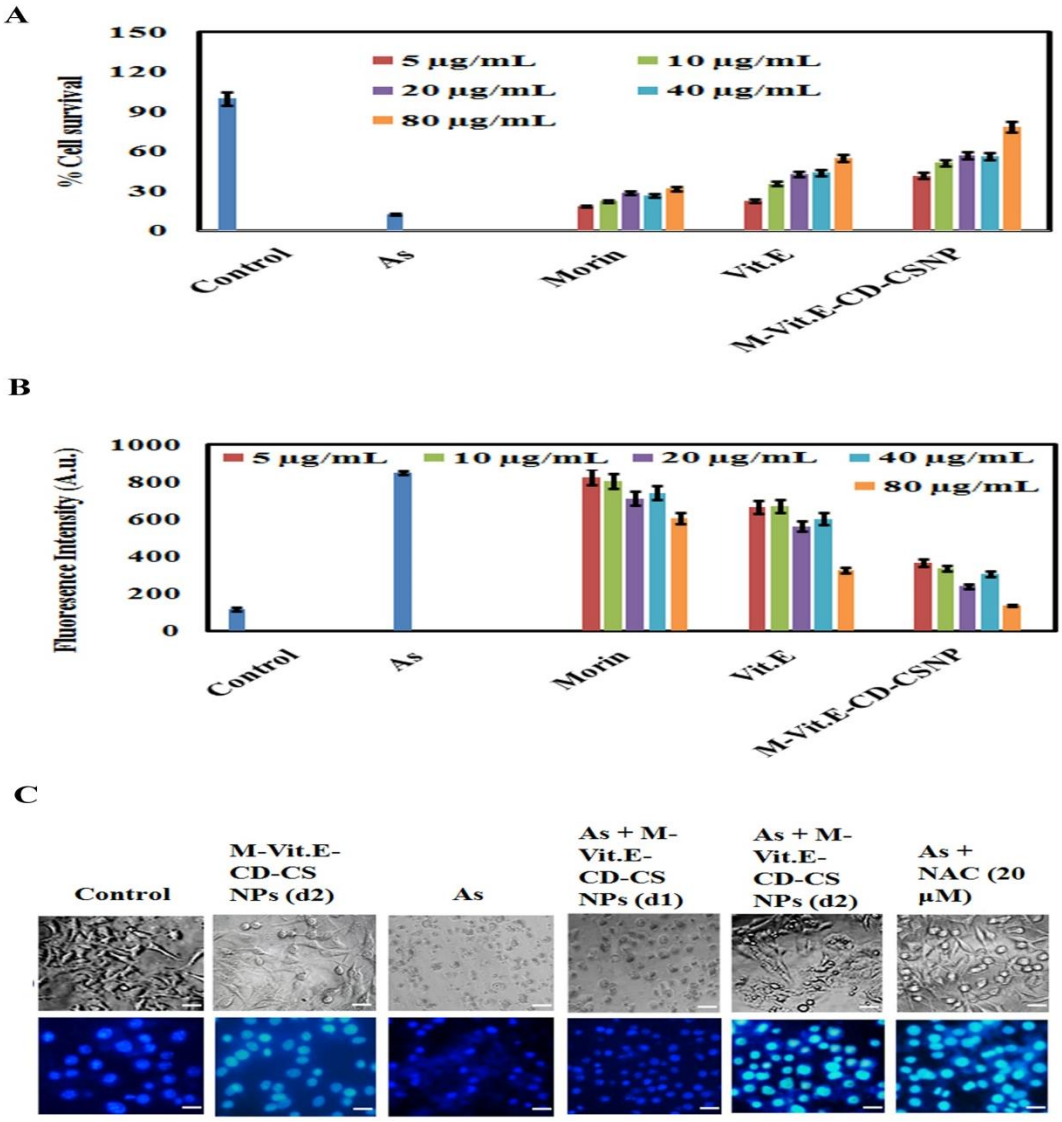

Figure 3: Effect of MOR, vitamin E and M-Vit.E-CD-CS NPs on arsenic treated HepG2 cells. (A) % cell survivability was measured by MTT assay. (B) ROS level was detected by fluorometrically. (C) Cell morphology was analysed using nuclear staining DAPI and bright field.

Effect of MOR, Vitamin E and M-Vit.E-CD-CSNPs on liver function markers, changing body weight, hematological parameters, kidney function markers and lipid profiles

A *non-poisonous* dose of MOR was 200 mg/kg as reported earlier [174]. Different doses of vitamin E and M-Vit.E-CD-CS NPs were administered in mice orally and the effect of them on the serum level of AST and ALT were measured. On every alternate day upto 50 mg/kg of vitamin E and 20 mg/kg of M-Vit.E-CD-CS NPs given orally for 30 days did not elevate the serum level of ALT and AST (Figure S2 & S3). Although, the serum level of ALT and AST uplifted following the treatment of 100 mg/kg body weight of vitamin E and 40 mg/kg body weight of M-Vit.E-CD-CS NPs. So, the effect of MOR, vitamin E and M-Vit.E-CD-CS NPs against arsenic intoxification was studied using the highest doses 200 mg/kg, 50 mg/kg and 20 mg/kg respectively.

S1:

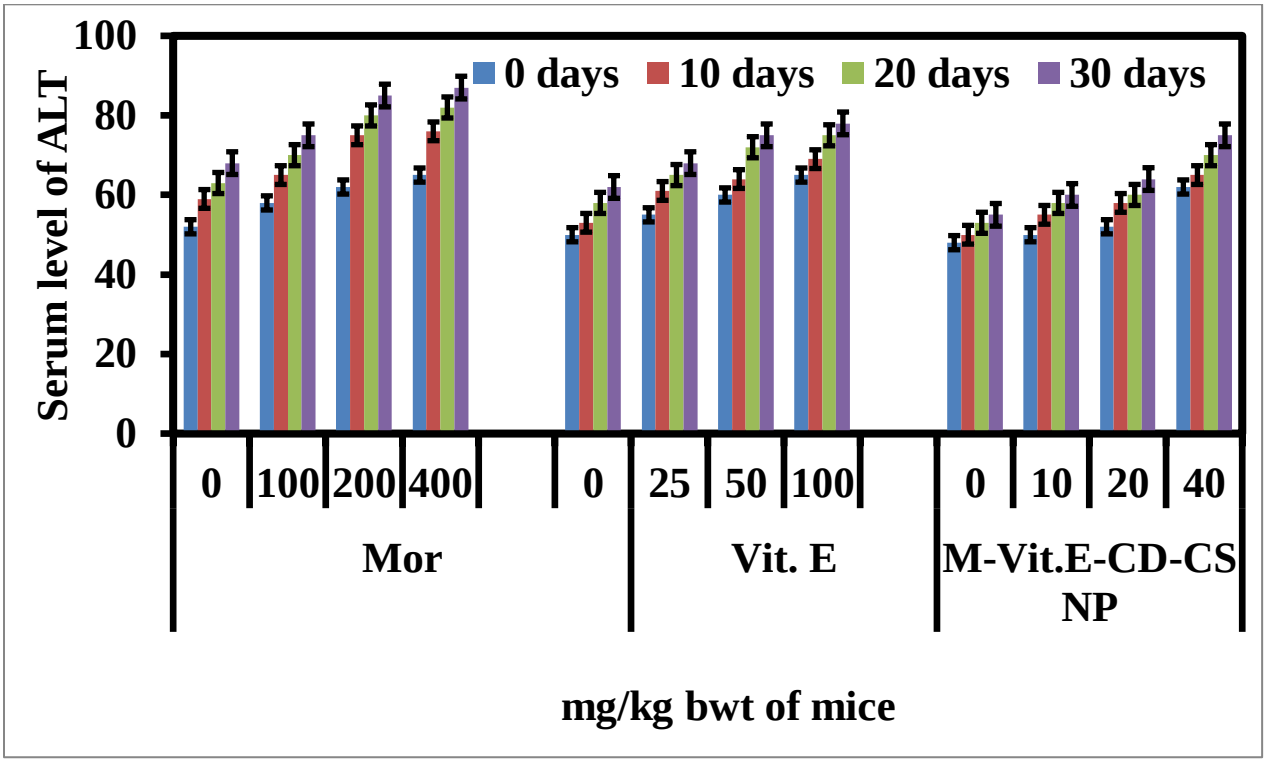

S3:

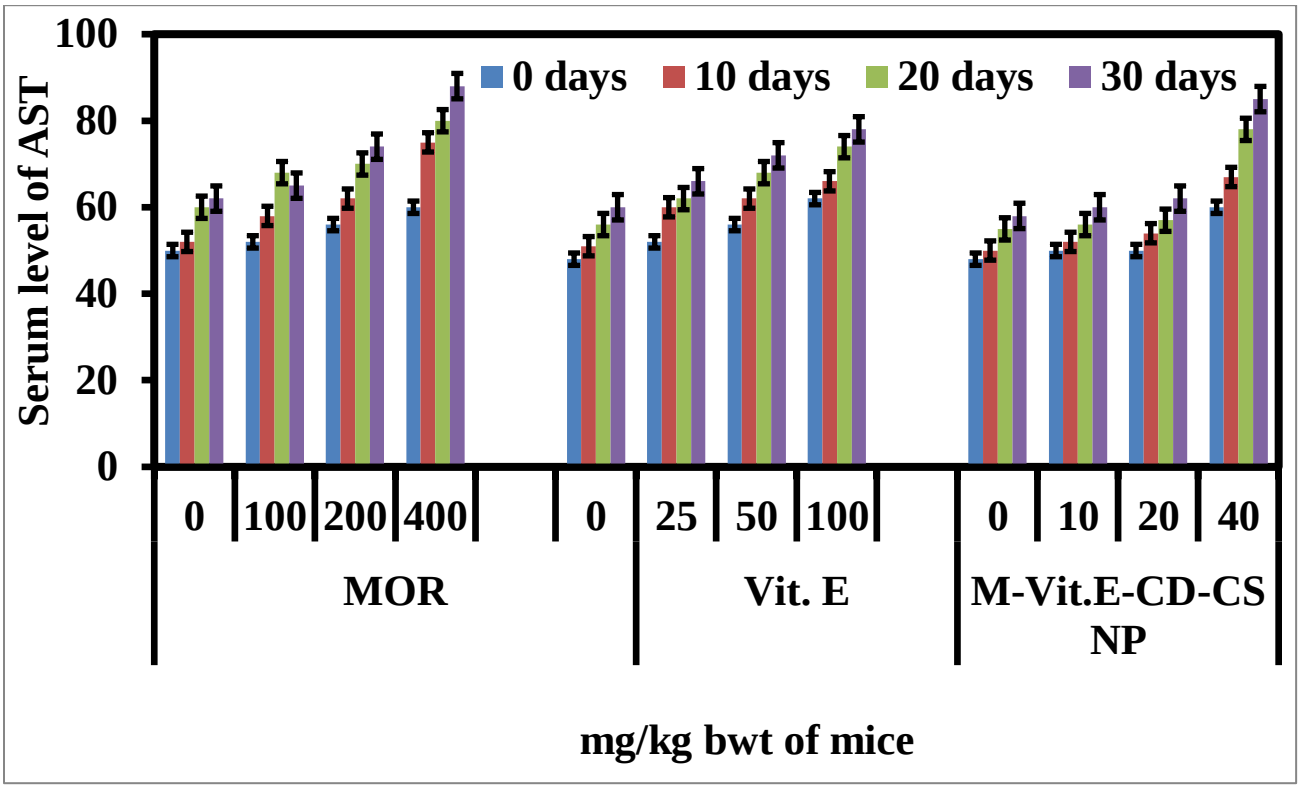

Fig S2 and S3: Effect of Morin (MOR), vitamin E and M-Vit.E-CD-CS NPs on liver function markers (ALT and AST). Different dosage of Morin (MOR), vitamin E and M-Vit.E-CD-CS NPs were orally given to the normal BALB/c mice and the serum level of ALT and AST were measured. Data is one of the three representative experiments ± SD.

We have taken dose of arsenic 40 mg/L as per our previous report [181]. Serum level of AST and ALT elevated gradually in arsenic induced mice (40 mg/L). Treatment of MOR (50, 100 and 200 mg/kg bwt), vitamin E (10, 25, and 50 mg/kg bwt) and M-Vit.E-CD-CS NPs (5, 10 and 20 mg/kg bwt) on every other day in the time of arsenic exposure dose dependently reduced the level of AST and ALT as shown in the Figure 4Aand 4B. The optimum effect was observed with 20 mg/kg M-Vit.E-CD-CS NPs, 200 mg/kg bwt of MOR and 50 mg/kg bwt of vitamin E. Thus, potency of M-Vit.E-CD-CS NPs was nearly 10 times higher than MOR and and 2.5 times higher than vitamin E.

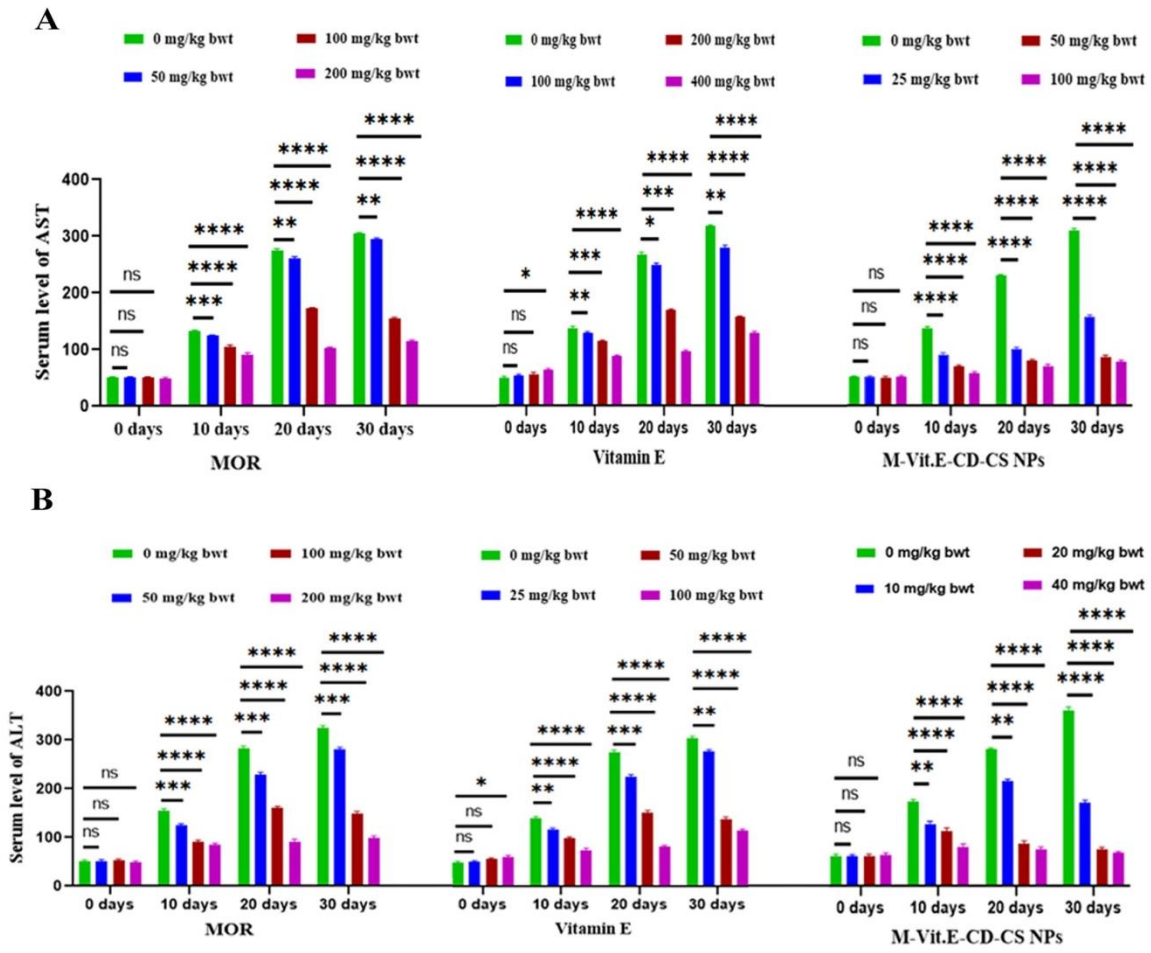

Figure 4: Effect of MOR, vitamin E and M-Vit.E-CD-CS NPs on arsenic induced elevation of (A) ALT (B) AST.

During arsenic exposure body weight of mice decreased along with the RBC level, platelet (PLT), hemoglobin (Hb) and HDL (High-density lipoprotein) also reduced and WBC (white blood cells), LDH (lactate dehydrogenase), kidney function markers e.g urea, uric acid and creatinine, lipid markers e.g cholesterol, triglycerides, and LDL (low density lipoprotein) became uplifted. Elevated level of LDH is suggested tissue damage. Treatment of mice with 20 mg/kg bwt M-Vit.E-CD-CS NPs, 200mg/kg bwt of MOR and 50 mg/kg bwt of vitamin E inverted the arsenic promoted transformation in body weight, level of the kidney function markers and blood parameters (Table 1). In addition, following the treatment with 20mg/kg bwt M-Vit.E-CD-CS NPs, 200mg/kg bwt of MOR, and 50 mg/kg bwt of vitamin E increased serum level of LDL

(Low-density lipoprotein), TG (Triglyceride) and TC (Total cholesterol), moderate level of HDL were remarkably changed (Table 1).

Table 1: Effect of oral administration of MOR and M-Vit.E-CD-CS NPs on haematological Parameters

Parameters	Control Group	Arsenic (40 mg/L) treated mice	Arsenic + MOR (200 mg/kg) treated mice	Arsenic + Vitamin E (50 mg/kg) treated mice	Arsenic + M-Vit.E-CD-CS NPs (20 mg/kg)
Body weight gain (gm)	**0.52 ± 0.06**	**0.29 ± 0.03**	**0.45 ± 0.04**	**0.39 ± 0.02**	**0.49 ± 0.03**
RBC : No. of cells (10^6/µL)	**8.1 ± 0.53**	**5.2 ± 0.35**	**6.8 ± 0.27**	**6.1 ± 0.33**	**7.5 ± 0.41**
WBC : No. of cells (10^3/µL)	**12.6 ± 0.13**	**16.2 ± 0.31**	**15.1 ± 0.24**	**15.8 ± 0.41**	**13.1 ± 0.22**
Hb (gm/dl)	**13.6 ± 0.38**	**11.7 ± 0.23**	**12.5 ± 0.47**	**12.1 ± 0.17**	**12.9 ± 0.38**
PLT (10^3/µL)	**556 ± 31.2**	**412 ± 28.2**	**512 ± 25.8**	**516 ± 36.2**	**545 ± 19.7**
LDH (U/L)	**401 ± 24.3**	**742 ± 31.3**	**495 ± 14.5**	**481 ± 16.6**	**412 ± 11.3**
Uric acid (mg/dL)	**2.61 ± 0.72**	**4.73 ± 0.51**	**3.09 ± 0.34**	**3.21 ± 0.51**	**2.76 ± 0.42**
Creatinine (mg/dL)	**0.51 ± 0.04**	**2.8 ± 0.13**	**1.7 ± 0.09**	**1.5 ± 0.06**	**0.61 ± 0.03**
Cholesterol (mg/dL)	**145 ± 7.6**	**281 ± 31.2**	**162 ± 11.2**	**173 ± 16.3**	**151 ± 4.5**
TG (mg/dL)	**85.1 ± 8.2**	**163 ± 12.1**	**92.4 ± 9.1**	**104.4 ± 6.2**	**89.3 ± 3.8**
HDL (mg/dL)	**61.8 ± 2.9**	**35.6 ± 4.1**	**45.1 ± 2.3**	**48.4 ± 3.1**	**55.3 ± 3.5**
LDL (mg/dL)	**76.2 ± 5.7**	**165.6 ± 10.8**	**92.5 ± 6.1**	**95.6 ± 5.3**	**81.1 ± 4.6**
Phospholipid (mg/dL)	**45.5 ± 7.5**	**22.1 ± 4.3**	**38.1 ± 2.9**	**35.3 ± 3.1**	**42.5 ± 3.1**

Values are expressed as mean ± SEM (n=3). P>0.05 when compared to normal group.

Effect of MOR, Vitamin E and M-Vit.E-CD-CSNPs on arsenic accumulation in various organs

The effect of vitamin E, MOR and M-Vit.E-CD-CS NPs treatment on arsenic accumulation in liver, brain, lung, heart, skin and kidney are represented in tabular form. Arsenic exposure results a remarkable rise in arsenic level in these organs. It also suggests that the arsenic accumulation is higher in liver than the other organs. Treatment of M-Vit.E-CD-CS NPs, vitamin E and MOR reduced the arsenic accumulation in these organs (Table 2).

Table 2: Arsenic deposition in different organ

	Arsenic concentration in µg/g of tissue in 30 days					
	Liver	**Kidney**	**Cerebellum**	**Lung**	**Heart**	**Skin**
Arsenic, 40 mg/L	**145.3 ± 5.1**	**29.8 ± 1.8**	**12.5± 4.4**	**14.6 ± 1.3**	**12.8 ± 5.6**	**4.8 ± 2.6**
Arsenic + MOR (200 mg/kg)	**110.4 ± 2.5**	**18.1 ± 1.4**	**8.2 ± 2.1**	**9.9 ± 1.9**	**8.5 ± 2.2**	**1.9 ± 0.6**
Arsenic + vitamin E (50 mg/kg)	**95.2 ± 2.4**	**15.1 ± 1.6**	**6.6 ± 1.3**	**7.1 ± 1.1**	**6.1 ± 0.8**	**0.7 ± 0.16**
Arsenic + M-Vit.E-CD-CS NPs (20 mg/kg)	**41.6 ± 3.3**	**3.1 ± 1.2**	**0.52 ± 0.07**	**1.2 ± 0.03**	**1.5 ± 0.21**	**0**

Values are expressed as mean ± SEM (n=3). P>0.05 when compared to normal group.

M-Vit.E-CD-CS NPs suppress oxidative stress in mice liver

Administration of vitamin E, MOR and M-Vit.E-CD-CS NPs significantly hindered ROS generation and increased level of MDA which is induced by arsenic exposure (Figure 4C and 4D).

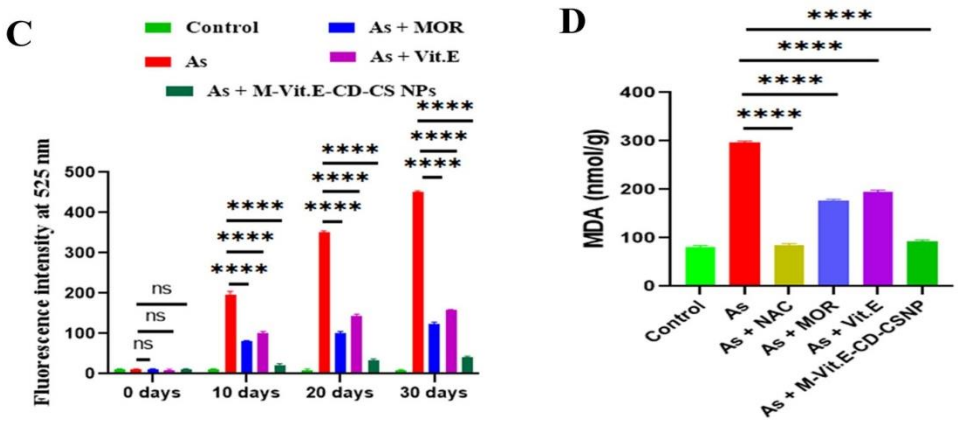

Figure 4: (C) ROS generation and (D) MDA level. MOR, vitamin E and M-Vit.E-CD-CS NPs level with the duration of its exposure. Indicated doses of MOR, vitamin E and M-Vit.E-CD-CS NPs were treated during arsenic exposure Data is one of the three representative experiments ± SD.

Effect of M-Vit.E-CD-CS NPson arsenic induced elevation of antioxidant factors

In the period of arsenic exposure, the level of anti-oxidant factors and anti-oxidant enzymes are reduced. So, we investigated the effect vitamin E, MOR and M-Vit.E-CD-CS NPs on arsenic induced decrease in anti-oxidant factors such SOD, catalase, GSH. SOD was up-regulated by vitamin E (50 mg/kg), MOR (200 mg/kg) and M-Vit.E-CD-CS NPs (20 mg/kg) in arsenic exposed mice (Figure 4A). The lowered levels of catalase and GSH in arsenic treated mice were increased receiving M-Vit.E-CD-CS NPs (Figure5B and 5C). Due to arsenic intoxification the level of nuclear Nrf2 and GPx were decreased which were further increased following by the treatment of M-Vit.E-CD-CS NPs (Figure 5D). Also, the study showed that cytosolic Nrf2 notably elevated in the arsenic exposed mice which are lowered following the treatment of M-Vit.E-CD-CS NPs (Figure 5D). Identical results were obtained in the amount of HO-1 and *NQO1* (Figure 5D).Effect of 20 mg/kg bwt M-Vit.E-CD-CS NPs was comparable with 200 mg/kg of MOR and 50 mg/kg of vitamin E. This indicated that M-Vit.E-CD-CS NPs has a powerful antioxidant activity against arsenic-induced liver damage.

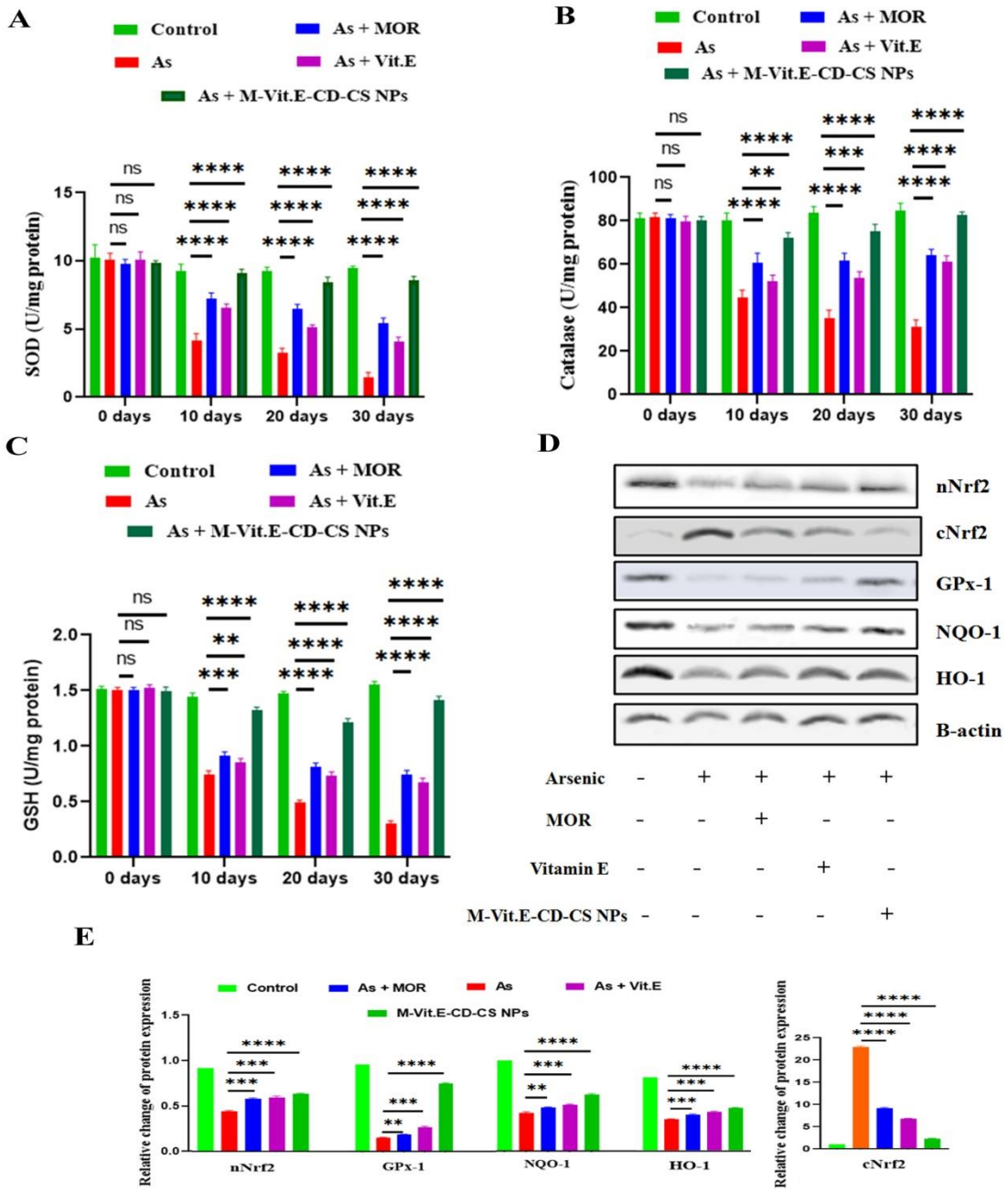

Figure 5: Effect of MOR, vitamin E and M-Vit.E-CD-CS NPs on antioxidant factors. M-Vit.E-CD-CS NPs (20mg/kg bwt), vitamin E (50 mg/kg bwt) and MOR (200 mg/kg bwt) were treated orally in mice during its exposure to arsenic. The level of (A) SOD (B) catalase (C) GSH in the liver tissue lysate of arsenic was measured by using assay kits. (D) the effect of MOR, vitamin E and M-Vit.E-CD-CS NPs on protein expression of cytosolic Nrf2, nuclear Nrf2, GPx, HO-1 and NQO1 (western blot analysis) in the liver tissue lysate.

M-Vit.E-CD-CS NPs inhibit apoptosis in liver tissue induced by arsenic

Arsenic induced inflation of DNA fragmentation, active caspase-3/caspase-9, and cytosolic cytochrome C were conquered by M-Vit.E-CD-CS NPs in the liver tissue lysate (Figure 6A and 6B). The effect of M-Vit.E-CD-CS NPs on DNA fragmentation was compared with the ROS-inhibitor NAC which showed that the effect of M-Vit.E-CD-CS NPs nearly same with NAC (Figure 6C). In the treated group of mice by arsenic+MOR, arsenic + vitamin E and arsenic+M-Vit.E-CD-CS NPs the level of Bax, Bad, p53, Apaf-1, and PUMA were found to be lowered in comparison to their elevated level in arsenic group. Arsenic exposure suppressed the level of anti-apoptotic protein Bcl-2 which was enhanced by the following treatment of MOR, vitamin E and M-Vit.E-CD-CS NPs (Figure 6D).

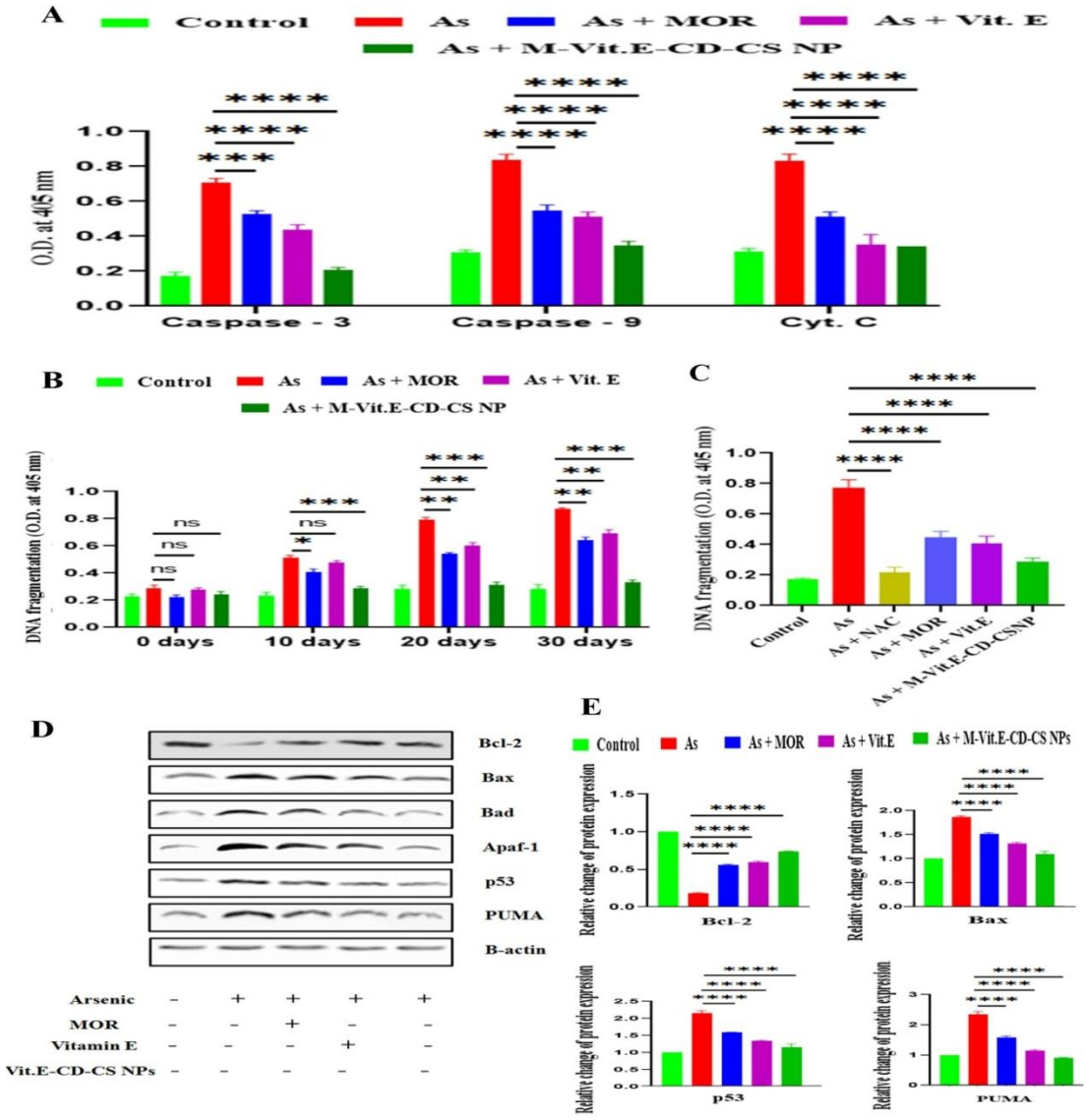

Figure 6: Effect of MOR, vitamin E and M-Vit.E-CD-CS NPs on liver tissue apoptosis. (A) the level of active caspase-3, active caspase-9, and cytosolic cytochrome C obtained using respective colorimetric assay kits. (B) & (C) Level of DNA fragmentation obtained using DNA fragmentation kit. (D) the effect of MOR, vitamin E and M-Vit.E-CD-CS NPs on the protein expression (western blot analysis) of Bcl-2, Bax, Bad, p53, Apaf-1 and PUMA in mice exposed to arsenic.

M-Vit.E-CD-CS NPs suppressed arsenic induced inflammatory responses:

The formation of pro-inflammatory mediators was enhanced due to the separation of IkBα from NF-kB in cytosol accelerate its shifting into the nucleus [182]. In the time of arsenic exposure, NF-kBp65 is extremely triggerd with the release of prominent level of inflammatory cytokines. The treatment of MOR, vitamin E and M-Vit.E-CD-CS NPs reduced the amount of these cytokines such as IL-1β, IL-6 and TNF-α increased by arsenic (Figure 7A). Arsenic exposure activated NF-kBp65 which was further suppressed following the treatment of MOR, vitamin E and M-Vit.E-CD-CS NPs (Figure 7B). The activation of NLRP3 inflammasome is occurred due to chronic arsenic exposure and the release of pro-inflammatory factors e.g. Caspase-1, IL-18 cause pyroptosis. The increasedlevel of NLRP3 inflammasome caused by arsenicand the amount of Caspase-1, and IL-18 in liver tissue was attenuated by M-Vit.E-CD-CS NPs treatment (Figure 7B).

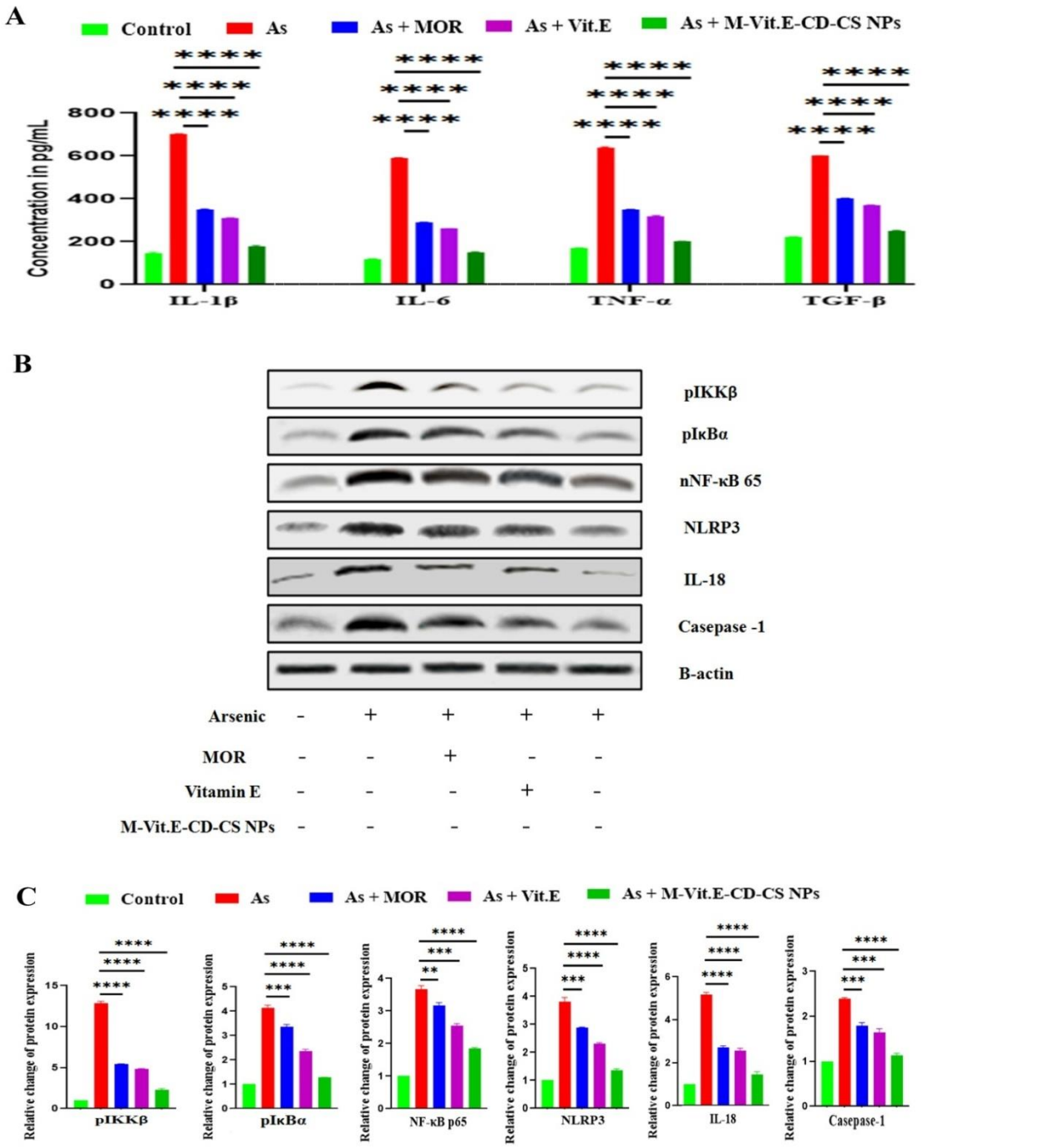

Figure 7: Effect of MOR, vitamin E and M-Vit.E-CD-CS NPs on the level of (A) TNF-α, IL-β, IL-6, TGF-β in the liver tissue lysate of arsenic challenged mice as seen in ELISA analysis. Data are one of the three representative experiments ± SD. (B) the effect of MOR, vitamin E and M-Vit.E-CD-CS NPs on protein expression of nuclear NF-kBp65, NLRP3, Caspase-1, IL-18 (western blot analysis).

M-Vit.E-CD-CS NPsameliorate liver tissue damage induced by arsenic

The histopathological changes were analyzed by using the H&E staining in the liver tissue section. The control liver tissue showed the cords of the normal hepatocytes in which sinusoids line were looking normal by Kupffer cells whereas diffused Kupffer cells, vascular changes, inflammatory cells infiltration were showed by arsenic exposure indicate the critical liver damage (Figure 8A). The repair of liver tissue took place in arsenic intoxicated mice injected with M-Vit.E-CD-CS NPs as compared with the free MOR and vitamin E treated mice (Figure 8A).

Tissue Distribution Study of M-Vit.E-CD-CS NPs in Various Organs

A single dose of M-Vit.E-CD-CS NPs orally given to the mice for several time point and the concentration of morin and vitamin E in liver, spleen, lungs, kidneys, and serum were recorded by HPLC. Figure 8A showed the different concentration of morin from M-Vit.E-CD-CS NPs in different the organs. At the time point 2h highest concentration of morin was present in liver and it was reduced slowly with time and was lowest at 72h. The sequence of the amount of morin and vitamin E in various organs was liver> kidney≥spleen> lung>serum. With the period of time, the concentration of morin and vitamin E in different organs was decreased steadily indicating the nominal or no deposition in the tissues and a gradual removal of the components (Figure 8B).

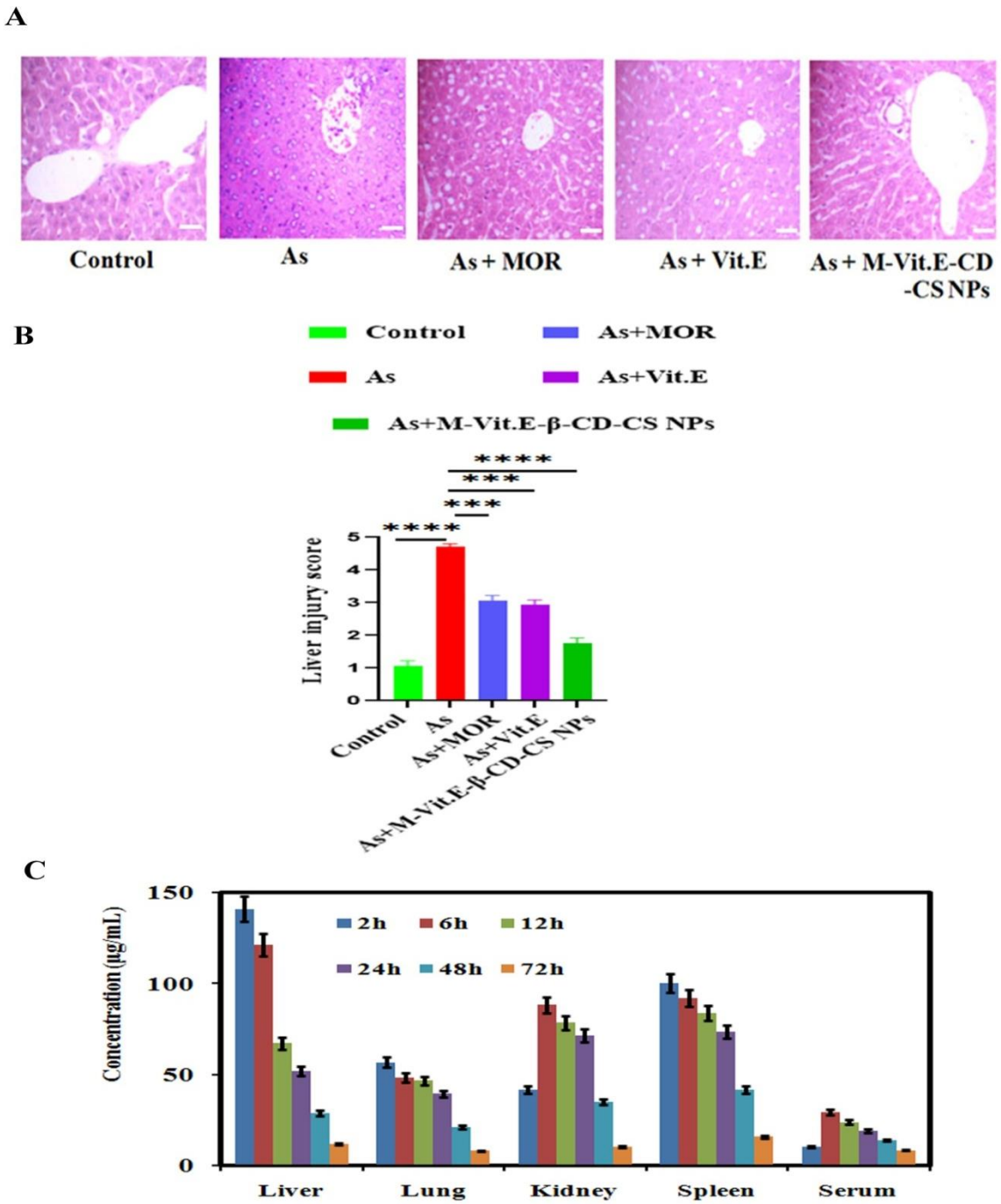

Figure 8: (A) Effect of MOR, vitamin E and M-Vit.E-CD-CS NPs on liver tissue histology Architecture of liver tissue section following treatment without or with MCNPs and MOR in arsenic exposed mice. (B)Tissue distribution studies of M-Vit.E-CD-CS NPs in various organs. Mean concentration of morin in liver, lungs, kidneys, spleen, and serum at 2, 6, 12, 24, 48, and 72 h after oral administration of single dose of M-Vit.E-CD-CS NPs (n = 3, mean ± SD) in mice.

Discussion:

CDs are widely used in pharmaceuticals, drug delivery systems, cosmetics, and the food and chemical industries. They can be found in commercially available medications, including tablets, eye drops, and ointments [178]. Their successful use in inclusion complexes with bioactive compounds has led to extensive investigations in several different application areas to try to overcome the limitations of certain substances. In the food industry CDs is used in the reduction of cholesterol in food, as dietary fibers, for controlling body weight and blood lipid profile, and as prebiotics, which enhance the intestinal microflora [183]. Although CDs are either non or only partly digestible by the enzymes of the human gastrointestinal (GI) tract and fermented by the gut microflora, they produce negligible cytotoxicity (mainly β-CD) in the body.

β-CD and chitosan both are used as nano drug delivery system. But there is previous report which suggest that compared to chitosan nanoparticles CD-g-CS nanoparticles showed better stability [29]. CDs can regulate various properties affecting the performance and therapeutic uses of drugs. Besides enhancing the hydrophilicity and the rate of dissolution of poorly water-soluble drugs CDs, also can reduce harmful reactions e.g. gastrointestinal or ocular irritation and other side effects [178]. They increase absorbency through the biological membranes, reduce vaporization and stabilizing flavors and enhance the tastiness. Several studies suggested that β-CD can enhance the drug loading efficicacy of nanoparticles and *decelerate* the release of drugs. CD inclusion complexes loaded Chitosan nanoparticles can result in mucoadhesive delivery systems, having combined effects of inclusion, bioavailability enhancement, and specific mucosal targeting.

Morin, a poorly water soluble flavonoid, and Vit E, a fat soluble antioxidant nutrient was chosen for testing the ability to load hydrophobic drug of the best NPs formulations in this study. The synthesized NPs were characterized in by using various technique. The results show that morin and Vit E were entrapped in the cavity of cyclodextrins. The inclusion complexes in which guest molecule was surrounded by hydrophobic environment of CDs cavity is ideal for delivering low solubility drug. Inclusion complexes have also been studies in order to significantly improve the hepatoprotective activity at lower of morin and Vit E. Morin was released sustainable but higher antioxidant and hepatoprotective activity was obtained upon inclusion complexed with β cyclodextrin. Results indicate that CDs could facilitate the association of complexed drug into

the NPs. Inclusion complexes formed with a host–guest molecule may exhibit improved chemical or biological properties compared to the host molecule alone.

Chitosan NPs also exhibits significant hepatoprotective effect in the handling of liver injury induced by alcohol, CCl4, acetaminophen, diethylnitrosamine (DEN) and concanavalin A [184-187]. Chitosan-graft-β-cyclodextrin nanoparticles were reported as a good carrier for controlled drug release [29].

Morin and vitamin E both has been reported to have hepatoprotective role in various disease model [154, 188].

However, their hydrophobic nature is the reason for poor bioavailabilty. To counter these drawbacks, we have synthesized β-CD-MOR-Vit.E inclusion complex loaded chitosan nanoparticles called as M-Vit.E-CD-CS NPs, which has prominent aqueous solubility therefore increased bioavailability. The efficacy of M-Vit.E-CD-CS NPs is much higher than that of MOR or vitamin E. The conservation of the significant FT-IR peak of the free compounds confirmed the formation of the nanoparticles. The average size of the nanoparticles is 178±1.5 nm. The TEM and AFM images confirmed the spherical shape of the nanoparticles.

Size of nanoparticle plays a crucial role and is key to achieving therapeutic efficacy depending on the physiological parameters such as blood circulation halflife, molecular targeting, and cellular uptake. Nanoparticles that fall between 5-200 nm tend to have a prolonged blood circulation [189]. Tissue distribution studies have revealed that M-Vit.E-CD-CS NPs accumulation increased in liver at 2h that gradually decreased upto 72h. This result suggested the slow elimination of nanoparticles from the blood circulation. The shape our synthesized nanoparticles were spherical and it also justify the previous report by Wang et al. which suggested that intake of the spherical MSNs by liver were increased constantly to the 72-h time point.

Cotreatment of MOR, Vitamin E or M-Vit.E-CD-CS NPs with arsenic in mice reduced liver function makers, ROS level, pro-apoptotic and inflammatory factors with elevation of antioxidant parameters and improvement of liver histopathology. Interestingly, effect of M-Vit.E-CD-CS NPs treatment showed better effects than free morin or vitamin E in all cases. All these beneficial outcomes can be associated to the therapeutic efficacy of M-Vit.E-CD-CS NPs.

Conclusion:

In this study, as a new carrier M-Vit.E-CD inclusion complex loaded chitosan nanoparticles are designed and synthesized which improved the solubility of MOR and vitamin E.Using readily available Morin and vitamin E as a hydrophobic drug and β-CD, chitosan as starting materials, the MOR-Vit.E-β-CD inclusion complex loaded Chitosan nanoparticles are effectively synthesized by an ionic gelation method.In vitro release study indicates that MOR and vitamin E are released pH-dependently from the nanoparticles in a sustainable way. Therefore, the newly synthesized drug carrier has a promising effect as a biodegradable transport system for sustained release of hydrophobic drugs in pH dependent manner. Our study indicates that M-Vit.E-CD-CS NPs has better hepatoprotective effect than free MOR and vitamin E against arsenic intoxicated liver injury in murine model. The better protective effect of M-Vit.E-CD-CS NPs can be attributed by the improved the solubility and bioavailability of MOR and vitamin E due to formation of nanocarrier. The antioxidant, anti-inflammatory and anti-apoptotic effects of M-Vit.E-CD-CS NPs can be accounted as primary reasons of the hepatoprotective activity. Therefore, MOR-Vit.E-β-CD inclusion complex loaded CS nanoparticles can be used as a potential therapeutic agent for liver damage for arsenic intoxification.

Chapter III:

Morin reduced gold nanoparticles ameliorates dextran sulfate sodium-induced Ulcerative Colitis via down-regulation of TLR4/NF-κB and NLRP3-inflammasome pathways and modulation of redox balance

Introduction:

Ulcerative colitis is considered to be a part of inflammatory bowel disease, occurred due to chronic inflammation. The causation of UC is not fully understood. UC is described by the increasing inflammatory cascade with the release of certain mediators. It is also capable of altering the bowel wall structure [191]. Patients usually suffer with extreme stomach pain, fecal blood, drastic weight loss and diarrhea [192]. The current treatment modalities only provide symptomatic relief from pain and inflammation [193]. The increasing number of UC globally, but unavailability of effective treatments is the major problem [194]. Over-expression of the inflammatory cytokines was correlated with the leukocytes, macrophages and neutrophil's infiltration in the UC's progression. Colon lesion resulting from damage of intestinal epithelial cells (IECs) causes ulceration [195].

At First mast cells, monocytes, macrophages, lymphocytes, and other immune cells are activated during the clinical induction of inflammation [196]. Then the cells are reinforced in the injury site, which results ROS formation and damage macromolecules including DNA. Also, those activated inflammatory cells generate lots of inflammatory mediators such as cytokines, chemokines, and prostaglandins [196].

Several evidences support that TLR4 (toll-like receptor 4) mediated immune dysfunction plays central role in the pathogenesis of ulcerative colitis [197] and it is overexpressed in UC. Besides the PAMP (pathogen activated molecular pattern) molecules, some endogenous molecules like heat shock proteins (HSPs) activate TLR4 [198]. After cell damage, molecules like HSPs are released in the extracellular milieu and triggers TLR4. TLR4 signaling pathways activate the transcription factor NF-kB [199], which regulates the expression of enormous number of inflammatory cytokines such as TNF-α, IL-1β, and IL-6, those have been involved in the deleterious effects of UC [199-201]. In TLR4 signaling the most commonly activated form of NF-kB is NF-kBp65 and NF-kBp50. They remain as inactive form in the cytoplasm by

interaction with IkB protein in normal cells. Stimulation of TLR4 triggers the phosphorylation at serine residues of IkB by its kinase (IKK: IkB kinase) which consists two catalytic subunit IKKα and IKKβ [202]. Phosphorylation of IkB results its degradation from NF-kB letting NF-kB to go to nucleus [202]. This TLR-mediated of inflammatory pathway is also known as the "Canonical pathway" [200].

Activation of the *TLR4-NF-kB* pathway promotes the stimulation of NLRP3-inflammasome [203]. NLRP3 inflammasome is linked with a variety of inflammatory conditions along with inflammatory bowel diseases [204]. Activated NLRP3 mediates caspase-1 activation and release of pro-inflammatory cytokines IL-1β and IL-18 [203]. Inhibition of pro-inflammatory cytokines production by down-regulation of TLR4/ NF-kB pathway might be a suitable treatment strategy for UC [205].

TGF-β is an immune-suppressive cytokine generated by many cell types and abundant in mammalian intestine [206]. Uncontrolled TGF-β signaling is noticed in the intestines of IBD patients. Dysregulated generation of the anti inflammatory cytokine, IL-10 has been correlated with ulcerative colitis [207]. Elevated levels of endogenous NO derived from iNOS (inducible form of NO synthase) has been shown as one of the mediator of intestinal inflammation in ulcerative colitis. Interaction of NO with superoxide anion produces peroxynitrite that contributes to tissue injury and over-expression of the inflammatory response.

Nrf2 plays a crucial role in protection of cells against oxidative stress. It regulates the transcription of various enzymes in detoxification and antioxidant responses [208]. Generally, Nrf2 found in the cytosol is tied with its endogenous inhibitor, Keap1. Under oxidative stress condition, cysteines in Keap1 are modified that causes dissociation of the Keap1-Nrf2 complex. Then, Nrf2 can rapidly translocate into the nucleus, where it can bind with ARE to control the expression of Phase II enzymes, along with HO-1 and NQO1, glutathione peroxidase, ferritin etc. which protect cells from various injuries [209].

Malondialdehyde (MDA) is a byproduct of lipid peroxidation and it is commonly used as a biomarker of oxidative stress [210]. MDA concentration correlates with the level of oxidative stress and lipid peroxidation and tissue damage. Myeloperoxidase is a enzyme which increases the production of reactive oxidant species. MPO-derived oxidants promote tissue injury in the time of inflammation and its role is implicated in diseases of heart, liver, lung, colon and kidney.

Numerous studies have shown that like tarpenoids, alkaloids, organosulphur compounds, phenolic compounds including morin exert protective effect on UC by antagonizing TLR4 [211]. Morin, a potent flavonoid was found in several fruits and vegetables. It is consumed in daily basis in our diet and also used as herbal medicines. It has been suggested to act as a food preservative [212]. It has enormous number of biological activities, such as, antioxidant and/or free radical scavenger properties, anti-inflammatory and anti-apoptotic effects in different biological systems. Some previous studies have proven the efficacy of morin in experimental models of rat colitis [213].

In experimental studies, among all nanoparticles (NP) used, gold nanoparticles (GNPs or AuNPs) are the most useful, with little or no systemic toxicity depending on dose. GNPs have shown exceptional properties such as easy synthesis, controllable shape, optics, excellent biocompatibility, and surface chemistry which make them more favorable for biomedical applications [214]. There are reports of the effect of chemically synthesized AuNPs in rat colitis model [215]. But the chemically-synthesized GNPs and advanced structures (nanorods, nanocages, nanostars etc.) need stabilizing and protecting agent that increase the toxicity of the prepared GNPs. A previous study suggest that the toxicity of gold nanoparticles of different shapes in HepG2 cells followed the order nanospheres>nanorods>nanostars [216]. Generally, spherical nanoparticles of size in between 15–50 nm show less toxicity [217].

So in the present study we have synthesized a spherical shaped morin reduced gold nanoparticles (MGNPs) and evaluated its protective efficacy on DSS-induced ulceration in murine colitis model.

Materials and Methods:

Materials:

Gold (III) chloride hydrate (HAuCl4) 99.99% pure, Morin hydrate, all primary and secondary antibodies were purchased from Sigma-Aldrich, MO, USA. Assays kits for the detection of serum ALT, AST, AP, SOD, catalase, GSH were bought from ARKRAY Healthcare Pvt. Ltd (Surat, India). IL-1β, IL-6, TGF-β and TNF-α were measured by ELISA kits from R&D system (MN, USA). DSS colitis-grade (36000− 50000 Da) was procured from MP Biomedicals (Costa Meca, CA). All other chemicals were available commercially and of a high degree of purity.

Synthesis of morin conjugated GNPs (MGNPs):

Morin was solubilized in milli Q water by increasing its pH to 8 and above using K2CO3. To this solution, HAuCl4 was added dropwise with continuous stirring in magnetic stirrer. Synthesis was carried out at pH of morin 8 and the ratio of morin to HAuCl4 1:1. The formed MGNPs were isolated by centrifuging the solution at 12,000 rpm for 20 min. The pellet obtained was washed twice in milli Q water at the same speed to remove any unreacted substances.

Characterization of MGNPs:

MGNP was characterized using techniques like UV absorbance, DLS, TEM, AFM, and FTIR according to the standard protocol.

Experimental animals:

BALB/c mice (6-8 weeks, male) were obtained from the animal house of CSIR-Indian Institute of Chemical Biology, Kolkata. The mice were randomly assigned to cages and acclimatized for 10 days at 22–24˚C temperature, 50–60 percent humidity and subject to light and dark cycles of 12:12 h, and the mice were fed with a certified standard diet; double distilled water was given. The animals were kept at 22–24˚C temperature, 50–60 percent humidity. The research procedure conducted on animals was as per the recommendations of the CSIR-Indian Institute of Chemical Biology Animal Ethics Committee.

Induction of colitis & experimental design:

After acclimatization for 10 days, the mice were arbitrarily divided into groups and were fed with standard chow diets. The experimental plan of this study was as follows: Groups of mice received (i) drinking water only for 16 days (ii) 3% DSS only via drinking water for 16 days, (iii) 3% DSS + Free MOR (200 mg/kg doses), (iv) 3% DSS + MGNPs (15 μg/kg and 150 μg/kg doses). Each dose of Free MOR and MGNPs were administered on every alternate day from 5 to day 15 of DSS challenged mice by oral gavage. Mice were sacrificed on day 16.

Body, organ weight & disease activity index assessment:

The body weight of each mouse was taken on a daily basis during the experimental period and the Colitis activity indexwas assessed by daily monitoring of weight loss, stool consistency and rectal bleeding. The distal 8 cm portion of the colon, liver and kidney of each mouse in all the experimental groups were removed and weighed. The clinical evaluation of the disease was quantitatively assessed by the scoring activity index as described by Zhang *et al*. with minor

modification, stool consistency and rectum bleeding. The score was calculated as follows: stool consistency (0: normal, 1 and 2: loose stool, 3 and 4: diarrhea) and rectal bleeding (0: normal, 1: stripes of blood, 2: obvious blood, 3 and 4: mostly blood).

Biochemical analysis of liver and kidney:

Blood samples were obtained by tail-vein puncture and kept at 4˚C undisturbed o/n. Samples were centrifuged thenext day(1109×*g*, 10 min, 4˚C) to obtain the serum from the experimental groups. Serum AST, ALT, ALP, SOD, GSH, catalase, urea, creatinine and uric acid activities were calculated according to the instruction brochure providedwith the commercial assay kits.

ROS and MDA estimation:

Supernatant of colon tissue tissue homogenate were mixed with dichlorofluoresceindiacetate (DCFDA) solution (10mM). The mixture was incubated at 37˚C for half an hour. Fluorescence intensity of the sample was measured using spectrofluorometer at 480 and 525 nm wavelengths of excitation and emission.MDA in colon tissue homogenate was assayed by using thiobarbituric acid (TBA) and measuring O.D. at 532 nm.

Determination of colonic myeloperoxidase activity:

The colon tissue activity of myeloperoxidase (MPO), which is linearly related to neutrophil infiltration in inflamedtissue, was measured spectrophotometrically at 650 nm and the activity was expressed as (unit/mg tissue) [**177**].

Assessment of hematological parameters:

A blood sample was collected. Hematological parameters were determined using an automatedhematological analyzer (Sysmex KX-21, IL, USA) with specific software for mice blood samples [32]. The white bloodcell (WBC) number, red blood cell number, hemoglobin concentration and platelet count were analyzed.

Assessment of serum cytokines by ELISA:

Blood sample collection was done by tail-vein puncture and kept overnight at 4°C. samples were centrifuged for 10 mins at 3000 rpm at 4 °C to obtain serum. The serum levels of interleukin 1β (IL-1β), Interleukin-10 (IL-10), interleukin 6 (IL-6), and TNF-α were evaluated using the commercial ELISA kit as per the guidelines and instruction (R&D Systems, MN).

Western blot analysis:

Protein concentrations in the supernatant of liver tissue lysate were measured using Bradford reagent. SDS-PAGE was performed to separate the proteins of supernatant using Semi dry transblot apparatus (Bio-Rad), and proteins of SDS gel were transferred to a polyvinylidene difluoride (PVDF) membrane(Merck Millipore). The membrane was blocked with 5% BSA and incubated with primary antibodies of the desired proteins and β-actin (1:1,000; Santa Cruz, CA, USA) for overnight at 4℃. Next the membrane was washed 3 times with PBS andincubated with an alkaline phosphatase-conjugated secondary antibody followed by addition of NBT/BCIP solution. Bands of the desired proteins and β-actin were detected.

Histological evaluation:

The fixed liver, kidney and colon tissues in 10% neutral buffered formalin (NBF) were embedded in paraffin, thinly sectioned, de-paraffinated and rehydrated using the standard histology procedure. Various pathological changes were assessed by using hematoxylin and eosin stains.

Statistical analysis:

The data of this study were obtained from three independent experiments. All the quantitative data were expressed as means ± standard deviation. (means ± SD). The significance of difference among treatment groups was performed using one-way analysis of variance (ANOVA). Data with value of $P < 0.05$ was considered as statistically significant.

Results:

MGNPs synthesis & characterization

MGNPs showed a characteristic wine red color (Fig. 1A). The appearence of the absorbance peak of MGNPs at 540 nm confirmed its identity (Fig. 1B). FTIR analysis of free MOR and MGNPs was done to analyse the presence of several functional groups. A broad peak was observed at 3500 cm^{-1} for MOR and 3488 cm^{-1} for MGNPs, reffered to O–H bond stretching and consistent with the presence of alcoholic and phenolic compounds. One more peak at 1645 cm^{-1}

for MOR and 1640 cm^{-1} for MGNPs specified the presence of amide (C=O) and alkene (C=C) groups. A significant dissimilarity was observed between the two peaks at 3398 cm^{-1} and 1640 cm^{-1} for MGNPs (Fig. 1C), signify the role of C=O and O–H bonds in the reduction of Au(III) ions to Au atoms. The size of MGNPs particles, obtained from the differential light scattering study was 33 nm (Fig. 1D). MGNPs were further analyzed by TEM analysis of the colloidal gold solution. TEM images showed the spherical monodispersed MGNPs without any aggregations (Fig 1E). Atomic force microscopy measurements showed the surface topology of MGNPs was uniform; they had a spherical shape and size also collaborates with the DLS result (Fig. 1F).

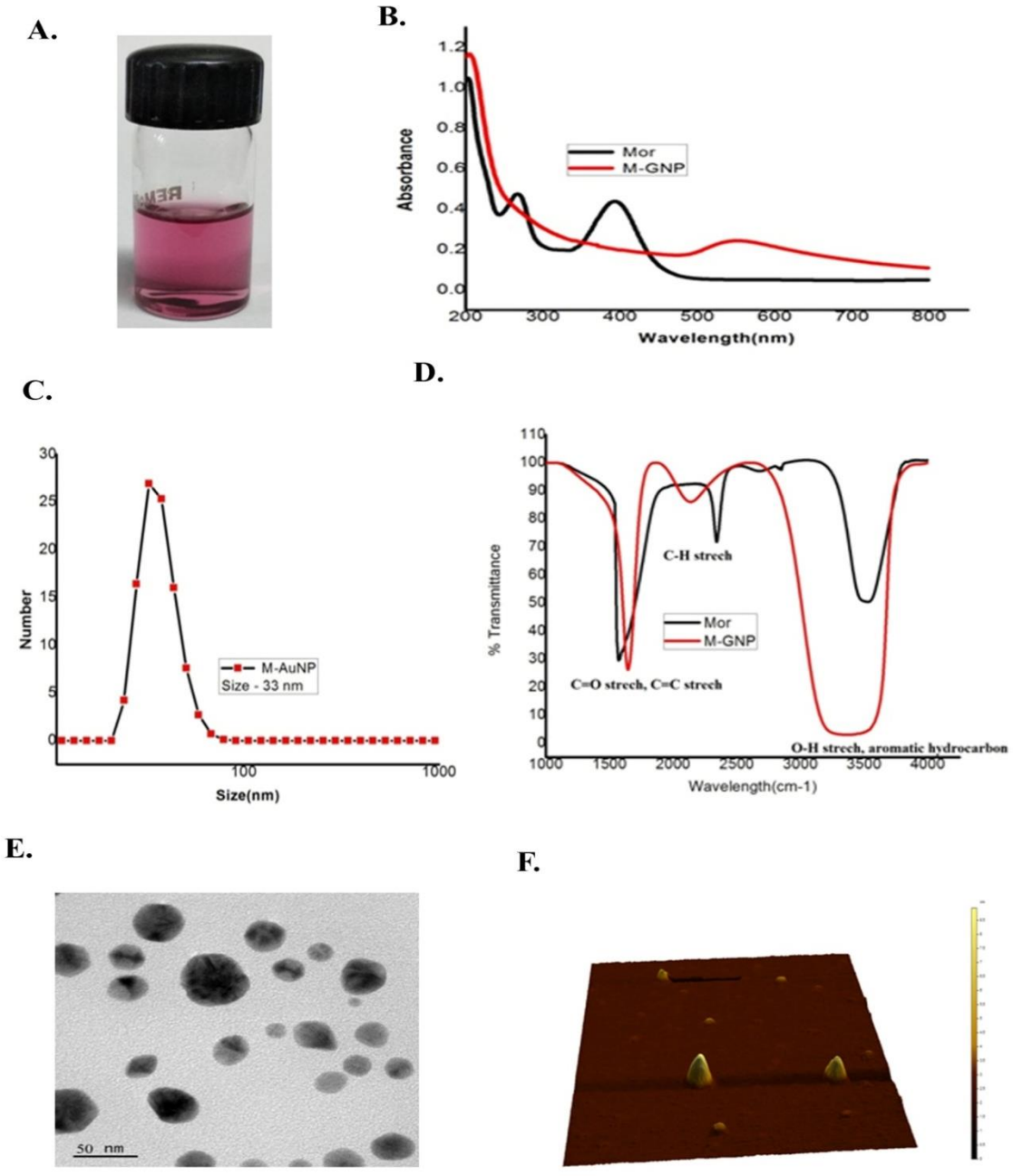

Figure 1: Characterization of Morin reduced Gold nanoparticles. (A) Picture of prepared of MGNPs. (B) UV–Visible spectra of morin and MGNPs. The red line shows the spectra of morin, black line shows the spectra of MGNPs. (C) Particle size distribution from differential light scattering (DLS) with MGNPs. (D) Fourier transform infrared spectroscopy (FTIR) spectra of Morin and MGNPs. (E) TEM images of MGNPs. (F) MGNPs particle surface topology determination using atomic force microscopy (AFM). The acquired images were analyzed using

scanning probe microscopy (SPM) tools for laboratory study. Result is the mean ± standard deviation (SD) from triplicate independent experiments.

Effect of MGNPs on Body, disease activity index and colonic shrinkage in DSS challenged mice

Non-toxic doses of MGNPs in murine model were determined by measuring the liver function markers ALT and AST following the oral treatment of 20, 60, and 180 mg/kg of MGNPs on day 1, 3, 5, 7, 9 and 11. No elevation of the liver function markers was noticed till 60mg/kg of MGNP treatment (data not shown).

Figure 2A showed the schematic presentation of treatment design of mice. DSS treatment lowered the body weight of mice and increased diarrhea and bloody stools (Disease Activity Index) those were recovered following the treatment of 150mg/kg Morin, 20 and 60 mg/kg of MGNPs and 75mg/kg of the anti-inflammatory ulcerative colitis drug, 5-ASA (5-aminosalicylic acid) at every alternate day (Figure 2C and 2D). Colon length shortened from DSS exposure was almost normalized following the treatment of 60 mg/kg of MGNPs (Figure 2E and 2F). Results show that MGNPs can resist the pathological changes caused by DSS.

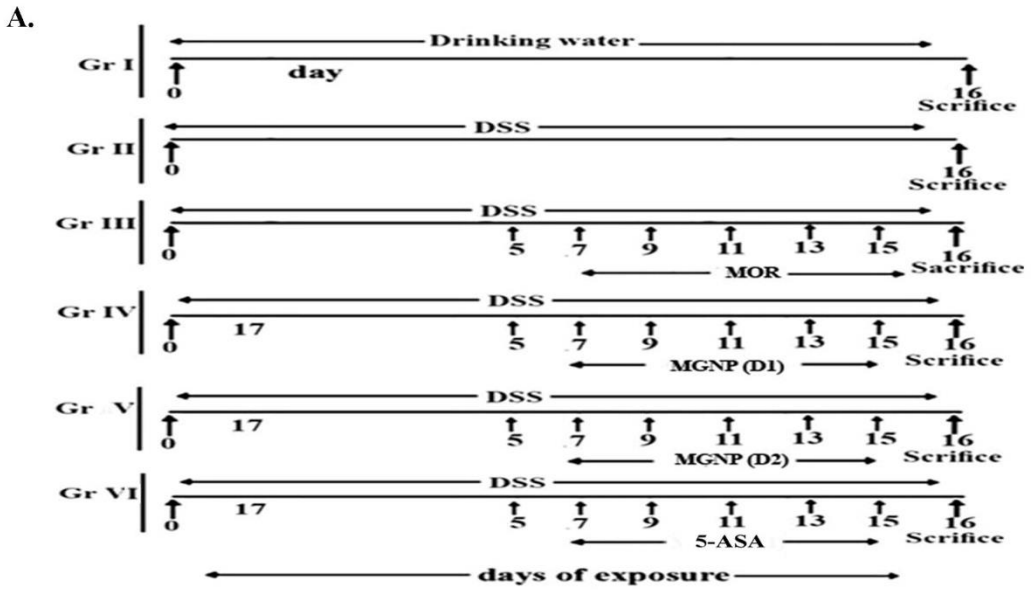
A.
Gr I
Drinking water
day
0
16
Scrifice
Gr II
DSS
0
16
Scrifice
Gr III
DSS
0
5
7
9
11
13
15
16
MOR
Sacrifice
Gr IV
DSS
0
17
5
7
9
11
13
15
16
MGNP (D1)
Scrifice
Gr V
DSS
0
17
5
7
9
11
13
15
16
MGNP (D2)
Scrifice
Gr VI
DSS
0
17
5
7
9
11
13
15
16
5-ASA
Scrifice
days of exposure

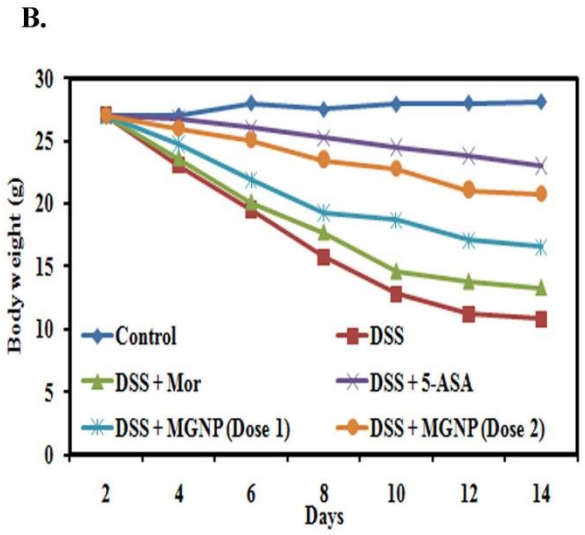
B.
Body weight (g)
30
25
20
15
10
5
0
2
4
6
8
10
12
14
Days
Control
DSS
DSS + Mor
DSS + 5-ASA
DSS + MGNP (Dose 1)
DSS + MGNP (Dose 2)

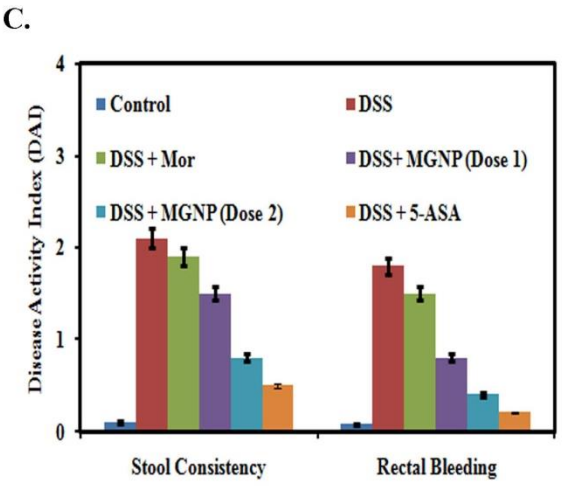
C.
Disease Activity Index (DAI)
4
3
2
1
0
Control
DSS
DSS + Mor
DSS+ MGNP (Dose 1)
DSS + MGNP (Dose 2)
DSS + 5-ASA
Stool Consistency
Rectal Bleeding

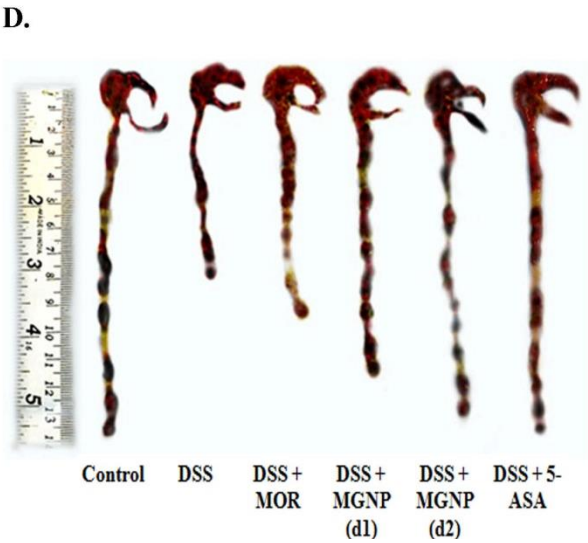
D.
Control
DSS
DSS + MOR
DSS + MGNP (d1)
DSS + MGNP (d2)
DSS + 5-ASA

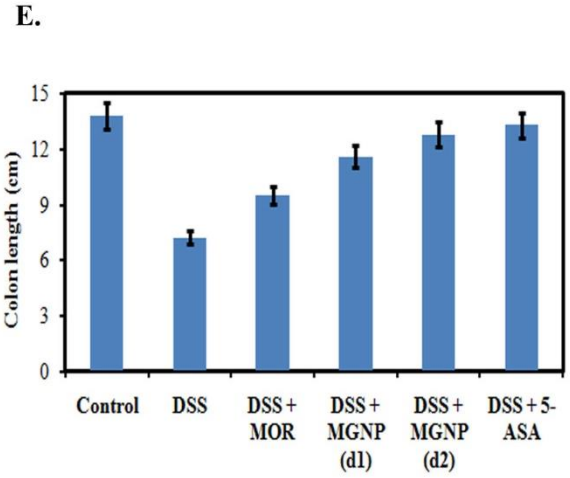
E.
Colon length (cm)
15
12
9
6
3
0
Control
DSS
DSS + MOR
DSS + MGNP (d1)
DSS + MGNP (d2)
DSS + 5-ASA

Figure 2: (A) Schematic representation of the experimental work plan for the development of Ulcerative Colitis using DSS and its amelioration by the treatment of MOR, MGNPs (d1 & d2), 5-ASA, Effect of gold nanoparticles on the (B) body weight, (C) disease activity index, (D) Macroscopic view of the whole colon from the cecum to the rectum in all of the experimental groups (E) Comparison of the colon length measured using a scale in all of the experimental groups.

Effect of MGNPs on liver and kidney function markers and haematological parameters altered by DSS

Serum level of liver function markers (AST, ALT, and ALP) increased in DSS-challenged mice was lowered upon the treatment of 150mg/kg Morin, 20 and 60 mg/kg of MGNPs and 75mg/kg of ASA as studied on day16 (Figure 3A, 3B and 3C). Effect of 60mg/kg of MGNPs was nearly same to that of 75mg/kg ASA and 3 higher than the effect of 150mg/kg of free morin (MOR). 150mg/kg Morin and 20 mg/kg of MGNPs showed almost same efficacy. Similar findings were observed for kidney function markers such as urea, uric acid and creatinine (Figure 3D, 3E and 3F). Table1 shows that MGNPs treatment reversed the DSS-induced alteration of blood haematological parameters. In contrast to DSS group, DSS + MGNPs (60 mg/kg) showed a significant increase in the red and white blood cells, hemoglobin and platelets which indicate the normalization of the hematological values. Thus MGNPs is found to play good protective role than free morin against DSS induced altered effect on kidney and liver function and hematological parameters.

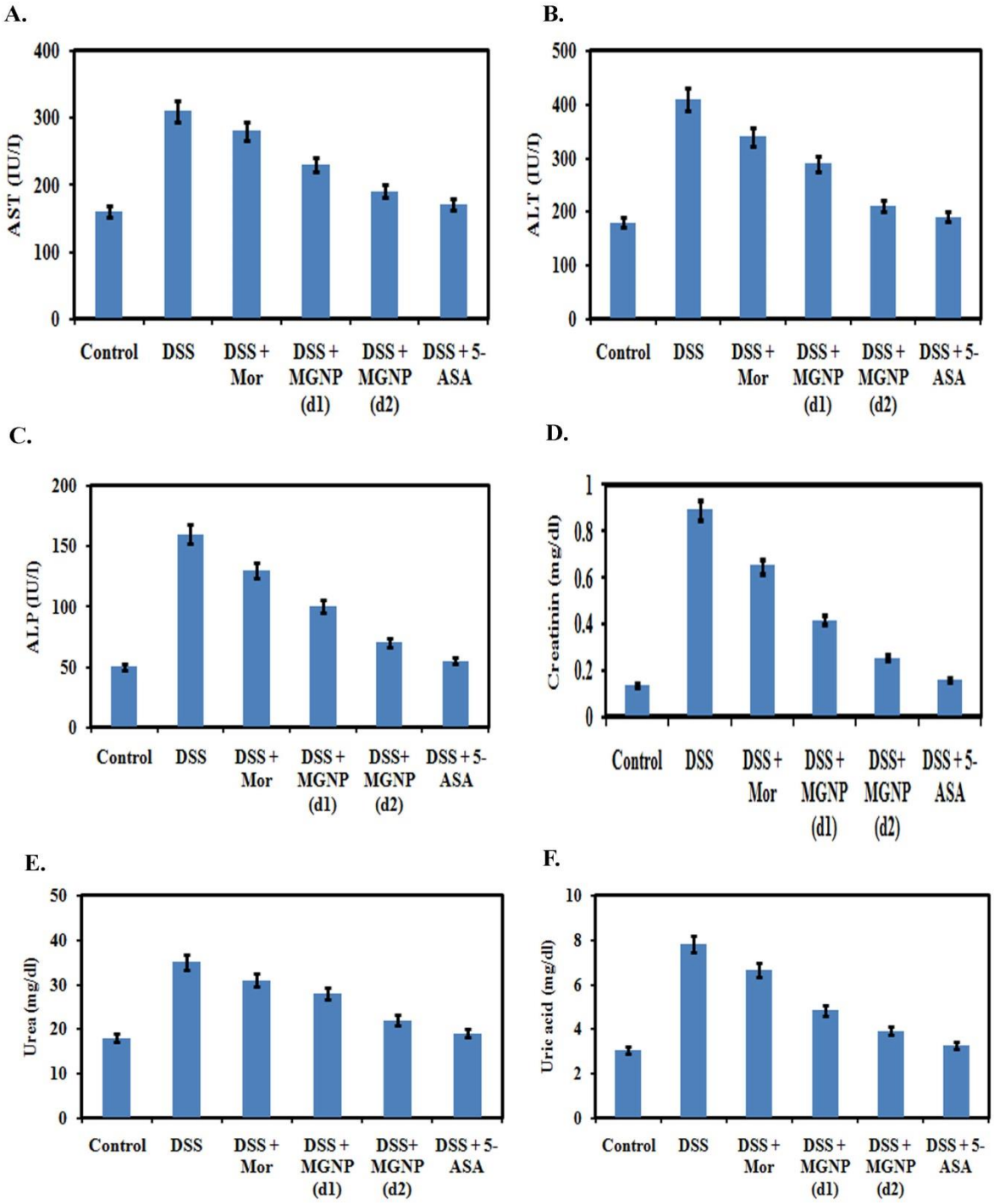

Figure 3: Effect of MOR, MGNPs (d1 & d2), 5-ASA on DSS-induced elevation of Liver and Kidney function markers. MOR, MGNPs (d1 & d2), 5-ASA level with the duration of its exposure. Indicated doses of MOR, MGNPs (d1 & d2), 5-ASA were treated during arsenic exposure. Data is one of the three representative experiments ± SD.

MGNPs suppresses ROS, MPO and MDA level and stimulates expression of antioxidant proteins

Oxidative stresses (ROS), myeloperoxidase (MPO), malondialdehyde (MDA) proportionally increased in the colon, kidney and liver of *DSS*-induced *colitis mice*. Treatment 150mg/kg Morin, 20 and 60 mg/kg of MGNPs and 75mg/kg of ASA suppressed the level of ROS, MPO and MDA (Figure 4A, 4B and 4C). Significant effect was noticed with 60 mg/kg of MGNPs and 75mg/kg of ASA. Degree of efficacy was same as found in Figure 3A, 3B and 3C.

Level of the antioxidant glutathione and the enzymes SOD and CAT were markedly elevated in DSS+ MGNPs treated group as compared to DSS challenged group only (Figure 4D, 4E and 4F). Similarly, expression of the antioxidant proteins GPx1 (glutathione peroxidase), HO-1 **(***heme oxygenase-1)*, NQO1 (NAD(P)H Quinone Dehydrogenase 1), nuclear level of their regulatory protein *Nrf2 (Nuclear* factor erythroid 2-related factor 2) are increased upon MGNPs treatment in DSS challenged mice with an opposite effect on cytosolic Nrf2 and Keap1 (repressor protein of Nrf2 in cytosol) (Figure 4G).

Fluorescence microscopy study for reveals similar effect of 60 mg/kg of MGNPs on DSS induced stimulation of Nrf2 and HO-1 (Figure 4H and Figure 4I).

Results shows that MGNPs can strongly modulate the DSS induced stimulation of ROS, MDA, and MPO, suppression of Nrf2 and its downstream antioxidant proteins. Effect of 60 mg/kg of MGNPs is higher than free 150mg/kg Morin.

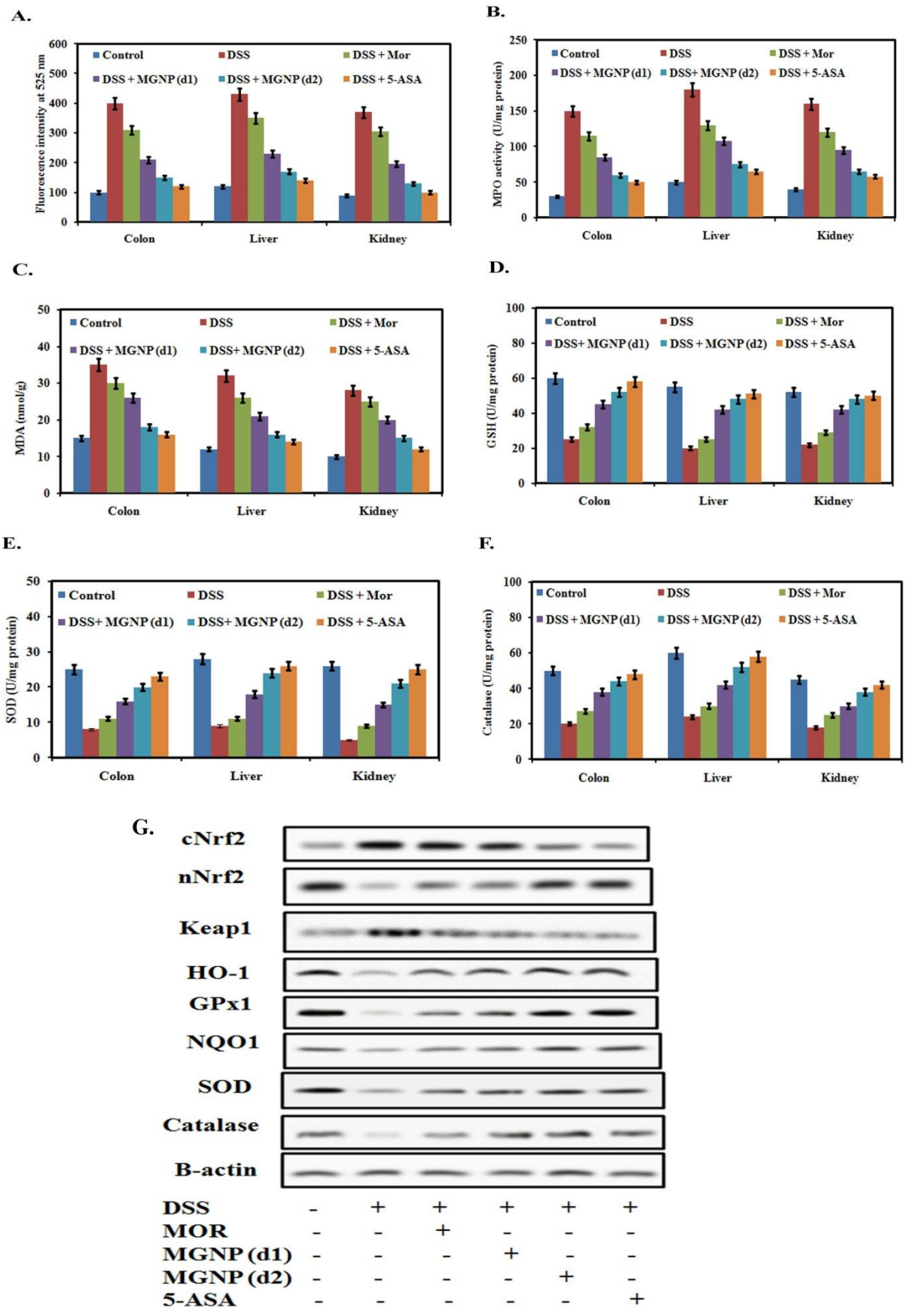
A.
Fluorescence intensity at 525 nm
Control
DSS
DSS + Mor
DSS + MGNP (d1)
DSS + MGNP (d2)
DSS + 5-ASA
Colon
Liver
Kidney
B.
MPO activity (U/mg protein)
C.
MDA (nmol/g)
D.
GSH (U/mg protein)
E.
SOD (U/mg protein)
F.
Catalase (U/mg protein)
G.
cNrf2
nNrf2
Keap1
HO-1
GPx1
NQO1
SOD
Catalase
B-actin
DSS - + + + + +
MOR - - + - - -
MGNP (d1) - - - + - -
MGNP (d2) - - - - + -
5-ASA - - - - - +

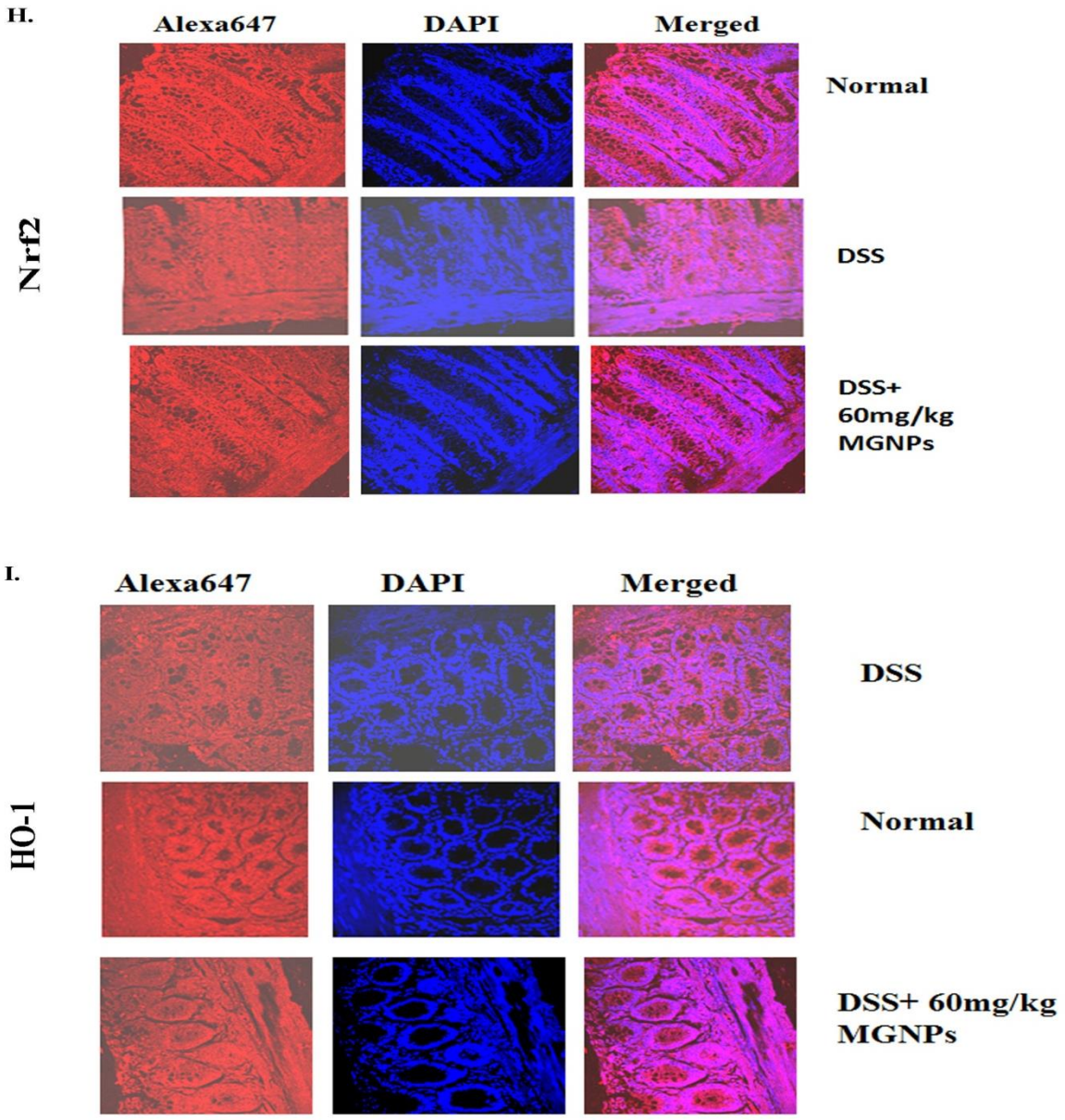

Figure 4: Effect of MOR and MCNPs on ROS generation and MDA level. Mice exposed to DSS via drinking water were treated with MOR, MGNPs (d1 & d2) and 5-ASA orally on every alternate day and the level of (A) ROS, (B) MDA were determined. Effect of MOR, MGNPs (d1 & d2) and 5-ASA on antioxidant factors. MOR, MGNPs (d1 & d2) and 5-ASA were treated orally in mice during its exposure to DSS. The level of (A) SOD (B) catalase (C) GSH in the liver tissue lysate of DSS was measured by using assay kits. (D) shows the effect of MOR, MGNPs (d1 & d2) and 5-ASA on protein expression of cytosolic Nrf2, nuclear Nrf2, Keap1, NQO-1, GPx, Catalase, SOD (western blot analysis) in the liver tissue lysate. (E) Expression of HO-1 and Nrf2 as seen in immunohistochemical analysis.

MGNPs prevent the DSS induced alteration of proinflammatory cytokines and inflammatory and anti-inflammatory factors

DSS-exposure caused a significant elevation in the production of proinflammatory cytokines IL-6, IL-1b, TNF-α and TGF-β in comparison with normal mice. Figure 5A showed that, treatment of 60 mg/kg MGNPs in DSS exposed mice significantly reduced the level of these cytokines. Level of protein expression of the proinflammatory cytokines (IL-6, IL-8, IL-17, and TNF-α), anti-inflammatory cytokine (IL-10 and TGF-β), inflammatory factor iNOS were reversed following administration of MGNPs in DSS exposed mice (Figure 5B).

Inflammatory cytokines are produced through activation of NF-kB p65. Studies on the upstream factors stimulating the NF-kB pathway showed that DSS triggered the expression of TLR-4, MyD88, p-IKKB, p-IkBα, and nNF-kBp65 that was markedly inhibited by 60 mg/kg MGNPs (Figure 5C). TLR4-NF-kB pathway also stimulates NLRP3 inflammasome that in turn produce inflammatory factors IL-1b and IL-18 via caspase-1 activation. DSS was found to activate NLRP3 and its downstream proteins caspase-1, IL-1β and IL-18 that was inhibited by MGNPs (Figure 5D). Fluorescence microscopy study reveals similar effect of 60 mg/kg of MGNPs on DSS induced stimulation of TLR4, NF-kBp65 and NLRP3 (Figure 5E, 5F and 5G).

Thus, 60 mg/kg of MGNPs can profoundly modulate the DSS induced inflammation via TLR4-NF-kB pathway and NLRP3 inflammasome.

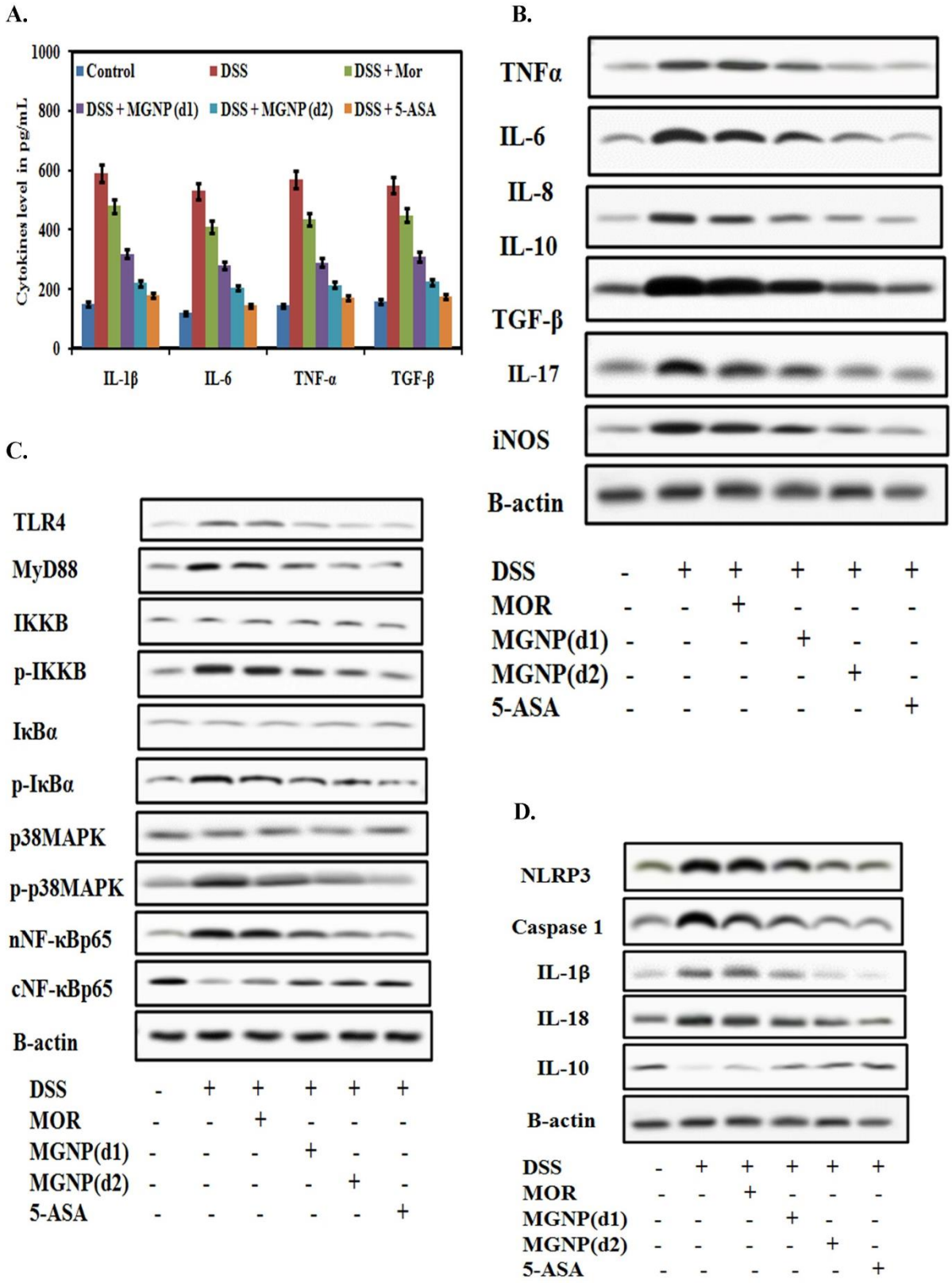
A.
1000
800
600
400
200
0
Control
DSS
DSS + Mor
DSS + MGNP (d1)
DSS + MGNP (d2)
DSS + 5-ASA
Cytokines level in pg/mL
IL-1β
IL-6
TNF-α
TGF-β
B.
TNFα
IL-6
IL-8
IL-10
TGF-β
IL-17
iNOS
B-actin
DSS - + + + + +
MOR - - + - - -
MGNP(d1) - - - + - -
MGNP(d2) - - - - + -
5-ASA - - - - - +
C.
TLR4
MyD88
IKKB
p-IKKB
IκBα
p-IκBα
p38MAPK
p-p38MAPK
nNF-κBp65
cNF-κBp65
B-actin
DSS - + + + + +
MOR - - + - - -
MGNP(d1) - - - + - -
MGNP(d2) - - - - + -
5-ASA - - - - - +
D.
NLRP3
Caspase 1
IL-1β
IL-18
IL-10
B-actin
DSS - + + + + +
MOR - - + - - -
MGNP(d1) - - - + - -
MGNP(d2) - - - - + -
5-ASA - - - - - +

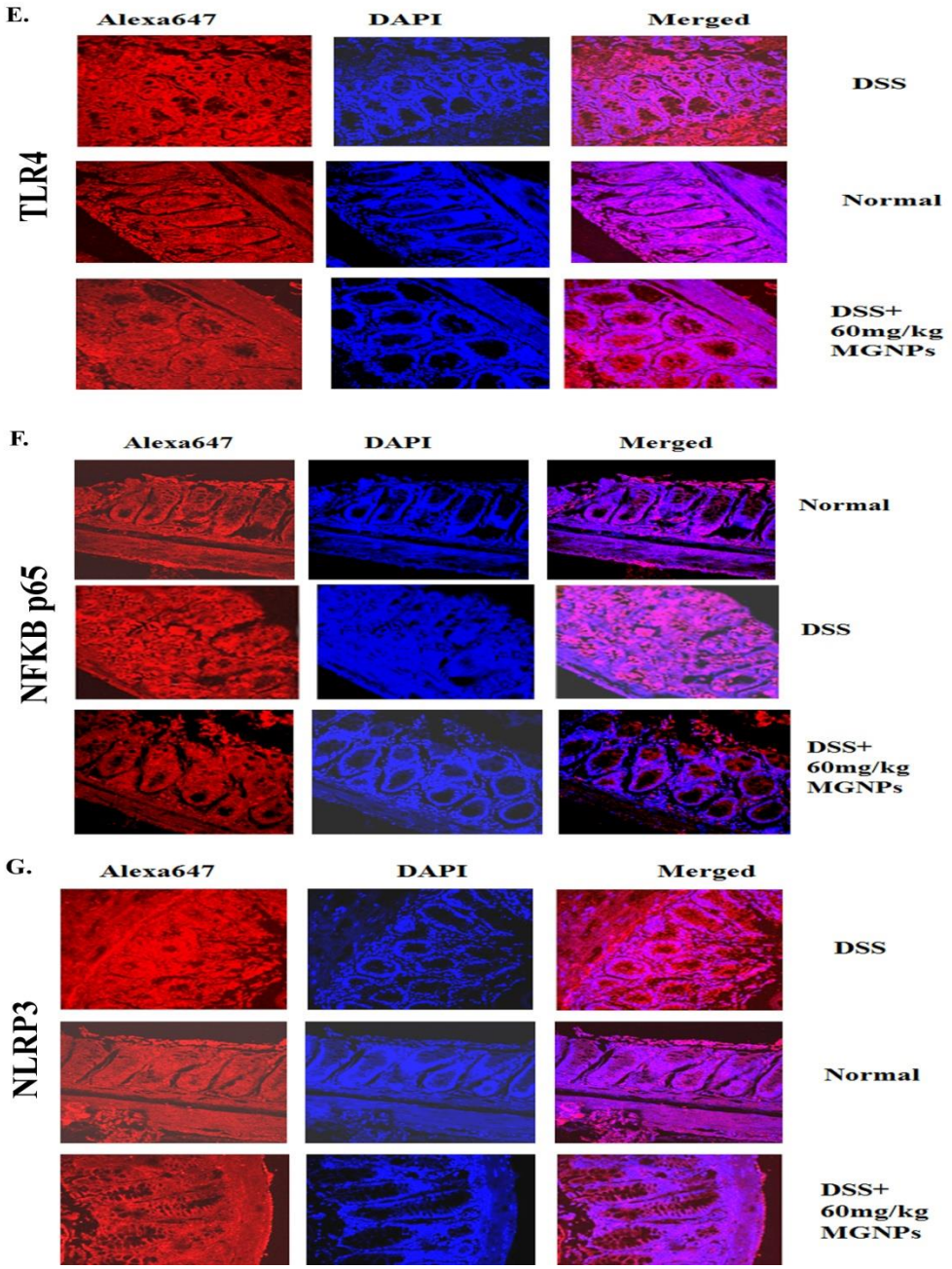

Figure 5: Effect of MOR, MGNPs (d1 & d2) and 5-ASA on the level of (A) TNF-α, IL-β, IL-6, TGF-β in the liver tissue lysate of arsenic challenged mice as seen in ELISA analysis. Data are one of the three representative experiments ± SD. (B) shows the effect of MOR, MGNPs (d1 & d2) and 5-ASA on protein expression of nuclear NF-kBp65 and NF-kBp50, IL-8, IL-6, IL-10, TGF-β, TNF-α, IL-17, iNOS, TLR4, MyD88, IKKB, p-IKKB, IκBα, p-IκBα, p38MAPK, p-p38MAPK (western blot analysis). (C) shows the expression of TLR4, NF-kBp65and NLRP3 (confocal images) in DSS exposed mice.

MGNPs restore the DSS induced histological changes of colon, liver and kidney

Over expressed inflammatory factors and ROS damage colonic, liver and kidney tissues in DSS induced ulcerative colitis. Damaged hepatocytes, portal inflammatory infiltration cells were seen in the liver tissue section of DSS-colitis group mice. When DSS exposed mice were treated with 60 mg/kg of MGNPs as shown in Figure 6A, liver histology was almost normal with the reduced dilation of sinusoids, clear central veins, undamaged hepatic cells and minimum or no infiltrated inflammatory cells.

The histological structure of kidney tissue showed normal renal tubules in the control group. But, the DSS-colitis group showed reduced and distorted glomeruli, dilated tubules, mild necrosis, and inflammatory infiltration cells, inflated epithelium with smaller capillary space and obstruction of renal blood vessel (Figure 6B). The DSS+MGNPs (60 mg/kg) or DSS + ASA group showed minimum infiltration of inflammatory cells, and the renal tubules appeared almost normal.

Histological studies of colon showed that DSS-colitis group has a serious damage in the normal framework of colon tissues with focal necrosis of the mucosa and submucosa along with inflammatory cell infiltration and ulceration. Treatment with 150mg/kg MOR, 20 and 60 mg/kg of MGNPs and 75mg/kg of ASA improved the crypt architecture (Figure 6C). The DSS exposed mice treated with 60 mg/kg of MGNPs or 75mg/kg of ASA showed almost normal mucosal architecture with a regular quantity of goblet cells, firmly packed glands with crypts.

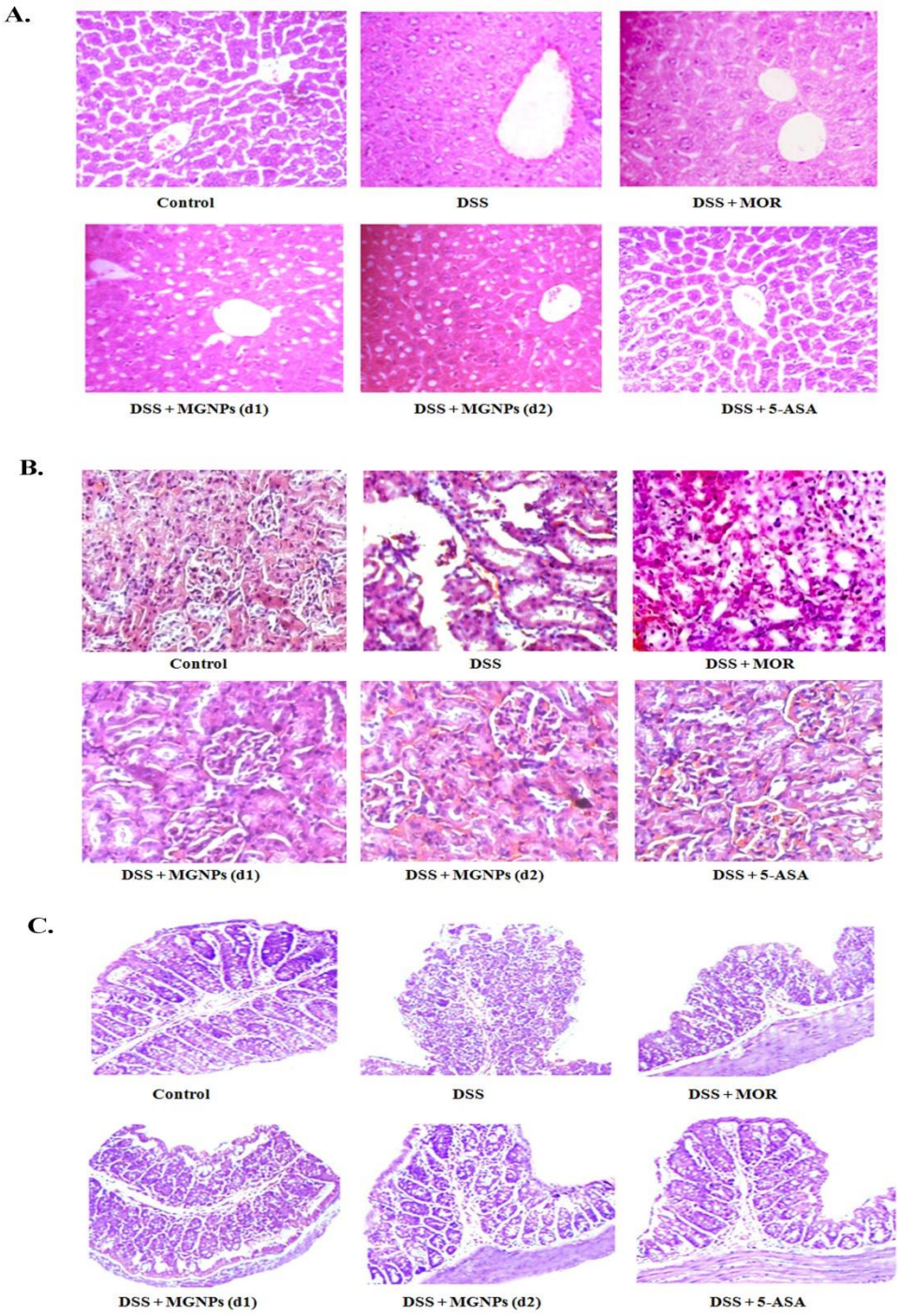

Figure 6: Effect of MOR, MGNPs (d1 & d2) and 5-ASA on liver, kidney and colon tissue apoptosis and histology. Architecture of liver tissue section following treatment without or with MOR, MGNPs (d1 & d2) and 5-ASA in DSS exposed mice.

Tissue Distribution Study of MGNPs in Various Organs

At several time points, content of nanoparticles in several organ and serum were examined by HPLC after treated with a single dose of MGNPs orally in mice. The Figure 7 shows, the different degree of MGNPs present in different organs. In liver highest concentration of MGNPs was found at 2h which slowly lowered with time and was lowest at 72h. In different organs, concentration of MGNPs followed the order, liver>kidney≥ colon> lung>serum. With time, in all organs the concentration of MGNPs was reduced slowly which indicate the negligible or no accumulation of MGNPs in the tissues and a moderate removal of the nanoparticles from the body.

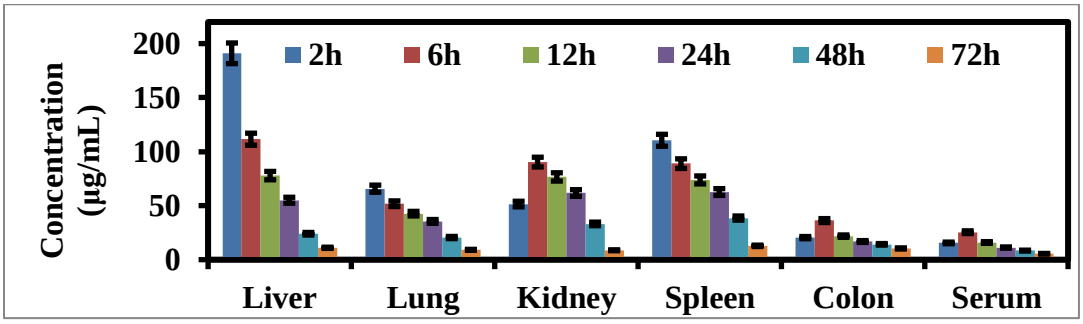

Figure 7: Tissue distribution studies of MGNPs in various organs.

Mean concentration of morin in liver, lungs, kidneys, spleen, and serum at 2, 6, 12, 24, 48, and 72 h after oral administration of single dose of MGNPs and (n = 3, mean ± SD) in mice.

Discussion:

Ulcerative colitis is characterized by chronic inflammatory disorder of the large intestine. It has been commonly accompanied with the release of inflammatory mediators together with pro-inflammatory cytokines and up-regulated reactive oxygen species (ROS) [218]. A absolute treatment of UCs is still missing. The primary complication arises because of the fact that the cause of UC is not fully understood. Therefore, preventive strategies were followed to cure UC.

Morin is the most abundant phytochemicals commonly available on many fruits and vegetables. It has antioxidant, anti-inflammatory, immunomodulatory and apoptotic properties [219]. But the therapeutic efficacy of morin (MOR) is severely limited due to its insolubility, poor bioavailability, high metabolism and rapid elimination from the human body [220]. There are several reports of the protective effect of different polyphenols like quercetin, tannic acid, gallic

acid, naringenine, berberine, EGCG, curcumin in the treatment of UC [221-227]. Also effect of Morin on an experimental model of acute colitis in rats was reported earlier [228]. But in best of my knowledge the effect of polyphenol reduced GNPs on UC is not reported till now.

GNPs are widely used sparkling tool for biomedical treatment. Unique properties and simple synthesis technique of GNPs make them perfect for the clinical area [229]. The GNPs preparation by "green synthesis" method is environment friendly and minimizes the production of harmful chemical and toxic byproducts. Antioxidant and anti-inflammatory effect of Gold nanoparticles (GNPs) was also reported [230].

In the present study, we prepared morin reduced spherical GNPs (MGNPs) with the size 33 nm which is stable for a long time without any presence of stabilizing agent. The previous studies have shown that GNPs at this size did not create any detectable toxicity examined by histology study, hematological analysis and serum biochemistry [231]. Toxicity study of GNPs by IP was performed by a group of researchers at the dose 320 to 3200 μg/kg/day which results no such effect on survival, weight, tissue histology and blood parameter [232].

In the present study we checked the effect of MGNPs on the orally treated colitis mice using doses 20 and 60 mg/kg. Effect of GNPs depends on their size, shape, zeta potential, stabilizing agent, the route of treatment, and duration [233]. A previous report indicate that the GNPs >15 nm are not toxic in any cell-type, and this is because these sizes did not cross the blood–brain barrier [234]. Schleh et al. suggested that orally treated GNPs in the size range of 5–200 nm were most bioavailable at the size of 18 nm in rats [245]. GNPs mainly enter to the cells by RME pathways [236]. The reported optimal particle size for RME is at 25–60 nm for spherical particles. MGNPs gave the smallest hydrodynamic size of 33 nm and so it was most suitable for RME in biological fluids. Therefore the effect of MGNPs is higher than free Morin.

In this present study we investigate the effect of morin reduced gold naonoparticles in DSS-induced ulcerative colitis. The primary biochemical results indicated the high level of liver function markers AST, ALT, ALP along with the elevated kidney function markers e.g. serum creatinine, urea and uric acid due to DSS induction with saline. This elevated biochemical markers are the indication of liver and kidney injury. The biochemical results of the DSS-colitis group are in harmony with the histological abnormalities of colon, liver and kidney. Alteration in colon, liver, and kidney histology of DSS-colitis mice were reverted in different degree following the treatment of 150mg/kg MOR, 20 and 60 mg/kg of MGNPs and 75mg/kg of ASA.

As seen in the biochemical and immunological studies, 60 mg/kg of MGNPs strongly prevented DSS induced histological abnormalities.

After oral administration of MGNPs in the DSS-colitis mice, it appeared to be accumulated in liver followed by kidney [237]. MPO activity was used as a biochemical indicator to identify inflammatory infiltration in the colon tissues [238] and it also participate in the inflammation [239]. Several studies suggested that the polyphenol has the efficacy in regulating the MPO activity, thereby regulates the MPO-mediated ROS production, tissue injury and colonic inflammation [240]. Our data showed that the high level of MPO activity in DSS exposed mice was significantly reduced following administration of 60mg/kg MGNPs which indirectly controlled antioxidants and thereby increased its anti-inflammatory properties.

Alteration of values of hematological parameters including WBC, RBC, Hb, PLT are the indication of inflammation as they help the body fight to infection and other diseases. The decreased values of these parameters are the indication of decrease in the immune system, and so the organ becomes susceptible to any infection. In our result, the DSS treatment showed the decrease in value of hematological parameters which were gradually restored upon treatment of 60mg/kg of MGNPs.

Colitis also increase the oxidative stress by ROS generation and a clear imbalance was observed in the antioxidant defense enzymes [241]. Our current study showed a notable reduced the level of some antioxidant markers e.g. GSH, SOD and CAT in colon, liver and kidney after the DSS-colitis induction and over production of ROS [242]. At the time of colitis down-regulations of the GSH levels and some essential trace elements, such as zinc and selenium was observed [243]. Those data was markedly uplifted in the DSS + MGNPs (60mg/kg) group. Spherical GNPs (2.5 mg/kg) was treated by IP in male Wister diabetic rats altered the oxidative stress; corrected the glucose and lipid profile levels [244]. Some previous work suggested that the anti-inflammatory and antioxidant properties of GNPs were observed because of its ability to regulate the ROS generation and early proinflammatory cytokines production and free radicals scavenging activity [245]. Furthermore, the level of lipid peroxidation marker MDA was markedly enhanced in the DSS-colitis group in comparison to the normal group. It was altered in the DSS + MGNPs 60 mg/kg group [246].

In colitis group an imbalance between proinflammatory and anti-inflammatory cytokines was observed and hence in the eternal body [247]. Our study showed that the DSS-colitis induction is

correlated with the over expression of pro-inflammatory cytokines such as TNF-α, IL-1β, IL-6 and TGF-β. The treatment of MGNPs strongly down-regulated the inflammatory response by controlling the levels of these pro-inflammatory cytokines. The previous work also suggested the similar observation, where GNPs blocked the proinflammatory cytokines (IL-2 and IL-6) production or showed the decrease in expression of IL-6 and TNF-α [248].

NF-κB is the main transcription factor which regulates the generation of proinflammatory cytokines [201]. NF-κB also takes part in controlling the activation of inflammasomes [203]. So, down-regulated NF-κB activation is an identification of chronic inflammatory diseases. The previous study suggests that morin constrained the activation of NF-κB and NF-κB regulated gene expression which results suppression of inflammation [248]. Western blot analysis showed that with upregulation of nuclear NF- κB p65 with DSS-colitis mice which gradually downregulated in the mice subjected MGNPs treatment. NF-κB also controlled the over-expression of iNOS during inflammation. Western blot analysis data showed that the level of iNOS was enhanced by DSS and this was significantly reduced in mice co-treated with MGNPs 60 mg/kg.

The tissue distribution study showed that accumulation of MGNPs in the liver is higher at 2h followed by colon and kidney. The concentration of MGNPs decreased in gradually upto 72h. A significant amount of MGNPs in the liver at all time points is the indication of intra-hepatic circulation and drug detoxification. Also, a trivial amount of MGNPs in the kidney, colon, lungs, and serum at 72 h demonstrated higher metabolism. Lower concentration of MGNPs in serum was suggesting the rapid penetration of MGNPs in various target organs, following the oral administration.

Conclusion:

We can conclude that, this study suggests the higher dose of MGNPs (60 mg/kg) showed the remarkable therapeutic efficacy on DSS-colitis. The greater effect MGNPs can be explained by the increase in bioavailability of morin. The anti-inflammatory activity can be thought about the primary responsible factors of the MGNPs to show the protective effect. The results suggested that MGNPs inhibited ROS production and enhanced antioxidant potential. It also improves the architecture of the damaged tissues, reduce the inflammation, and restrain the response of inflammatory cytokine. Therefore MGNPs may represent a therapeutic option for colitis treatment.

References:

1. Natural Antioxidants in Foods and Medicinal Plants: Extraction, Assessment and Resources. Dong-Ping Xu,Ya Li,Xiao Meng,Tong Zhou,Yue Zhou, Jie Zheng, Jiao-Jiao Zhang, and Hua-Bin Li. Int J Mol Sci. 2017 Jan; 18(1): 96. Doi: 10.3390/ijms18010096.
2. The growing use of herbal medicines: issues relating to adverse reactions and challenges in monitoring safety. Martins Ekor.Front Pharmacol. 2013; 4: 177. Doi: 10.3389/fphar.2013.00177.
3. Plant polyphenols as dietary antioxidants in human health and disease. Kanti Bhooshan Pandey and Syed Ibrahim Rizvi. Oxid Med Cell Longev. 2009 Nov-Dec; 2(5): 270–278. Doi: 10.4161/oxim.2.5.9498.
4. Oxidative Stress: Harms and Benefits for Human Health. Gabriele Pizzino, Natasha Irrera, Mariapaola Cucinotta, Giovanni Pallio, Federica Mannino, Vincenzo Arcoraci, Francesco Squadrito, Domenica Altavilla, and Alessandra Bitto. Oxid Med Cell Longev. 2017; 2017: 8416763. Doi: 10.1155/2017/8416763.
5. Important Flavonoids and Their Role as a Therapeutic Agent. Asad Ullah,Sidra Munir,Syed Lal Badshah,Noreen Khan,Lubna Ghani,Benjamin Gabriel Poulson,Abdul-Hamid Emwas,and Mariusz Jaremko.Molecules. 2020 Nov; 25(22): 5243.doi: 10.3390/molecules25225243.
6. Drug development: Lessons from nature. Sunil Mathur and Clare Hoskins. Biomed Rep. 2017 Jun; 6(6): 612–614. Doi: 10.3892/br.2017.909.
7. Morin: a promising natural drug, Curr. Med. Chem. A. Caselli, P. Cirri, A. Santi, P. Paoli. 23 (8) (2016) 774–791.
8. Morin hydrate: botanical origin, pharmacological activity and its applications: a mini-review, J.V. Gopal, Pharm. J. 5 (2013) 123–126.
9. Overview of morin and its complementary role as an adjuvant for anticancer agents, S. Solairaja, M.Q. Andrabi, N.R. Dunna, S. Venkatabalasubramanian, Nutr. Cancer (2020) 1–16.
10. Solid state electrochemical oxidation mechanisms of morin in aqueous media, Electroanal. P. Janeiro, A.M.O. Brett, Int. J. Dev. Fund. Prac. Asp. Elect. 17 (2005) 733–738.

11. Efficacy of Morin as a Potential Therapeutic Phytocomponent: Insights into the Mechanism of Action. Amarendranath Choudhury, Indrajeet Chakraborty, Tuhin Subhra Banerjee, Dhilleswara Rao Vana and Dattatreya Adapa. International Journal of Medical Research & Health Sciences, 2017, 6(11): 175-194. ISSN No: 2319-5886.
12. Morin sulfates/glucuronides exert anti-inflammatory activity on activated macrophages and decreased the incidence of septic shock, S.-H. Fang, Y.-C. Hou, W.-C. Chang, S.-L. Hsiu, P.-D.L. Chao, B.-L. Chiang, Life Sci. 74 (6) (2003) 743–756.
13. Morin protects LPS-induced mastitis via inhibiting NLRP3 inflammasome and NF-κB signaling pathways, S. Yu, X. Liu, D. Yu, E. Changyong, J. Yang, Inflammation 43 (2020) 1293–1303.
14. Suppression in PHLPP2 induction by morin promotes Nrf2-regulated cellular defenses against oxidative injury to primary rat hepatocytes, F. Rizvi, A. Mathur, S. Krishna, M.I. Siddiqi, P. Kakkar, Redox Biol. 6 (2015) 587–598.
15. Antioxidant and cytoprotective effects of morin against hydrogen peroxide-induced oxidative stress are associated with the induction of Nrf- 2mediated HO-1 expression in V79-4 Chinese hamster lung fibroblasts, M. Lee, H.J. Cha, E. Choi, M. Han, S. Kim, G.Y. Kim, S. Hong, C. Park, S.K. Moon, S.J. Jeong, Int. J. Mol. Med. 39 (2017) 672–680.
16. The flavonoid morin from Moraceae induces apoptosis by modulation of Bcl-2 family members and Fas receptor in HCT 116 cells, H.B. Hyun, W. Lee, S.I. Go, A. Nagappan, C. Park, M. Han, S. Hong, G. Kim, G. Kim, J. Cheong, Int. J. Oncol. 6 (2015) 2670–2678.
17. Morin augments anticarcinogenic and antiproliferative efficacy against 7, 12-dimethylbenz (a)-anthracene induced experimental mammary carcinogenesis, R. Nandhakumar, K. Salini, S.N. Devaraj, Mol. Cell. Biochem. 364 (1–2) (2012) 79–92.
18. Morin regulates the expression of NF-κB-p65, COX-2 and matrix metalloproteinases in diethylnitrosamine induced rat hepatocellular carcinoma, V. Sivaramakrishnan, S.N. Devaraj, Chem. Biol. Interact. 180 (3) (2009) 353–359.
19. Attenuation of N-nitrosodiethylamine-induced hepatocellular carcinogenesis by a novel flavonol-Morin, V. Sivaramakrishnan, P.N.M. Shilpa, V.R.P. Kumar, S.N. Devaraj, Chem. Biol. Interact. 171 (1) (2008) 79–88.

20. Morin attenuates cigarette smoke-induced lung inflammation through inhibition of PI3K/AKT/NF- κB signaling pathway, Cai Baoning, Gan Xiangfeng, He Jinxi, Zhixiong Wei, Bo Qiao, Int. Immunopharmacol. 63 (2018) 198–203.
21. The effects of morin on lipopolysaccharide-induced acute lung injury by suppressing the lung NLRP3 inflammasome,Z. Tianzhu, Y. Shihai, D. Juan, Inflammation 37 (6) (2014) 1976–1983.
22. Morin hydrate inhibits TREM-1/TLR4-mediated inflammatory response in macrophages and protects against carbon tetrachloride-induced acute liver injury in mice, X. Li, Q. Yao, J. Huang, B. Xu, Q. Jin, F. Cheng, C. Tu, Front. Pharmacol. 10 (2019) 1089.
23. Morin exerts neuroprotection via attenuation of ROS induced oxidative damage and neuroinflammation in experimental diabetic neuropathy, P. Bachewal, C. Gundu, V.G. Yerra, A.K. Kalvala, A. Areti, A. Kumar, Biofactors 44 (2018) 109–122.
24. Morin mitigates chronic constriction injury (CCI)-induced peripheral neuropathy by inhibiting oxidative stress induced PARP over-activation and neuroinflammation, P. Komirishetty, A. Areti, R. Sistla, A. Kumar, Neurochem. Res. 41 (2016) 2029–2042.
25. Ameliorative effect of morin hydrate, a flavonoid against gentamicin induced oxidative stress and nephrotoxicity in sprague-dawley rats, V.G. Jonnalagadda, S. Pittala, M. Lahkar, V. Pradeep, Int. J. Pharm. Pharm. Sci. 6 (2013) 852–856.
26. The insulin-mimetic effect of Morin: a promising molecule in diabetes treatment, P. Paoli, P. Cirri, A. Caselli, F. Ranaldi, G. Bruschi, A. Santi, G. Camici, Biochim. Biolphys. Acta 1830 (2013) 3102–3111.
27. Morin protects gastric mucosa from nonsteroidal anti-inflammatory drug, indomethacin induced inflammatory damage and apoptosis by modulating NF-κB pathway, K. Sinha, P. Sadhukhan, S. Saha, P.B. Pal, P.C. Sil, Biochim. Biophys. Acta (BBA) Gen. Subj. 50 (2015) 769–783.
28. Role of MAPK/NF-κB pathway in cardioprotective effect of Morin in isoproterenol induced myocardial injury in rats, V.K. Verma, S. Malik, S.P. Narayanan, E. Mutneja, A.K. Sahu, J. Bhatia, D.S. AryaMol. Biol. Rep. 46 (2019) 1139–1148.
29. Nanotechnology, Book Chapter-36, Information Resources in Toxicology (Fourth Edition), 2009, Pages 321-328. https://doi.org/10.1016/B978-0-12-373593-5.00036-7.

30. Nanomedicine, Book Chapter 12,Immune Rebalancing, The Future of Immunosuppression, 2016, Pages 251-274. https://doi.org/10.1016/B978-0-12-803302-9.00012-9.
31. Applications of nanoparticles in biology and medicine. OV Salata, J Nanobiotechnology. 2004; 2: 3.doi: 10.1186/1477-3155-2-3.
32. Biopolymer and polymer nanoparticles and their biomedical applications. Book Chapter 11,Handbook of Nanostructured Materials and Nanotechnology, Volume 5, 2000, Pages 577-635.
33. The Potential Advantages of Nanoparticle Drug Delivery Systems in Chemotherapy of Tuberculosis. Kevin Kisich, Michael D. Iseman, and Leonid Heifets, Svetlana Gelperina, Am J Respir Crit Care Med. 2005 Dec 15; 172(12): 1487–1490. Doi: 10.1164/rccm.200504-613PP.
34. Drug Bioavailability. Gary Price, Deven A. Patel.In: StatPearls [Internet]. 2022 Jun 23. PMID: **32496732,** Bookshelf ID: NBK557852.
35. Chitin and Chitosan: Production and Application of Versatile Biomedical, Nanomaterials. Daniel Elieh-Ali-Komiand Michael R Hamblin, Int J Adv Res (Indore). 2016 Mar; 4(3): 411–427.
36. Chitosan nanoparticles containing *Physalis alkekengi-L* extract: preparation, optimization and their antioxidant activity, Reza Mahmoudi, Maryam Tajali Ardakani, Behnam Hajipour Verdom, Abouzar Bahgeri, Hossein Mohammad-Beigi, Farhang Aliakbari, Zeinab Salehpour, Mohsen Alipour, Sajad Afrouz and Hassan Bardania, *Bull. Mater. Sci.* (2019) 42:131. https://doi.org/10.1007/s12034-019-1815-3.
37. Chitosan Nanoparticles at the Biological Interface: Implications for Drug Delivery, Noorjahan Aibani, Raj Rai, Parth Patel, Grace Cuddihy, and Ellen K. Wasan, Pharmaceutics. 2021 Oct; 13(10): 1686. Doi: 10.3390/pharmaceutics13101686.
38. Contribution of Tocopherols in Commonly Consumed Foods to Estimated Tocopherol Intake in the Chinese Diet, Yu Zhang, Xin Qi, Xueyan Wang, Xuefang Wang, Fei Ma, Li Yu, Jin Mao, Jun Jiang, Liangxiao Zhang, and Peiwu Li, Front Nutr. 2022; 9: 829091. doi: 10.3389/fnut.2022.829091.
39. Vitamins C and E: Beneficial effects from a mechanistic perspective, Maret G. Traberand Jan F. Stevens, Free Radic Biol Med. Free Radic Biol Med. 2011 Sep 1; 51(5): 1000–1013. Doi: 10.1016/j.freeradbiomed.2011.05.017.

40. Vitamin E as a Treatment for Nonalcoholic Fatty Liver Disease: Reality or Myth?,Hamza El Hadi, Roberto Vettor, and Marco Rossato, Antioxidants, 2018 Jan; 7(1): 12. Doi: 10.3390/antiox7010012.
41. Cyclodextrinsthe Molecular Container. Sanjoy Kumar Das, Rajan Rajabalaya, Sheba David, Nasimul Gani, Jasmina Khanam, Arunabha Nanda. Research Journal of Pharmaceutical, Biological and Chemical Sciences.2013, RJPBCS Volume 4, ISSN: 0975-8585.
42. Controlled drug delivery mediated by cyclodextrin-based supramolecular self-assembled carriers: From design to clinical performances, Jana GHITMAN, Stefan Ioan VOICU, Carbohydrate Polymer Technologies and Applications. https://doi.org/10.1016/j.carpta.2022.100266.
43. Recent Advances in Host–Guest Self-Assembled Cyclodextrin Carriers: Implications for Responsive Drug Delivery and Biomedical Engineering, Jitendra Wankar, Niranjan G. Kotla, Sonia Gera, Swetha Rasala, Abhay Pandit, Yury A. Rochev. Adv. Func. Mat., 05 February 2020, https://doi.org/10.1002/adfm.201909049.
44. Cyclodextrin Based Nanoparticles for Drug Delivery and Theranostics, Dipak Dilip Gadade and Sanjay Sudhakar Pekamwar, Adv Pharm Bull. 2020 Jun; 10(2): 166–183. Doi: 10.34172/apb.2020.022.
45. Recent Advances in Metal Decorated Nanomaterials and Their Various Biological Applications: A Review, Asim Ali Yaqoob, Hilal Ahmad, Tabassum Parveen, Akil Ahmad, Mohammad Oves, Iqbal M. I. Ismail, Huda A. Qari, Khalid Umar, and Mohamad Nasir Mohamad Ibrahim, Front Chem. 2020; 8: 341. 2020 May 19. doi: 10.3389/fchem.2020.00341.
46. Gold nanoparticles (GNPs) in biomedical and clinical applications: A review, Muzahidul I. Anik, Niaz Mahmud, Abdullah Al Masud, Maruf Hasan, October 2021, Nano Select 3(4), DOI: 10.1002/nano.202100255.
47. Biocompatibility and Cytotoxicity of Gold Nanoparticles: Recent Advances in Methodologies and Regulations, Małgorzata Kus-Liśkiewicz, Patrick Fickers, and Imen Ben Tahar, Int J Mol Sci. 2021 Oct; 22(20): 10952, doi: 10.3390/ijms222010952.

48. Gold nanoparticles: a novel paradigm for targeted drug delivery, Inorganic and nano-metal chemistry, Kamalavarshini S, Ranjani S, Hemalatha S, https://doi.org/10.1080/24701556.2021.2025077.
49. Physical Properties of Different Gold Nanoparticles: Ultraviolet-Visible and Fluorescence Measurements, Mohamed Anwar K Abdelhalim, Mohsen Mady, Magdy Ghannam, May 2012, Journal of Nanomedicine & Nanotechnology, DOI: 10.4172/2157-7439.1000133.
50. Green Synthesis of Gold Nanoparticles: A novel, Environment-Friendly, Economic, Safe Approach, Niladry Sekhar Ghosh, Ekta Pandey, Madan Kaushik, Jai Prakash Kadian, Bhupendra Chauhan, Ajeet yadav and Ranjit Singh, Biomedical and pharmacology journal, DOI : https://dx.doi.org/10.13005/bpj/2301.
51. Toxicity and Biokinetics of Colloidal Gold Nanoparticles. Mi-Rae Jo, Song-Hwa Bae, Mi-Ran Go, Hyun-Jin Kim, Yun-Gu Hwang, Soo-Jin Choi, *Nanomaterials* 2015, *5*(2), 835-50; https://doi.org/10.3390/nano5020835.
52. A review on gold nanoparticles (GNPs) and their advancement in cancer therapy, Shabbir Hussain and Muhammad Amjad, International Journal of Nanomaterials, Nanotechnology and Nanomedicine, ISSN: 2455-3492, 7(1):019-025. DOI: 10.17352/2455-3492.000040.
53. Micro-Computed Tomography Detection of Gold Nanoparticle-Labelled Mesenchymal Stem Cells in the Rat Subretinal Layer, Pooi Ling Mok, Sue Ngein Leow, Avin Ee-Hwan Koh, Hairul Harun Mohd Nizam, Suet Lee Shirley Ding, Chi Luu, Raduan Ruhaslizan,[4] Hon Seng Wong, Wan Haslina Wan Abdul Halim, Min Hwei Ng, Ruszymah Binti Hj. Idrus, Shiplu Roy Chowdhury, Catherine Mae-Lynn Bastion, Suresh Kumar Subbiah, Akon Higuchi, Abdullah A. Alarfaj, and Kong Yong Then, Int J Mol Sci. 2017 Feb; 18(2): 345, doi: 10.3390/ijms18020345.
54. Functionalized Gold Nanoparticles and Their Biomedical Applications, Pooja M. Tiwari, Komal Vig, Vida A. Dennis, and Shree R. Singh, Nanomaterials (Basel). 2011; 1(1): 31–63, doi: 10.3390/nano1010031.
55. The Applications of Gold Nanoparticles in the Diagnosis and Treatment of Gastrointestinal Cancer, Zhijing Yang, Dongxu Wang, Chenyu Zhang, Huimin Liu, Ming Hao, Shaoning Kan, Dianfeng Liu, and Weiwei Liu. Front Oncol. 2021; 11: 819329, doi: 10.3389/fonc.2021.819329.

56. Gold nanoparticles as novel agents for cancer therapy, S Jain, MB, Bch, D G Hirst, PhD, and J M O'Sullivan, MD, Br J Radiol. 2012 Feb; 85(1010): 101–113, doi: 10.1259/bjr/59448833.

57. Gold nanoparticles for photothermal cancer therapy. Jeremy B. Vines, Jee-Hyun Yoon, Na-Eun Ryu, Dong-Jin Lim and Hansoo Park, Front. Chem., 05 April 2019, Nanoscience, https://doi.org/10.3389/fchem.20.19.00167.

58. Gold nanoparticle mediated combined cancer therapy, Celina Yang, Kyle Bromma, Caterina Di Ciano-Oliveira, Gaetano Zafarana, Monique van Prooijen & Devika B. Chithrani, Cancer Nanotechnology, volume 9, Article number: 4 (2018).

59. Therapeutic effects of the gold nanoparticle on obesity-triggered neuroinflammation: a review, Jessica Abel, Mariella Reinol da Silva, Ana Beatriz Costa, Mariana Pacheco de Oliveira, Larissa Espindola da Silva, Larissa Marques Dela Vedova, Talita Farias Mendes, Gisele Tartari, Jonathann Correa Possato, Gabriela Kozuchovski Ferreira, Ricardo Andrez Machado de Avila, Gislaine Tezza Rezin, J Drug Target, 2022 Sep 15;1-8.DOI: 10.1080/1061186X.2022.2120613.

60. Potential of Gold Nanoparticles for Noninvasive Imaging and Therapy for Vascular Inflammation. Hisanori Kosuge, Maki Nakamura, Ayako Oyane, Kazuko Tajiri, Nobuyuki Murakoshi, Satoshi Sakai, Akira Sato, Atsushi Taninaka, Taishiro Chikamori, Hidemi Shigekawa & Kazutaka Aonuma, Molecular Imaging and Biology volume 24, pages692–699 (2022).

61. Linlin Chen, Huidan Deng, Hengmin Cui, Jing Fang, Zhicai Zuo, Junliang Deng, Yinglun Li, Xun Wang, and Ling Zhao, Inflammatory responses and inflammation-associated diseases in organs, Oncotarget. 2018 Jan 23; 9(6): 7204–7218. Doi: 10.18632/oncotarget.23208.

62. Inflammatory and Molecular Pathways in Heart Failure-Ischemia, HFpEF and Transthyretin Cardiac Amyloidosis. Michels da Silva D, Langer H, Graf T. Int J Mol Sci. 2019 May 10;20(9).

63. Effects of short- and long-term exposures to particulate matter on inflammatory marker levels in the general population. Tsai DH, Riediker M, Berchet A, Paccaud F, Waeber G, Vollenweider P, Bochud M. Environ Sci Pollut Res Int. 2019 Jul;26(19):19697-19704.

64. Chronic Inflammation, Roma Pahwa; Amandeep Goyal; Ishwarlal Jialal, StatPearls, 2022, NCBI Bookshelf. A service of the National Library of Medicine, National Institutes of Health.

65. Anti-Inflammatory Therapy in Chronic Disease: Challenges and Opportunities, Ira Tabas and Christopher K. Glass, Science. 2013 Jan 11; 339(6116): 166–172. Doi: 10.1126/science.1230720.

66. Oxidative Stress: Harms and Benefits for Human Health, Gabriele Pizzino, Natasha Irrera, Mariapaola Cucinotta, Giovanni Pallio, Federica Mannino, Vincenzo Arcoraci, Francesco Squadrito, DomenicaAltavilla, and Alessandra Bitto, Oxid Med Cell Longev. 2017; 2017: 8416763.Doi: 10.1155/2017/8416763.

67. Oxidative Stress and Inflammation, Samreen Soomro, Mar. 31, 2019, 1, Open Journal of Immunology DOI: 10.4236/oji.2019.91001.

68. Cardiovascular Diseases, Cancers, and Chronic Obstructive Pulmonary Diseases, Howson CP, Harrison PF, Law M, 1996, NCBI Bookshelf. A service of the National Library of Medicine, National Institutes of Health.

69. Reactive Oxygen Species in Inflammation and Tissue Injury, Manish Mittal, Mohammad Rizwan Siddiqui, Khiem Tran, Sekhar P. Reddy, and Asrar B. Malik, Antioxid Redox Signal. 2014 Mar 1; 20(7): 1126–1167. Doi: 10.1089/ars.2012.5149.

70. Oxidative Stress: An Essential Factor in the Pathogenesis of Gastrointestinal Mucosal Diseases, Asima Bhattacharyya, Ranajoy Chattopadhyay, Sankar Mitra, and Sheila E. Crowe, Physiol Rev. 2014 Apr; 94(2): 329–354. Doi: 10.1152/physrev.00040.2012.

71. Lipid Peroxidation, Encyclopedia of Toxicology (Second Edition), Zhengwei Cai, 2005, Pages 730-734.

72. Heavy Metals Toxicity and the Environment, Paul B Tchounwou, Clement G Yedjou, Anita K Patlolla, and Dwayne J Sutton, EXS. 2012; 101: 133–164.Doi: 10.1007/978-3-7643-8340-46.

73. Free radicals in the physiological control of cell function, Wulf Dröge, Physiol Rev, 2002 Jan;82(1):47-95. Doi: 10.1152/physrev.00018.2001.
74. Systematic Understanding of Pathophysiological Mechanisms of Oxidative Stress-Related Conditions—Diabetes Mellitus, Cardiovascular Diseases, and Ischemia–Reperfusion Injury, Mengxue Wang, Yun Liu, Yin Liang, Keiji Naruse and Ken Takahashi, Front. Cardiovasc. Med., doi: 10.3389/fcvm.2021.649785.
75. Free radicals, antioxidants and functional foods: Impact on human health, V. Lobo, A. Patil, A. Phatak, and N. Chandra, Pharmacogn Rev. 2010 Jul-Dec; 4(8): 118–126. Doi: 10.4103/0973-7847.70902.
76. Reactive oxygen species (ROS) and response of antioxidants as ROS-scavengers during environmental stress in plants, Kaushik Das and Aryadeep Roychoudhury, Frontiers in Environ. Sci., Doi: 10.3389/fenvs.2014.00053.
77. Natural Antioxidants in Foods and Medicinal Plants: Extraction, Assessment and Resources, Dong-Ping Xu,[1] Ya Li,[1] Xiao Meng,[1] Tong Zhou,[1] Yue Zhou,[1] Jie Zheng,[1] Jiao-Jiao Zhang,[1] and Hua-Bin Li, Int J Mol Sci. 2017 Jan; 18(1): 96. Doi: 10.3390/ijms18010096.
78. The importance of antioxidants which play the role in cellular response against oxidative/nitrosative stress: current state, Ergul Belge Kurutas, Nutr J. 2016; 15: 71. Doi: 10.1186/s12937-016-0186-5.
79. Nuclear factor (erythroid-derived 2)-like-2 factor (Nrf2), a key regulator of the antioxidant response to protect against atherosclerosis and nonalcoholic steatohepatitis, Anisha A Gupte [1], Christopher J Lyon, Willa A Hsueh, Curr Diab Rep, 2013 Jun;13(3):362-71.Doi: 10.1007/s11892-013-0372-1.
80. NRF2, a Key Regulator of Antioxidants with Two Faces towards Cancer, Jaieun Kim and Young-Sam Keum, Oxidative Medicine and Cellular Longevity, https://doi.org/10.1155/2016/2746457.
81. The Molecular Mechanisms Regulating the KEAP1-NRF2 Pathway, Liam Baird and Masayuki Yamamoto, Mol Cell Biol. 2020 Jul; 40(13): e00099-20. Doi: 10.1128/MCB.00099-20.
82. Nrf2:INrf2(Keap1) Signaling in Oxidative Stress, James W. Kaspar, Suresh K. Niture, and Anil K. Jaiswal, Free Radic Biol Med. 2009 Nov 1; 47(9): 1304–1309. Doi: 10.1016/j.freeradbiomed.2009.07.035.

83. Signal amplification in the KEAP1-NRF2-ARE antioxidant response pathway, Shengnan Liu, Jingbo Pi, Qiang Zhan, Redox Biology, https://doi.org/10.1016/j.redox.2022.102389.
84. Nrf2 in Cancer, Detoxifying Enzymes and Cell Death Programs, Tabitha Jenkins, Jerome Gouge, *Antioxidants* 2021, *10*(7), 1030; https://doi.org/10.3390/antiox10071030.
85. Redox Regulation of Cell Survival by the Thioredoxin Superfamily: An Implication of Redox Gene Therapy in the Heart, Md. Kaimul Ahsan, Istvan Lekli, Diptarka Ray, Junji Yodoi, and Dipak K. Das, Antioxid Redox Signal. 2009 Nov; 11(11): 2741–2758. Doi: 10.1089/ars.2009.2683.
86. Apoptosis, Pyroptosis, and Necrosis: Mechanistic Description of Dead and Dying Eukaryotic Cells, Susan L. Fink[1] and Brad T. Cookson, Infect Immun. 2005 Apr; 73(4): 1907–1916. Doi: 10.1128/IAI.73.4.1907-1916.2005.
87. Apoptosis: A Review of Programmed Cell Death, Susan Elmore, Toxicol Pathol. 2007; 35(4): 495–516. Doi: 10.1080/01926230701320337.
88. Caspase Functions in Cell Death and Disease, David R. McIlwain, Thorsten Berger, and Tak W. Mak, Cold Spring Harb Perspect Biol. 2013 Apr; 5(4): a008656. doi: 10.1101/cshperspect.a008656.
89. Mechanisms of Action of Bcl-2 Family Proteins, Aisha Shamas-Din, Justin Kale, Brian Leber, and David W. Andrews, Cold Spring Harb Perspect Biol. 2013 Apr; 5(4): a008714, doi: 10.1101/cshperspect.a008714.
90. Apoptosis: A review of pro-apoptotic and anti-apoptotic pathways and dysregulation in disease, Mauria A. O'Brien, DVM and Rebecca Kirby, J Vet Emerg Crit Care (San Antonio). 2008 Dec; 18(6): 572–585, doi: 10.1111/j.1476-4431.2008.00363.x.
91. The Role of Mitochondria in Apoptosis, Chunxin Wang and Richard J. Youle, Annu Rev Genet, Annu Rev Genet. 2009; 43: 95–118. Doi: 10.1146/annurev-genet-102108-134850.
92. Mechanisms of cytochrome *c* release from mitochondria, C Garrido, L Galluzzi, M Brunet, P E Puig, C Didelot & G Kroemer, Cell Death & Differentiation volume 13, pages1423–1433 (2006).
93. Emerging roles of caspase-3 in apoptosis, Alan G. Porter and Reiner U. JaÈ nicke, Cell Death and Differentiation (1999) 6, 99 ± 104.

94. Akt Regulates Cell Survival and Apoptosis at a Postmitochondrial Level, Honglin Zhou,[a] Xin-Ming Li,[a] Judy Meinkoth,[a] and Randall N. Pittman, J Cell Biol. 2000 Oct 30; 151(3): 483–494. doi: 10.1083/jcb.151.3.483.
95. A new role for the PI3K/Akt signaling pathway in the epithelial-mesenchymal transition, Wenting Xu, Zhen Yang, and Nonghua Lu, Cell Adh Migr. 2015 Jul-Aug; 9(4): 317–324. doi: 10.1080/19336918.2015.1016686.
96. The IκB kinase complex in NF-κB regulation and beyond, Michael Hinz and Claus Scheidereit, EMBO Rep. 2014 Jan; 15(1): 46–61. doi: 10.1002/embr.201337983.
97. Role of p53 in Cell Death and Human Cancers, Toshinori Ozaki and Akira Nakagawara, Cancers (Basel). 2011 Mar; 3(1): 994–1013. doi: 10.3390/cancers3010994.
98. The p53 family and programmed cell death, E. Christine Pietsch, Stephen M. Sykes, Steven B. McMahon, and Maureen E. Murphy, Oncogene. 2008 Oct 27; 27(50): 6507–6521, doi: 10.1038/onc.2008.315.
99. P53 Regulates Progression of Injury and Liver Regeneration After Acetaminophen Overdose. Prachi Borude, Bharat Bhushan, Hemantkumar Chavan, James L. Weemhoff, Hartmut Jaeschke, Partha Krishnamurthy, Udayan Apte, The FASEB journal. https://doi.org/10.1096/fasebj.31.1.
100. Hepatic hypoxia-inducible factors inhibit PPARα expression to exacerbate acetaminophen induced oxidative stress and hepatotoxicity. Li D, Du Y, Yuan X, Han X, Dong Z, Chen X, Wu H, Zhang J, Xu L, Han C, Zhang M, Xia Q. Free Radic Biol Med. 2017;110:102-116.
101. Oxidative stress as a crucial factor in liver diseases, Halina Cichoż-Lach and Agata Michalak, World J Gastroenterol. 2014 Jul 7; 20(25): 8082–8091. doi: 10.3748/wjg.v20.i25.8082.
102. Arsenic as an environmental and human health antagonist: A review of its toxicity and disease initiation, John Olabode Fatoki, Jelili Abiodun Badmus, Journal of Hazardous Materials Advances.
103. Biological effects and epidemiological consequences of arsenic exposure, and reagents that can ameliorate arsenic damage in vivo. Rao CV, Pal S, Mohammed A, Farooqui M, Doescher MP, Asch AS, Yamada HY. Oncotarget. 2017;8(34): 57605-57621.
104. Biomarkers of oxidative stress and damage in human populations exposed to arsenic. De Vizcaya-Ruiz A, Barbier O, Ruiz-Ramos R, Cebrian ME. Mutat Res. 2009;674(1-2):85-92.

105. Molecular mechanisms of hepatic apoptosis, K Wang, Cell Death Dis. 2014 Jan; 5(1): e996. Doi: 10.1038/cddis.2013.499.
106. Regulation of apoptosis in health and disease: the balancing act of BCL-2 family proteins, Rumani Singh, Anthony Letai, and Kristopher Sarosiek, Nat Rev Mol Cell Biol., Nat Rev Mol Cell Biol. 2019 Mar; 20(3): 175–193.doi: 10.1038/s41580-018-0089-8.
107. Uncovering pathogenic mechanisms of inflammatory bowel disease using mouse models of Crohn's disease-like ileitis: What is the right model? Cominelli F, Arseneau KO, Rodriguez-Palacios A, Pizarro TT. *Cell. Mol. Gastroenterol. Hepatol.* 4(1), 19–23 (2017).
108. Innate immune mechanisms of colitis and colitis-associated colorectal cancer. Saleh M, Trinchieri G. *Nat. Rev. Immunol.* 11(1), 9–20 (2011).
109. Ulcerative colitis, Ryan Ungaro, Saurabh Mehandru, Patrick B Allen, Laurent Peyrin-Biroulet, and Jean-Frédéric Colombel, Lancet. 2017 Apr 29; 389(10080): 1756–1770. doi: 10.1016/S0140-6736(16)32126-2.
110. Tumour Necrosis Factor Alpha in Intestinal Homeostasis and Gut Related Diseases, Barbara Ruder, Raja Atreya, and Christoph Becker, Int J Mol Sci. 2019 Apr; 20(8): 1887. Doi: 10.3390/ijms20081887.
111. The Dual Role of Neutrophils in Inflammatory Bowel Diseases, Odile Wéra, Patrizio Lancellotti, and Cécile Oury, J Clin Med. 2016 Dec; 5(12): 118. Doi: 10.3390/jcm5120118.
112. Programmed cell death and its role in inflammation, Yong Yang, Gening Jiang, Peng Zhang, and Jie Fan, Mil Med Res. 2015; 2: 12. Doi: 10.1186/s40779-015-0039-0.
113. Cell death of intestinal epithelial cells in intestinal diseases, Saravanan Subramanian, Hua Geng, and Xiao-Di Tan, Sheng Li Xue Bao. 2020 Jun 25; 72(3): 308–324.
114. Arsenic exposure: A public health problem leading to several cancers. I Palma-Lara, M Martínez-Castillo, J C Quintana-Pérez, M G Arellano-Mendoza, F Tamay-Cach, O L Valenzuela-Limón, E A García-Montalvo, A Hernández-Zavala. Regul Toxicol Pharmacol; 2020 Feb;110:104539. Doi: 10.1016/j.yrtph.2019.104539.
115. Arsenic: toxicity, oxidative stress and human disease. K Jomova, Z Jenisova, M Feszterova, S Baros, J Liska, D Hudecova, C J Rhodes, M Valko. J Appl Toxicol. 2011 Mar;31(2):95-107. doi: 10.1002/jat.1649.
116. Sodium arsenite induced reactive oxygen species generation, nuclear factor (erythroid-2 related) factor 2 activation, heme oxygenase-1 expression, and glutathione elevation in

Chang human hepatocytes. Bing Li , Xin Li, Bo Zhu, Xinyu., Environ Toxicol. 2013 Jul; 28(7):401-10. doi: 10.1002/tox.20731.

117. An appraisal on molecular and biochemical signalling cascades during arsenic-induced hepatotoxicity. Kaviyarasi Renu, Anusha Saravanan, Anushree Elangovan, Sineka Ramesh, Sivakumar Annamalai, Arunraj Namachivayam, Praveena Abel, Harishkumar Madhyastha, Radha Madhyastha, Masugi Maruyama, Vellingiri Balachandar, Abilash Valsala Gopalakrishnan. 2020 Nov 1;260:118438. doi: 10.1016/j.lfs.2020.118438.
118. Hydrogen Sulfide Alleviates Liver Injury Through the S-Sulfhydrated-Kelch-Like ECH-Associated Protein 1/Nuclear Erythroid 2-Related Factor 2/Low-Density Lipoprotein Receptor-Related Protein 1 Pathway. Shuang Zhao, Tianyu Song, Yue Gu, Yihua Zhang, Siyi Cao, Qing Miao, Xiyue Zhang, Hongshan Chen, Yuanqing Gao, Lei Zhang , Yi Han, Hong Wang, Jun Pu, Liping Xie, Yong Ji, .Hepatology. 2021 Jan;73(1):282-302. doi: 10.1002/hep.31247.
119. Oxidative stress-related liver dysfunction by sodium arsenite: Alleviation by Pistacia lentiscus oil.Fahima Klibet , Amel Boumendjel , Mohamed Khiari , Abdelfattah El Feki , Cherif Abdennour , Mahfoud Messarah. pharm Biol. 2016;54(2):354-63. doi: 10.3109/13880209.2015.1043562.
120. Morin treatment for acute ethanol exposure in rats.Anbu Singaravelu [1], Karthikkumar Venkatachalam, Richard L Jayaraj, Padma Jayabalan, Saravanan Nadanam , Biotech Histochem. 2021 Apr; 96(3):230-241. doi: 10.1080/10520295.2020.1785548. Epub 2020 Jun 29.
121. Mechanisms of poor oral bioavailability of flavonoid Morin in rats: From physicochemical to biopharmaceutical evaluations. Jianbo Li, Yang Yang, Erjuan Ning, Youmei Peng, Jinjie Zhang. Eur J Pharm Sci. 2019 Feb 1;128:290-298. doi: 10.1016/j.ejps.2018.12.011. Epub 2018 Dec 14.
122. Chitosan nanoparticles containing *Physalis alkekengi-L* extract: preparation, optimization and their antioxidant activity. Reza Mahmoudi, Maryam Tajali Ardakani, Behnam Hajipour Verdom, Abouzar Bahgeri, Hossein Mohammad-Beigi, Farhang Aliakbari, Zeinab Salehpour, Mohsen Alipour, Sajad Afrouz and Hassan Bardania. *Bull. Mater. Sci.* (2019) 42:131. https://doi.org/10.1007/s12034-019-1815-3.

123. Determination of arsenic in environmental and biological samples using toluidine blue or safanine O by simple spectrophotometric method. Chand Pasha and Badiadka Narayana. Bulletin of environmental contamination and toxicology; 81, 47-51 92008).
124. Lipid peroxidation measured as thiobarbituric acid-reactive substances in tissue slices: characterization and comparison with homogenates and microsomes. C G Fraga [1], B E Leibovitz, A L Tappel. Free Radic Biol Med. 1988;4(3):155-61. doi: 10.1016/0891-5849(88)90023-8.
125. Pharmacokinetics and Tissue Distribution Study of Pinosylvin in Rats by Ultra-High-Performance Liquid Chromatography Coupled with Linear Trap Quadrupole Orbitrap Mass Spectrometry. Fu, Y.; Sun, X.; Wang, L.; Chen, S. Evidence-Based Complementary Altern. Med. 2018, 2018, No. 4181084.
126. Corchorusin-D Directed Apoptosis of K562 Cells Occurs through Activation of Mitochondrial and Death Receptor Pathways and Suppression of AKT/PKB Pathway. Sumana Mallicka, Bikas C. Pal, Joseph R. Vedasiromoni, Deepak Kumar, Krishna Das Saha. Cellular Physiology and Biochemistry. 2012; 12;30(4):915-926.
127. The Role of Reactive Oxygen Species in Arsenic Toxicity. Yuxin Hu, Jin Li, Bin Lou, Ruirui Wu, Gang Wang, Chunwei Lu, Huihui Wang, Jingbo Pi and Yuanyuan Xu; Biomolecules 2020, 10, 240; doi:10.3390/biom10020240.
128. Molecular Mechanisms That Link Oxidative Stress, Inflammation, and Fibrosis in the Liver. Erika Ramos-Tovar and Pablo Muriel. Antioxidants (Basel). 2020 Dec; 9(12): 1279. doi: 10.3390/antiox9121279.
129. Drug pricing & challenges to hepatitis C treatment access. Brandy Henry. J Health Biomed Law. Author manuscript; available in PMC 2018 Sep 24. J Health Biomed Law. 2018 Sep; 14: 265–283.
130. The Role of Polyphenols in Human Health and Food Systems: A Mini-Review. Hannah Cory, Simone Passarelli, John Szeto, Martha Tamez and Josiemer Mattei. Front. Nutr., 21 September 2018 | https://doi.org/10.3389/fnut.2018.00087.
131. The Potential and Action Mechanism of Polyphenols in the Treatment of Liver Diseases, Sha Li, Hor Yue Tan, Ning Wang, Fan Cheung, Ming Hong, and Yibin Feng. Oxid Med Cell Longev. 2018; 2018: 8394818. doi: 10.1155/2018/8394818.

132. Hepatoprotective effect of morin on ethanol-induced hepatotoxicity in rats.Santhanam Gowri Shankari, Krishnamoorthy Karthikesan, Abdul Mohammed Jalaludeen, Natarajan Ashokkumar. J Basic Clin Physiol Pharmacol. 2010; 21(4):277-94. Doi: 10.1515/jbcpp.2010.21.4.277.
133. Morin protects acute liver damage by carbon tetrachloride (CCl_4) in rat. Hee Seung Lee, Kyung-Hee Jung, Sang-Won Hong, In-Suh Park, Chongmu Lee, Hyo-Kyung Han, Don-Haeng Lee, Soon-Sun Hong. Arch Pharm Res. 2008 Sep;31(9):1160-5. doi: 10.1007/s12272-001-1283-5.
134. Potential protective effects of quercetin and curcumin on paracetamol-induced histological changes, oxidative stress, impaired liver and kidney functions and haematotoxicity in rat. Mokhtar I Yousef, Sahar A M Omar, Marwa I El-Guendi, Laila A Abdelmegid. Food Chem Toxicol. 2010 Nov;48(11):3246-61. doi: 10.1016/j.fct.2010.08.034.
135. Protective Effect of Resveratrol against Hepatotoxicity of Cadmium in Male Rats: Antioxidant and Histopathological Approaches. Najah M. Al-Baqami and Reham Z. Hamza. *Coatings* 2021, *11*(5), 594; https://doi.org/10.3390/coatings11050594.
136. Protective effect of chitosan treatment against acetaminophen-induced hepatotoxicity. Eda Ozcelik, Sema Uslu, Nilufer Erkasap, Hadi Karimi. Kaohsiung J Med Sci. 2014 Jun;30(6):286-90. doi: 10.1016/j.kjms.2014.02.003.
137. Chitosan Nanoparticles as hepatoprotective agent against alcohol and fatty diet stress in rats. Mohamed Ahmed Abdelhakim, Mohamed S Radwan, Aya H Rady. January 2017, Biochemistry International 4(1):5-10.
138. Antioxidant Capacity and Hepatoprotective Role of Chitosan-Stabilized Selenium Nanoparticles in Concanavalin A-Induced Liver Injury in Mice. Kaikai Bai, Bihong Hong, Jianlin He, and Wenwen Huang. Nutrients. 2020 Mar; 12(3): 857. doi: 10.3390/nu12030857.
139. Protective effect of chitosan treatment against acetaminophen-induced hepatotoxicity. Eda Ozcelik, Sema Uslu, Nilufer Erkasap, Hadi Karimkhani. The Kaohsiung journal of medical sciences. 30(6), June 2014; DOI:10.1016/j.kjms.2014.02.003.
140. Hepatoprotective and antioxidant activity of quercetin loaded chitosan/alginate particles in vitro and in vivo in a model of paracetamol-induced toxicity. Virginia Tzankova, Denitsa Aluani, Magdalena Kondeva-Burdina, Yordan Yordanov, Feodor Odzhakov, Alexandar

Apostolov, Krassimira Yoncheva. Biomed Pharmacother. 2017 Aug;92:569-579. doi: 10.1016/j.biopha.2017.05.008.

141. The hepatic-targeted, resveratrol loaded nanoparticles for relief of high fat diet-induced nonalcoholic fatty liver disease. Wendi Teng, Liyun Zhao, Songtao Yang, Chengying Zhang, Meiyu Liu, Jie Luo, Junhua Jin, Ming Zhang, Chen Bao, Dan Li, Wei Xiong , Yuan Li, Fazheng Ren. J Control Release. 2019 Aug 10;307:139-149. doi: 10.1016/j.jconrel.2019.06.023.
142. Evaluation of the hepatoprotective effect of curcumin-loaded solid lipid nanoparticles against paracetamol overdose toxicity: Role of inducible nitric oxide synthase. Rasha M Hussein, Mohamed A Kandeil, Norhan A Mohammed, Rasha A Khallaf . J Liposome Res. 2022 Feb 8;1-11. doi: 10.1080/08982104.2022.2032737.
143. Arsenic induces apoptosis in mouse liver is mitochondria dependent and is abrogated by N-acetylcysteine. Amal Santra , Abhijit Chowdhury, Subhadip Ghatak, Ayan Biswas, Gopal Krishna Dhali. Toxicol Appl Pharmacol. 2007 Apr 15;220(2):146-55. doi: 10.1016/j.taap.2006.12.029.
144. Apoptosis: A Review of Programmed Cell Death. Susan elmore. Toxicol Pathol. 2007; 35(4): 495–516. doi: 10.1080/01926230701320337.
145. The effect of inflammatory cytokines in alcoholic liver disease. Kawaratani H, Tsujimoto T, Douhara A *et al. Mediators Inflamm.* 2013, 495156 (2013).
146. Tuning the size of poly(lactic-co-glycolic acid) (PLGA) nanoparticles fabricated by nanoprecipitation. Huang W, Zhang C. *Biotechnol. J.* 13(1) 700203 (2018).
147. Chitosan nanoparticles in drug therapy of infectious and inflammatory diseases. Rajitha P, Gopinath D, Biswas R, Sabitha M, Jayakumar R. Expert Opin Drug Deliv. 2016 Aug;13(8):1177-94. doi: 10.1080/17425247.2016.1178232. Epub 2016 May 2.
148. Bioimaging of Intact Polycaprolactone Nanoparticles Using Aggregation-Caused Quenching Probes: Size-Dependent Translocation via Oral Delivery. Haisheng He, Yunchang Xie, Yongjiu Lv, Jianping Qi, Xiaochun Dong , Weili Zhao, Wei Wu, Yi Lu. Adv Healthc Mater. 2018 Nov;7(22):e1800711. doi: 10.1002/adhm.201800711.
149. Biodegradable polymeric nanoparticles based drug delivery systems. Avnesh Kumari , Sudesh Kumar Yadav, Subhash C Yadav. Colloids Surf B Biointerfaces. 2010 Jan 1;75(1):1-18. doi: 10.1016/j.colsurfb.2009.09.001.

150. Phase solubility studiesof pure (-)-α-bisabolol and camomile essential oil with β-cyclodextrin, Waleczek, K.J.; Cabral Marques, H.M.; Hempel, B.; Schmidt, P.C.; Eur. J. Pharm. Biopharm. 2003, 55, 247–251.
151. Recent advances on chitosan-based micro- and nanoparticles in drug delivery. Sunil, A.A.; Nadagouda, N.M.; Tejraj, M.A. J. Control. Release **2004**, 100, 5–28.
152. Antitumor activity of mitoxantrone-loaded chitosan microspheres against Ehrlich ascites carcinoma. Jameela, S.R.; Latha, P.G.; Subramoniam, A.; Jayakrishnan, A. J. Pharm. Pharmacol. **1996**, 48, 685–688.
153. Tumor targeted delivery of encapsulated dextran–doxorubicin conjugate using chitosan nanoparticles as carrier. Mitra, S.; Gaur, U.; Ghosh, P.C.; Maitra, A.N. J. Control. Release **2001**, 74, 317–323.
154. Chitosan nanoparticle as protein delivery carrier – systematic examination of fabrication conditions for efficient loading and release. Gan, Q.; Wang, T. Colloid Surface B. **2007**, 59, 24–34.
155. In vivo uptake of chitosan microparticles by murine Peyer's patches: visualization studies using confocal laser scanning microscopy and immuno-histochemistry. Lubben, I.M.; Konings, F.A.J.; Borchard, G.; Verhoef, J.C.; Junginger, H.E. J. Drug Target. **2001**, 9, 39–47.
156. Chitosan DNA nanoparticles as gene delivery carriers: synthesis, characterization and transfection efficiency. Mao, H.Q.; Roy, K.; Troung-Le, V.L.; Janes, K.A.; Lim, K.Y.; Wang, Y.; August, J.T.; Leong, K.W. J. Control. Release **2001**, 70, 399–421.
157. Pharmacokinetic interaction between diltiazem and morin, a flavonoid, in rats. Choi, J. S., and Han, H. K. Pharmacol. Res. Commun.**2005**, 52, 5, 386-91.
158. Morin hydrate: A comprehensive review on novel natural dietary bioactive compound with versatile biological and pharmacological potential. Rajput, S. A.; Wang, X.; Yan, H. Biomed. Pharmacother.**2021**, 138, 111511.
159. Determination of flavonoids and phenolics and their distribution in almonds. Milbury, P.E. et al. J. Agric. Food Chem.**2006**, 54, 14, 5027-33.
160. Characterization of the interaction between human serum albumin and morin. Xie, M-X, et al. Biochimica et Biophysica Acta. **2006**, 1760, 8, 1184-91.

161. Protection against arsenic-induced hematological and hepatic anomalies by supplementation of vitamin C and vitamin e in adult male rats. Mondal, R.; Biswas, S.; Chatterjee, A. *et al.* J. Basic Clin. Physiol. Pharmacol.**2016**,27(6), 643–652.
162. Increased oxidative stress associated with the severity of the liver disease in various forms of hepatitis B virus infection. Bolukbas, C.; Bolukbas, F.F.; Horoz, M.; Aslan, M.; Celik, H. *et al*. Infec. Dis. **2005**, 5: 95-95.
163. Hepatoprotective Effect of Vitamin E. Adikwu, E.; Nelson, B. Am J Pharmacol Toxicol **2012**, 7 (4), 154-163.
164. Sodium arsenite induced reactive oxygen species generation, nuclear factor (erythroid-2 related) factor 2 activation, heme oxygenase-1 expression, and glutathione elevation in Chang human hepatocytes. Li,B.; Li, X.; Zhu,B.; Xinyu. Environ Toxicol. **2013**, 28(7):401-10.
165. Arsenic-induced oxidative stress and its reversibility. Flora, S.J. Free Radic. Biol. Med.**2011**, 51, 257–281.
166. An overview of chemical inhibitors of the Nrf2-ARE signaling pathway and their potential applications in cancer therapy. Zhu, J.; Wang, H.; Chen, F.; Fu, J.; Xu, Y.; hou, Y.; Kou, H.H.; Zhai, C.; Nelson, M.B.; Zhang, Q.; et al. Free Radic. Biol. Med. **2016**, 99, 544–556.
167. An Nrf2/small Maf heterodimer mediates the induction of phase II detoxifying enzyme genes through antioxidant response elements. Itoh, K.; Chiba, T.; Takahashi, S.; Ishii, T.; Igarashi, K.; Katoh, Y.; Oyake, T.; hayashi, N.; Satoh, K.; hatayama, I.; et al. Biochem. Biophys. Res. Commun. **1997**, *236*, 313–322.
168. Nrf2 redirects glucose and glutamine into anabolic pathways in metabolic reprogramming. Mitsuishi, Y.; Taguchi, K.; Kawatani, Y.; Shibata, T.; Nukiwa, T.; Aburatani, H.; Yamamoto, M.; Motohashi, H. Cancer Cell**2012**, *22*, 66–79.
169. Small Maf proteins serve as transcriptional cofactors for keratinocyte differentiation in the Keap1-Nrf2 regulatory pathway. Motohashi, H.; Katsuoka, F.; Engel, J.D.; Yamamoto, M. Proc.Natl. Acad. Sci. USA**2004**, *101*, 6379–6384.
170. The absence of Nrf2 enhances NF-κB-dependent inflammation following scratch injury in mouse primary cultured astrocytes. Pan, H.; Wang, H.; Wang, X.; Zhu, L.; Mao, L. Mediat. Inflamm**2012**, *2012*, 217580.

171. An enzyme-mediated controlled release system for curcumin based on cyclodextrin/cyclodextrin degrading enzyme. Roozbehi, S.; Dadashzadeh, S.; Sajedi, R. H. Enzyme Microb. Technol. 2021, 144, 109727.
172. Preparation, characterization and pharmacokinetic studies of tacrolimus-dimethyl-β-cyclodextrin inclusion complex-loaded albumin nanoparticles. Gao, S.; Sun, J.; Fu, D.; Zhao, H.; Lan, M.; Gao, F. Int. J. Pharm**2012**, 427, 410–416.
173. Chitosan nanoparticles containing Physalis alkekengi-L extract: preparation, optimization and their antioxidant activity. Mahmoudi, R.; Ardakani, M. T.; Verdom, B. H.; Bagheri, A.; Beigi, H. M.; Aliakbari, F.; Salehpour, Z.; Alipour, M.; Afrouz, S.; Bardania, H. Bull. Mater. Sci. 2019, 42:131.
174. Morin encapsulated Chitosan nanoparticles (MCNPs) ameliorate arsenic induced liver damage through improvement of antioxidant system,prevention of apoptosis and inflammation in mice. Mondal, S.; Das, S.; Mahapatra, P.K.; Saha, K.D; Nanoscale Adv. **2022,** (D2NA00167E).
175. Yuan, Z.; Ye, Y. Gao, F.; Yuan, H.; Lan, M.; Lou, K.; Wang, W. Chitosan-graft-_-cyclodextrin nanoparticles as a carrier for controlled drug release. Int. J. Pharm. **2013,** 446, 191– 198.
176. Determination of arsenic in environmental and biological samples using toluidine blue or safanine O by simple spectrophotometric method. Pasha, C.; Narayana, B. Bull Environ Contam Toxicol**2008,**81, 47-51 92008.
177. Lipid peroxidation measured as thiobarbituric acid-reactive substances in tissue slices: characterization and comparison with homogenates and microsomes. Fraga,C. G.; Leibovitz, B. E.; Tappel,A. L. Free Radic Biol Med. **1988**, 4(3):155-61.
178. Cyclodextrin–Drug Inclusion Complexes: In Vivo and In Vitro Approaches. Carneiro, S. B.; Duarte, F. Í. C.; Heimfarth, L.; Quintans, J. S. S.; Quintans-Júnior, L. J.; Veiga Júnior, V. F.; Lima, Á. A. N. Int J Mol Sci. **2019 Feb**; 20(3): 642.
179. Pharmacokinetics and Tissue Distribution Study of Pinosylvin in Rats by Ultra-High-Performance Liquid Chromatography Coupled with Linear Trap Quadrupole Orbitrap Mass Spectrometry. Fu, Y.; Sun, X.; Wang, L.; Chen, S. Evidence-Based Complementary Altern. Med. **2018**, 2018, 4181084.

180. Structure and properties of chitosan/sodium dodecyl sulfate composite films. Jiang, S.; Qiao, C.; Wang, X.;Li, Z.; Yang, G. RSC Adv. **2022**, 12(7): 3969–3978. Doi: 10.1039/d1ra08218c.
181. Enhanced protective activity of Nano formulated andrographolide against arsenic induced liver damage. Das, S.; Pradhan, G. K.; Das, S.; Nath, D.; Saha, K. D. Chem.-Biol. Interact.**2015,** DOI: 10.1016/j.cbi.2015.10.011.
182. The effect of inflammatory cytokines in alcoholic liver disease. Kawaratani, H.; Tsujimoto, T.; Douhara, A. *et al.* Mediators Inflamm**2013**, 495156.
183. Cyclodextrins in Food Technology and Human Nutrition: Benefits and Limitations. Fenyvesi, É.; Vikmon, M.; Szente; L. Crit Rev Food Sci Nutr.**March 2015**; 56(12).
184. t hart na, van der plaats a, leuvenink hg, wiersema-buist j, olinga p, vanluyn mj, verkerke gj, rakhorst g, ploeg rj. initial blood washout duringorgan procurement determines liver injury and function after preservationand reperfusion. am j transplant. 2004;4:1836–44. (16) (pdf) sedum sarmentosum bunge extract ameliorates lipopolysaccharide- and d-galactosamine-induced acute liver injury by attenuating the hedgehog signaling pathway via regulation of mir-124 expression.
185. Chitosan nanoparticles as hepatoprotective agent against alcohol and fatty diet stress in rats. Abdelhakim,M. A.; Radwan,M. S.; Rady, A. H. Biochem. Int. **2017**, 4(1):5-10.
186. Antioxidant Capacity and Hepatoprotective Role of Chitosan-Stabilized Selenium Nanoparticles in Concanavalin A-Induced Liver Injury in Mice. Bai,K.; Hong,B.; He,J.; Huang, W. Nutrients **2020**, 12(3): 857.
187. Hepatoprotective and antioxidant activity of quercetin loaded chitosan/alginate particles in vitro and in vivo in a model of paracetamol-induced toxicity. Tzankova,V.; Aluani,D.; Kondeva-Burdina,M.; Yordanov, Y.; Odzhakov,F.; Apostolov, A.; Yoncheva,K. Biomed Pharmacother **2017**, 92:569-579.
188. Morin protects acute liver damage by carbon tetrachloride (CCl_4) in rat. Lee,H. S.; Jung,K. H.; Hong,S. W.; Park, I. S.; Lee, C.; Han,H. K.; Lee, D. H.; Hong, S. S. Arch Pharm Res **2008**, 31(9):1160-5.
189. Review: A history of cyclodextrins, Crini, G.; Chem. Rev. **2014**, 114, 10940–10975.

190. Uncovering pathogenic mechanisms of inflammatory bowel disease using mouse models of Crohn's disease-like ileitis: What is the right model? Cominelli F, Arseneau KO, Rodriguez-Palacios A, Pizarro TT. *Cell. Mol. Gastroenterol. Hepatol.* 4(1), 19–23 (2017).
191. Can ulcerative colitis be cured by acupuncture? Iseri SO. *J. Aust. Tradit-Med. So.* 19(2), 94–95 (2013).
192. Kaplan GG. The global burden of IBD: from 2015 to 2025. *Nat. Rev. Gastroenterol. Hepatol.* 12(12), 720–727 (2015).
193. Worldwide incidence and prevalence of inflammatory bowel disease in the 21st century: A systematic review of population-based studies. Ng, S.C.; Shi, H.Y.; Hamidi, N.; Underwood, F.E.; Tang,W.; Benchimol, E.I.; Panaccione, R.; Ghosh, S.;Wu, J.C.Y.; Chan, F.K.L.; et al. Lancet **2017**, 390, 2769–2778.
194. Neutrophils cascading their way to inflammation. Sadik, C.D., Kim, N.D. & Luster, A.D. *Trends Immunol*. **32,** 452–460 (2011).
195. Mast Cell: A multi-functional master cell, Melissa Krystal-Whittemore, Kottarappat N. Dileepan, John G. Front. Immunol., 2016, https://doi.org/10.3389/fimmu.2015.00620.
196. Toll-like Receptors and Inflammatory Bowel Disease. Yue Lu,[1] Xinrui Li,[1] Shanshan Liu,[1] Yifan Zhang,[2] and Dekai Zhang, Front Immunol. 2018; 9: 72. doi: 10.3389/fimmu.2018.00072.
197. The role of pattern-recognition receptors in innate immunity: update on Toll-like receptors, Taro Kawai, Shizuo Akira, *Nature Immunology* volume 11, pages373–384 (2010).
198. Signaling to NF-kappaB by Toll-like receptors, Taro Kawai [1], Shizuo Akira, 2007 Nov;13(11):460-9. doi: 10.1016/j.molmed.2007.09.002.
199. NF-κB signaling in inflammation. Ting Liu,[1] Lingyun Zhang,[1] Donghyun Joo,[1] and Shao-Cong Sun, Signal Transduct Target Ther. 2017; 2: 17023. doi: 10.1038/sigtrans.2017.23.
200. Pro-Inflammatory Cytokines in the Pathogenesis of IBD, Warren Strober[#] and Ivan J. Fuss, Gastroenterology. 2011 May; 140(6): 1756–1767. doi: 10.1053/j.gastro.2011.02.016.
201. The NF-κB Family of Transcription Factors and Its Regulation. Andrea Oeckinghaus[1,2] and Sankar Ghosh, Cold Spring Harb Perspect Biol. 2009 Oct; 1(4): a000034. doi: 10.1101/cshperspect.a000034.

202. The NLRP3 Inflammasome: An Overview of Mechanisms of Activation and Regulation. Nathan Kelley, Devon Jeltema, Yanhui Duan, and Yuan He, Int J Mol Sci. 2019 Jul; 20(13): 3328. doi: 10.3390/ijms20133328.
203. Role of NLRP3 inflammasome in inflammatory bowel diseases, Evanthia Tourkochristou, Ioanna Aggeletopoulou, Christos Konstantakis, and Christos Triantos, World J Gastroenterol. 2019 Sep 7; 25(33): 4796–4804. doi: 10.3748/wjg.v25.i33.4796.
204. Targeting NF-κB pathway for treating ulcerative colitis: comprehensive regulatory characteristics of Chinese medicines, Peng-De Lu[1] and Yong-Hua Zhao, Chin Med. 2020; 15: 15. doi: 10.1186/s13020-020-0296-z.
205. TGF-β in inflammatory bowel disease: a key regulator of immune cells, epithelium, and the intestinal microbiota, Sozaburo Ihara, Yoshihiro Hirata, Kazuhiko Koike, Journal of Gastroenterology volume 52, pages777–787 (2017).
206. Anti-inflammatory effect of IL-10 mediated by metabolic reprogramming of macrophages. W. K. Eddie IP, Namiko Hoshi, Dror S. Shouval, Scott Snapper, Ruslan Medzhitov. *SCIENCE,* 5 May 2017, Vol 356, Issue 6337, pp. 513-519, DOI: 10.1126/science.aal3535
207. Role of Nrf2 in Oxidative Stress and Toxicity. Qiang Ma,Annu Rev Pharmacol Toxicol. 2013; 53: 401–426. doi: 10.1146/annurev-pharmtox-011112-140320.
208. Emerging Roles of Nrf2 and Phase II Antioxidant Enzymes in Neuroprotection, Meijuan Zhang, Chengrui An, Yanqin Gao, Rehana K. Leak, Jun Chen, and Feng Zhang, Prog Neurobiol. 2013 Jan; 100: 30–47. doi: 10.1016/j.pneurobio.2012.09.003.
209. Reliability of malondialdehyde as a biomarker of oxidative stress in psychological disorders. Maryam Khoubnasabjafari, Khalil Ansarin, and Abolghasem Jouyban, Bioimpacts. 2015; 5(3): 123–127. Doi: 10.15171/bi.2015.20.
210. Phytochemicals targeting Toll-like receptors 4 (TLR4) in inflammatory bowel disease. Wenbin Dai, Longhai Long, Xiaoqiang Wang,Sen Li, and Houping Xu, Chin Med. 2022; 17: 53. Doi: 10.1186/s13020-022-00611-w.
211. Morin as a Preservative for Delaying Senescence of Banana. Hong Zhu, Jiali Yang, Yueming Jiang, Jun Zeng, Xuesong Zhou, Yanglin Hua, and Bao Yang, Biomolecules. 2018 Sep; 8(3): 52. Doi: 10.3390/biom8030052.
212. Intestinal anti-inflammatory activity of morin on chronic experimental colitis in the rat. J Gálvez , G Coelho, M E Crespo, T Cruz, M E Rodríguez-Cabezas, A Concha, M

Gonzalez, A Zarzuelo, Aliment Pharmacol Ther, 2001 Dec;15(12):2027-39, Doi: 10.1046/j.1365-2036.2001.01133.x.

213. Gold Nanoparticles in Biology and Medicine: Recent Advances and Prospects, L.A. Dykman and N.G. Khlebtsov, Acta Naturae. 2011 Apr-Jun; 3(2): 34–55.
214. Therapeutic effect of gold nanoparticles on DSS-induced ulcerative colitis in mice with reference to interleukin-17 expression. Amira M. Abdelmegid, Fadia K. Abdo, Fayza E. Ahmed, and Asmaa A. A. Kattaia, Sci Rep. 2019; 9: 10176, Doi: 10.1038/s41598-019-46671-1.
215. Shape-dependent cytotoxicity and cellular uptake of gold nanoparticles synthesized using green tea extract, You Jeong Lee, Eun-Young Ahn, and Youmie Park. Nanoscale Res Lett. 2019; 14: 129. Doi: 10.1186/s11671-019-2967-1.
216. Nanoparticles: Properties, applications and toxicities, IbrahimKhan, KhalidSaeed, IdreesKhan, Arabian J. of Chemistry. Volume 12, Issue 7, November 2019, Pages 908-931. https://doi.org/10.1016/j.arabjc.2017.05.011.
217. Hashizume, M.; Higuchi, Y.; Uchiyama, Y.; Mihara, M. IL-6 plays an essential role in neutrophilia under inflammation. Cytokine, 2011, 54, 92–99.
218. D. A. Martin and B. W. Bolling, "A review of the efficacy of dietary polyphenols in experimental models of inflammatory bowel diseases," *Food & Function*, vol. 6, no. 6, pp. 1773–1786, 2015.
219. Morin encapsulated chitosan nanoparticles (MCNPs) ameliorate arsenic induced liver damage through improvement of the antioxidant system and prevention of apoptosis and inflammation in mice. Sanchaita Mondal[1,2], Sujata Das[1], Pradip Kumar Mahapatra[2], Krishna Das Saha, Nanoscale Adv., . 2022 May 17;4(13):2857-2872, DOI: 10.1039/d2na00167e.
220. Plant polyphenols as dietary antioxidants in human health and disease. Kanti Bhooshan Pandey and Syed Ibrahim Rizvi, Oxid Med Cell Longev. 2009 Nov-Dec; 2(5): 270–278. Doi: 10.4161/oxim.2.5.9498.
221. Efficacy of quercetin derivatives in prevention of ulcerative colitis in rats. Ruzena Sotnikova, Viera Nosalova, and Jana Navarova, Interdiscip Toxicol. 2013 Mar; 6(1): 9–12, doi: 10.2478/intox-2013-0002.

222. Tannic acid modulates intestinal barrier functions associated with intestinal morphology, antioxidative activity, and intestinal tight junction in a diquat-induced mouse model Meiwei Wang, Huijun Huang, Shuang Liu, Yu Zhuang, Huansheng Yang, Yali Li, Shuai Chen, Lixia Wang, Lanmei Yin, Yuanfeng Yaod and Shanping He. RSC Adv., 2019, 9, 31988, DOI: 10.1039/c9ra04943f.
223. Gallic acid improved inflammation via NF-κB pathway in TNBS-induced ulcerative colitis. Lei Zhu, PeiQing Gu, Hong Shen, Int Immunopharmacol, 2019 Feb;67:129-137. Doi: 10.1016/j.intimp.2018.11.049.
224. Protective effect of naringenin on acetic acid-induced ulcerative colitis in rats. Salim S Al-Rejaie, Hatem M Abuohashish, Maher M Al-Enazi, Abdullah H Al-Assaf, Mihir Y Parmar, and Mohammed M Ahmed, World J Gastroenterol. 2013 Sep 14; 19(34): 5633–5644. Doi: 10.3748/wjg.v19.i34.5633.
225. Protective role of berberine on ulcerative colitis through modulating enteric glial cells-intestinal epithelial cells-immune cells interactions. Heng Li, Chen Fan, Huimin Lu, Chunlan Feng, Peilan He , Xiaoqian Yang, Caigui Xiang , Jianping Zuo, Wei Tang, Acta Pharm Sin B, 2020 Mar;10(3):447-461. Doi: 10.1016/j.apsb.2019.08.006.
226. Protective Role of Curcumin and Flunixin Against Acetic Acid-Induced Inflammatory Bowel Disease via Modulating Inflammatory Mediators and Cytokine Profile in Rats. Boobalan Gopu [1], Rasakatla Dileep, Matukumalli Usha Rani, C S V Satish Kumar [1], Matham Vijay Kumar, Alla Gopala Reddy, J Environ Pathol Toxicol Oncol, 2015;34(4):309-20. Doi: 10.1615/jenvironpatholtoxicoloncol.2015013049.
227. Effects of morin on an experimental model of acute colitis in rats. M A Ocete [1], J Gálvez, M E Crespo, T Cruz, M González, M I Torres, A Zarzuelo, Pharmacology, 1998 Nov;57(5):261-70. Doi: 10.1159/000028250.
228. An Overview of the Synthesis of Gold Nanoparticles Using Radiation Technologies. Lucas Freitas de Freitas, Gustavo Henrique Costa Varca, Jorge Gabriel dos Santos Batista, and Ademar Benévolo Lugão, Nanomaterials (Basel). 2018 Nov; 8(11): 939. Doi: 10.3390/nano8110939.
229. Pharmacological Role of Functionalized Gold Nanoparticles in Disease Applications. Wen-Chin Ko, Su-Jane Wang, Chien-Yu Hsiao, Chen-Ting Hung, Yu-Jou Hsu, Der-Chen

Chang,[7] and Chi-Feng Hung, Molecules. 2022 Mar; 27(5): 1551. Doi: 10.3390/molecules27051551.

230. Assessment of the in Vivo Toxicity of Gold Nanoparticles. Yu-Shiun Chen,Yao-Ching HungIan Liau,G Steve Huang, Nanoscale Res Lett. 2009; 4(8): 858–864. Doi: 10.1007/s11671-009-9334-6.
231. Toxicologic effects of gold nanoparticles in vivo by different administration routes. Xiao-Dong Zhang, Hong-Ying Wu, Di Wu, Yue-Ying Wang, Jian-Hui Chang, Zhi-Bin Zhai, Ai-Min Meng, Pei-Xun Liu, Liang-An Zhang, and Fei-Yue Fan. Int J Nanomedicine. 2010; 5: 771–781. Doi: 10.2147/IJN.S8428.
232. Gold Nanoparticles: Multifaceted Roles in the Management of Autoimmune Disorders. Khadijeh Koushki, Sanaz Keshavarz Shahbaz, Mohsen Keshavarz, Evgeny E. Bezsonov, Thozhukat Sathyapalan, and Amirhossein Sahebkar, Biomolecules. 2021 Sep; 11(9): 1289. Doi: 10.3390/biom11091289.
233. Investigating the optimum size of nanoparticles for their delivery into the brain assisted by focused ultrasound-induced blood–brain barrier opening. Seiichi Ohta, Emi Kikuchi, Ayumu Ishijima, Takashi Azuma, Ichiro Sakuma, and Taichi Ito, Sci Rep. 2020; 10: 18220. Doi: 10.1038/s41598-020-75253-9.
234. Size and surface charge of gold nanoparticles determine absorption across intestinal barriers and accumulation in secondary target organs after oral administration, Carsten Schleh, Manuela Semmler-Behnke, Jens Lipka, Alexander Wenk, Stephanie Hirn, Martin Schäffler, Günter Schmid, Ulrich Simon, and Wolfgang G Kreyling, Nanotoxicology. 2012 Feb; 6(1): 36–46. Doi: 10.3109/17435390.2011.552811.
235. Size-Dependent Gold Nanoparticle Interaction at Nano–Micro Interface Using Both Monolayer and Multilayer (Tissue-Like) Cell Models Darren Yohan. Charmainne Cruje. Xiaofeng Lu. Devika B. Chithrani, Nano-Micro Lett. (2016) 8(1):44–53 DOI 10.1007/s40820-015-0060-6.
236. Effects of Dextran Sulfate Sodium-Induced Ulcerative Colitis on the Disposition of Tofacitinib in Rats. Sung Hun Bae, Hyo Sung Kim, Hyeon Gyeom Choi, Sun-Young Chang, and So Hee Kim, Biomol Ther (Seoul). 2022 Nov 1; 30(6): 510–519. Doi: 10.4062/biomolther.2022.049.

237. Myeloperoxidase as an Active Disease Biomarker: Recent Biochemical and Pathological Perspectives. Amjad A. Khan, Mohammed A. Alsahli, and Arshad H. Rahmani, Med Sci (Basel). 2018 Jun; 6(2): 33. Doi: 10.3390/medsci6020033.
238. Targeting myeloperoxidase (MPO) mediated oxidative stress and inflammation for reducing brain ischemia injury: potential application of natural compounds. Shuang Chen, Hansen Chen, Qiaohui Du and Jiangang Shen. Front. Physiol., 19 May 2020. https://doi.org/10.3389/fphys.2020.00433.
239. Polyphenol Content and Modulatory Activities of Some Tropical Dietary Plant Extracts on the Oxidant Activities of Neutrophils and Myeloperoxidase. Cesar N. Tsumbu, Ginette Deby-Dupont, Monique Tits, Luc Angenot, Michel Frederich, Stephane Kohnen, Ange Mouithys-Mickalad, Didier Serteyn, and Thierry Franck, Int J Mol Sci. 2012; 13(1): 628–650. Doi: 10.3390/ijms13010628.
240. Pathomechanisms of Oxidative Stress in Inflammatory Bowel Disease and Potential Antioxidant Therapies. Tian Tian, Ziling Wang, and Jinhua Zhang, Oxid Med Cell Longev. 2017; 2017: 4535194. Doi: 10.1155/2017/4535194.
241. New Insights into the Role of Trace Elements in IBD. Georgiana-Emmanuela Gîlcă-Blanariu, Smaranda Diaconescu, Manuela Ciocoiu, and Gabriela Ștefănescu. Biomed Res Int. 2018; 2018: 1813047. Doi: 10.1155/2018/1813047.
242. Pancreatic Response to Gold Nanoparticles Includes Decrease of Oxidative Stress and Inflammation in Autistic Diabetic Model. Manar Selim, Yashmina M Abd Elhakim, Laila Y Al-Ayedhi, 2015, Cellular Physiology and Biochemistry 35(2):586-600, DOI:10.1159/000369721.
243. Spherical neutral gold nanoparticles improve anti-inflammatory response, oxidative stress and fibrosis in alcohol-methamphetamine-induced liver injury in rats. Thaís Gomes de Carvalho, Vinícius Barreto Garcia, Aurigena Antunes de Araújo, Luiz Henrique da Silva Gasparotto, Heloiza Silva, Gerlane Coelho Bernardo Guerra, Emilio de Castro Miguel, Renata Ferreira de Carvalho Leitão, Deiziane Viana da Silva Costa, Luis J Cruz, Alan B Chan, Raimundo Fernandes de Araújo Júnior, Int J Pharm, 2018 Sep 5;548(1):1-14. Doi: 10.1016/j.ijpharm.2018.06.008.
244. Therapeutic Potential of Quercetin Loaded Nanoparticles: Novel Insights in Alleviating Colitis in an Experimental DSS Induced Colitis Model. Safaa I. Khater, Marwa M. Lotfy,

Maher N. Alandiyjany, Leena S. Alqahtani, Asmaa W. Zaglool, Fayez Althobaiti, Tamer Ahmed Ismail, Mohamed Mohamed Soliman, Saydat Saad, and Doaa Ibrahim, Biomedicines. 2022 Jul; 10(7): 1654. Doi: 10.3390/biomedicines10071654.

245. Changes of the cytokine profile in inflammatory bowel diseases. Györgyi Műzes, Béla Molnár, Zsolt Tulassay, and Ferenc Sipos, World J Gastroenterol. 2012 Nov 7; 18(41): 5848–5861. Doi: 10.3748/wjg.v18.i41.5848.
246. Inhibitor of Differentiation-2 Protein Ameliorates DSS-Induced Ulcerative Colitis by Inhibiting NF-κB Activation in Neutrophils. Jie Ren, Dong Yan, Yichun Wang, Jiaojiao Zhang, Min Li, Wancheng Xiong, Xueqian Jing, Puze Li, Weidong Zhao, Xiwen Xiong, Minna Wu, and Genshen Zhong , Front Immunol. 2021; 12: 760999. Doi: 10.3389/fimmu.2021.760999.
247. Morin (3,5,7,2',4'-Pentahydroxyflavone) abolishes nuclear factor-kappaB activation induced by various carcinogens and inflammatory stimuli, leading to suppression of nuclear factor-kappaB-regulated gene expression and up-regulation of apoptosis. Sunil K Manna [1], Rishi S Aggarwal, Gautam Sethi, Bharat B Aggarwal, Govindarajan T Ramesh, Clin Cancer Res, 2007 Apr 1;13(7):2290-7. Doi: 10.1158/1078-0432.CCR-06-2394.

Publications related to thesis:

- S. Mondal, S. Das, P. K. Mahapatra, K. D. Saha; Morin encapsulated chitosan nanoparticles (MCNPs) ameliorate arsenic induced liver damage through improvement of the antioxidant system and prevention of apoptosis and inflammation in mice. Nanoscale Adv., 2022, 4, 2857. DOI: 10.1039/d2na00167e.
- S. Mondal, S. Das, P. K. Mahapatra, K. D. Saha; Morin-VitaminE-β-cyclodextrinInclusion Complex Loaded Chitosan Nanoparticles (M-Vit.E-CD-CSNPs) Ameliorate Arsenic-Induced Hepatotoxicityina Murine Model. Molecules **2022**, 27, 5819. doi.org/10.3390/molecules27185819.

Publications on collaborative work:

- S. Mondal, M. Saha, M. Ghosh, S. Santra, M. A. Khan, KD Saha, M. R. Molla; Programmed supramolecular nanoassemblies: enhanced serum stability and cell specific triggered release of anti-cancer drugs. nanoscale-advances.,2019,DOI:10.1039/c9na00052f.
- S. Mukherjee, S. Ganguly, K. Manna, S. Mondal, S. Mahapatra, D. Das; Green Approach To Synthesize Crystalline Nanoscale ZnIICoordination Polymers: Cell Growth Inhibition and Immunofluorescence Study. Inorg. Chem. 2018 Apr 2;57(7):4050-4060.
- S. Dey, R. Purkait, C. Patra, M. Saha, S. Mondal, K D Saha, C. Sinha; Highly selective and sensitive recognition of Zn(II) by a novel coumarinyl scaffold following spectrofluorometric technique and its application in living cells. *New J. Chem.,* 2018, 42, 16297—16306.
- P. Singh, S. Mondal, M. Saha, KD saha, PK Maiti, K. Sen. Toxicity of pristine and β-cyclodextrin modified mesoporous alumina towards normal and cancer cell lines. August 2019Journal of the Indian Chemical Society 96(8):1109
- A. Mondal, C. Das, M. Corbella, A. Bauz, A. Frontera, M. Saha,S. Mondal, KD Saha, SK Chattopadhyay; Biological Promiscuity of a binuclear Cu(II) complex of aminoguanidine Schiff base: DNA binding, Anticancer Activity and Histidine sensing ability of the complex. *New J. Chem.*, 2020, DOI: 10.1039/C9NJ05712A
- Biswajit Bera, Sanchaita Mondal, Saswati Gharami, Rahul Naskar, Krishna Das Saha and Tapan K. Mondal, Palladium (II) and platinum (II) complexes with ONN donor pincer ligand: synthesis, characterization and in vitro cytotoxicity study. *New J. Chem.*, 2022, 46, 11277, DOI: 10.1039/d2nj01894b.

Seminars and Symposiums attended:

- 3rd regional science and technology congress (southern region), 2018, organized by Bidhannagar college, govt of West Bengal & Department of science and Biotechnology, govt of West Bengal.
- Professor Asima Chatterjee Centenary Seminar (PACCS – 2018) on recent inventions in Chemical and Allied Sciences, University of Calcutta.
- 6th world congress on Nanomedical Sciences, Chemistry Biology interface: Synergestic in new Frontiers (CBISNF – 2019) and Science and technology for the future mankind, university of Delhi.